A Single-Well Injection-Withdrawal (SWIW) experiment with synthetic groundwater

Rune Nordqvist, Anna Lindquist, Pernilla Thur, Johan Byegård, Erik Gustafsson

Geosigma AB

November 2015

SKB

A Single-Well Injection-Withdrawal (SWIW) experiment with synthetic groundwater

Rune Nordqvist, Anna Lindquist, Pernilla Thur,
Johan Byegård, Erik Gustafsson

Geosigma AB

Abstract

A series of SWIW (Single-Well Injection-Withdrawal) tests with synthetic groundwater were carried out in borehole KA2858A at the Äspö HRL. The experimental sequence included supporting investigations of hydrogeology and water chemistry at the site as well as *in situ* measurements of groundwater flow using the dilution method. Three single-tracer preparatory SWIW tests were performed that provided preliminary results for the final design of the main tests. Two main synthetic SWIW tests employing a wide range of tracers were performed, one without and one with a waiting phase (93 hours) between tracer injection and recovery pumping. The tracers were either added or removed to the synthetic injection water. Added tracers comprised Uranine, Li, NO_3, Mg, Cs and Rb while removed tracers comprised Cl, Na, Ca, K and Rn (radon).

The main SWIW tests resulted in well-defined breakthrough curves for all employed tracers. Estimation of tracer recovery indicated complete recovery for all tracers with a sufficiently long back-pumping period. There are clear and consistent differences between the tests with and without waiting phase, respectively, for all tracers. The differences are qualitatively consistent with what can be expected if diffusion takes place during the waiting phase. However, detailed analysis of the potential impact of the background flow during the waiting period indicated that the background flow may be important for the early parts of the breakthrough curves from the SWIW test with a waiting phase. A complicating factor is that the determination of the background flow rate is uncertain due to high sampling flow rates relative to the formation flow rate. Further analysis of the early parts of the breakthrough curves requires that the background flow, possibly with more accurate correction for the sampling flow rate, and diffusion are considered simultaneously.

The late-time breakthrough for the added tracers clearly indicates diffusive mass transfer, shown by straight lines in log-log tracer breakthrough plots. This result is not affected by the background groundwater flow. The log-log slopes often approach the value of -1.5, which is the ideal value for homogenous matrix diffusion. Interesting observations are that sorbing tracers generally have somewhat flatter slopes and that all the SWIW test with a waiting phase also results in flatter slopes. Basic simulations with a homogenous matrix diffusion model suggest that such a model is not sufficient to explain both early and late parts of the tracer breakthrough.

This report comprises a summary of all investigations carried out in connection with the SWIW experiments with synthetic groundwater. A first evaluation of experimental data has been made in order to explore alternatives for interpretation of the results. A large volume of experimental data is now available for further analysis.

Sammanfattning

Ett antal SWIW-tester (Single-Well Injection-Withdrawal) med syntetiskt grundvatten har genomförts i tunnelborrhål KA2858 i Äspölaboratoriet. I samband med spårämnesförsöken gjordes även hydraultester, vattenkemisk provtagning samt mätningar av grundvattenflöde genom utspädningsmetoden. Tre förberedande SWIW-tester genomfördes för planeringen av två huvudförsök. I de två huvudförsöken injicerades ett stort antal spårämnen med olika transportegenskaper. Skillnaden mellan de båda huvudförsöken bestod i att det första genomfördes utan väntetid efter injicieringsfasen medan en väntetid på 93 timmar tillämpades i det andra. De spårämnen som studerades var antingen tillsatta eller borttagna från det syntetiska grundvatten som användes för injicering. Tillsatta spårämnen utgjordes av Uranin, Li, NO_3, Mg, Cs och Rb medan bortagna spårämnen utgjordes av Cl, Na, Ca, K samt Rn.

Huvudförsöken resulterade i väldefinierade genombrottskurvor för samtliga spårämnen. Experimentdata tyder på att allt injicerat spårämne kan återpumpas till experimentsektionen. Tydliga skillnader i resultat kan observeras mellan de båda huvudförsöken med respektive utan väntefas. En kvalitativ bedömning indikerar att skillnaderna mellan försöken är ung efär vad som kan förväntas om diffusionsprocesser är verksamma under väntefasen. Dock visar en mer detaljerad analys av potentiell inverkan av befintligt grundvattenflöde att detta kan vara en viktig faktor att ta hänsyn till, särskilt vid utvärdering av den tidiga delen av genombrottskurvorna för SWIW-testet med väntefas. En komplicerande faktor är att bestämningen av grundvattenflödet med hjälp av utspädningsmetoden är osäker på grund av att provtagningsflödet och grundvattenflödet är av ungefär samma storlek. Vidare analys av framförallt de tidiga delarna av genombrottskurvorna bör göras där man tar hänsyn till bakrundsflöde och diffusionsprocesser samtidigt, samt eventuellt ta fram en mer noggrann metod för att korrigera för höga provtagningsflöden vid utspädningsmätningar.

De senare delarna av genombrottskurvorna för tillsatta spårämnen visar, oavsett storleken på bakgrundsflödet, att diffusion i sprickformationen är en aktiv process under SWIW-testerna. Genombrottskurvor plottade i log-log skala ger i regel lutningar som verkar gå mot -1.5, vilket teoretiskt kan förväntas då man har matrisdiffusion under ideala förhållanden. Det finns dock ett antal intressanta avvikelser, t.ex. att sorberande ämnen allmänt ger något flackare lutning samt att försök med väntetid verkar ge flackare lutning för samtliga spårämnen. Enkla simuleringar med matrisdiffusion indikerar att olika diffusionsprocesser kan behövas för att förklara både början och slutet på spårämnesgenombrotten.

Denna rapport utgör en sammanfattning samtliga undersökningar utförda i samband med SWIWterna med syntetiskt grundvatten. En första relativt grundläggande utvärdering av experimentdata har gjorts i syfte att utforska olika tolkningsmöjligheter. En stor mängd experimentdata finns därmed tillgängliga och som bör analyseras vidare.

Contents

1 Introduction

1.1 Background

The Swedish Nuclear Fuel and Waste Management (SKB) have the task of managing Swedish nuclear and radioactive waste. SKB has been conducting advanced research for thirty years with focus on the final disposal of all spent nuclear fuel. The Äspö Hard Rock Laboratory (Äspö HRL) is an underground facility operated by SKB that provides opportunities for research, development and demonstration in a realistic and relatively undisturbed underground crystalline rock environment at depths planned for a future deep repository.

The SKB disposal concept comprises three protective barriers; a Cu canister, a buffer made up of bentonite clay and the geosphere (crystalline bedrock). The geosphere provides a natural environment in which the function of the technical barriers is maintained over a very long period. Should the primary barriers (canister, buffer) fail, it is envisioned that radioactive substances become dissolved in the groundwater water and then follow the natural pathways of the flowing groundwater. However, even in such a case, the processes of diffusion and sorption provide significant additional retention mechanisms for radionuclide transport that are considered to be important for the overall safety analysis. The transport and retention properties of solutes in rock fractures have been studied using field tracer test for about three decades. These tests have typically provided clear demonstrations of solute retention but often with ambiguity regarding detailed interpretation about the various processes involved. The overall intention of the present synthetic SWIW test is to increase the understanding of processes that govern radionuclide transport by providing data that may be used to compare behaviour of a large number of tracers with different properties in tests with different contact times with the rock.

Single-Well Injection-Withdrawal tests (SWIW, sometimes also referred to as push-pull tests) have been used frequently in the site investigations at Forsmark and Oskarshamn (Nordqvist 2008) with the main objective to demonstrate and investigate transport properties of non-sorbing and sorbing solutes in fractures. The SWIW test was carried out in isolated borehole sections representing features with large water-bearing capacity relative the adjacent rock. In a typical SWIW test, one or more tracers are added to the injection water (consisting of natural groundwater sampled prior to the injections) and the tracer breakthrough during the recovery/pump-back phase is evaluated. In the SWIW test with synthetic groundwater reported herein, however, the injection water is prepared so that some of the naturally occurring ions are absent in the tracers solution while other ions are added. Thus, this type of SWIW experiment has the potential to address the out-diffusion of dissolved species from hydraulically stagnant parts of the tested feature. Furthermore, in order to make comparisons with the tracer techniques normally used in SWIW tests it could be valuable if a set of non-sorbing and sorbing tracers are added to the tracer injection solution.

A basic idea with the synthetic SWIW experiment is that a multitude of added and removed tracers with different sorption and diffusion properties will provide data that have potential to give further knowledge about diffusion characteristics in the rock, or whether diffusive transport in stagnant water is important for the tailing often observed in field tracer experiments. An important feature of the synthetic test is that it is carried out with and without a waiting phase (during which the tracers may undergo further diffusion).

Radon-222 ($t_{1/2}$=3.8 d) is a radioactive non-sorbing tracer which is produced from the decay of Ra-226 ($t_{1/2}$=1,600 y) in the rock matrix. It is assumed that it reaches the groundwater by diffusion from the rock pores to the fractures. Since this tracer therefore is continuously produced from the rock matrix, it will not be depleted to the same extent as the other tracers. Therefore, the breakthrough characteristics of this tracer will be different and could possibly provide additional information of the extent of the diffusion from the rock matrix.

SWIW tests with synthetic groundwater were investigated in a feasibility study (Nordqvist et al. 2008). One conclusion of this study was that there may be potential for distinguishing between slow and fast diffusion processes by performing a combination of tests with and without a waiting phase and was also suggested that it is important to use many tracers with different characteristics regarding diffusion and sorption.

Other aspects of the feasibility study were to investigate the possibility to produce a synthetic groundwater with such a low content of the natural groundwater components (chloride, sodium and calcium) that quantification can be made of the diffusion of these species from the matrix pore water to the synthetic groundwater. Also the cost for production of the synthetic water and the whole proposed experiment were investigated.

A number of recommendations regarding the experimental site, tracers and test procedures resulted from the study.

The scoping simulations in the feasibility study show, despite that the studied examples are comprised of simple systems and do not cover all possible combinations of transport domain attributes, that a wide range of tracer behaviour may be expected depending on the relative influences of stagnant zones, rock matrix and sorption in the fracture. Expected results are complex because the induced flow during the injection in the fracture carries tracer away that may have been picked up from stagnant zones and/or the matrix. Tracers with different diffusion and sorption properties may have potential to show differences between different transport geometries. The proposed SWIW experiment presents a possibility to use a relatively large number of tracers with different properties which provides better opportunities to use combinations of tracers to constrain interpretation of experimental results. It should also have the potential to provide valuable opportunities to study a number of interesting aspects regarding SWIW experiments in general. For example, it should be possible to study possible differences depending on which rock volume is tested, i.e. comparing breakthrough from injected tracers with tracers already present in the formation.

The present report presents the results from the main SWIW tests with synthetic groundwater together with some preparatory tests performed at the Äspö Hard Rock laboratory during 2010. The report also presents some basic evaluation and discussion of the results.

1.2 Objectives

The main objective is to increase the understanding of the dominating retention processes in fractured rock. Specifically, experimental data are sought that may provide more information whether fast or slow diffusion processes dominate, i.e. diffusion from stagnant zones or rock matrix, in the studied time and spatial scales.

An additional objective is to obtain supporting information to the SWIW tests performed during the site investigations in Forsmark and Oskarshamn.

1.3 Scope

The scope of the project includes two almost identical SWIW tests in the same borehole section, with the only difference being the waiting period between the injection period and the pump-back period added in one of the tests. The breakthrough curves from the pump-back phase are then compared and evaluated.

Since the site chosen for the experiment was not very well characterised, a number of investigations and preparatory SWIW tests were performed in order to investigate the prerequisites for successfully performing SWIW tests with synthetic groundwater. The preparatory investigations include:

- Capacity (i.e. transmissivity) test.
- Groundwater flow measurements.
- Water sampling and chemical analyses.
- Re-instrumentation of borehole equipment to minimize the experimental volume.

When the preparatory investigations concluded that the site was suitable for performing SWIW tests, a total of three preparatory SWIW tests were performed in order to optimize the performance of the main SWIW tests.

- SWIW test 1: Only one tracer (Uranine); in an injection solution with natural groundwater withdrawn prior to the injection. Without waiting phase.

- SWIW test 2: Only one tracer (Amino-G Acid); in an injection solution with natural groundwater withdrawn prior to the injection. With waiting phase of 48 h.

The preliminary evaluation of the two first preparatory tests indicated that it would be possible to extend the waiting period. Hence, a third preliminary test was carried out.

- SWIW test 3: Only one tracer (Uranine); in an injection solution with natural groundwater withdrawn prior to the injection. With waiting phase of 91 h.

Based on all information from the three preparatory SWIW tests and other investigations, the main synthetic SWIW tests were carried out:

- SWIW test 4: Injection of synthetic groundwater. Without waiting phase.

- SWIW test 5: Injection of synthetic groundwater. With waiting phase 93h.

The two SWIW tests in which synthetic groundwater were injected are referred to as the main tests in this report. The simpler tests performed prior to the main tests using only one tracer added to groundwater sampled prior to the injection are referred to as preparatory SWIW tests.

1.4 Test site

1.4.1 Requirements

The test site should be well characterized, have a low hydraulic gradient (i.e. low background flow) and with no high-conductivity features in the immediate vicinity. The borehole KA2858A was selected based on a review of available boreholes. Since the chosen borehole was not very well characterized a number of tests were performed to test its suitability for SWIW tests. These tests were performed from January to September 2010 and included a capacity test (transmissivity), groundwater flow measurements, re-instrumentation and preliminary SWIW tests. Basic borehole data are presented in Table 1-1 and Table 1-2.

1.4.2 Borehole data

Table 1-1. Borehole data KA2858A (coordinate system ÄSPÖ96).

Northing (m)	7,465.220
Easting (m)	2,221.980
Elevation (m.a.s.l.)	–379.380
Bearing (°)	287
Inclination (°)	–4.3
Diameter (mm)	56

Table 1-2. Basic data for borehole section KA2858A:2.

	Prior to re-instrumentation	After re-instrumentation
Secup (m)	39.77	
Seclow (m)	40.77	
Diameter (mm)	56	
Section volume (L)	1.51	0.65
Volume circulation loop (L)	2.51	0.95
Distance to tunnel (m)	34	
Position of anomaly (m)	40.23	

1.4.3 Geology

Borehole KA2858A is, together with borehole KA2862A, situated in the so called Rex Block (Figure 1-1) 2,860 m down in the Äspö tunnel, 380 m below the ground surface. The mineralogy of the core and fracture fills has been studied in detail by The British Geological Survey (West et al. 1997) from where the information below is gathered.

The REX Block is situated in a lithological transition between Småland Granite, dominating above 2,845 m in the tunnel, and Äspö Diorite/fine-grained granite, which dominates between 2,845 and 2,890 m. Except for a thin pegmatite vein, the bedrock mapping of the REX Block shows exclusively Äspö Diorite.

The borehole KA2858A is 59.7 m long with orientation 287°/–4.3° (bearing relative to the local north of Äspö). The lithology is dominated by Äspö Diorite (62.3%), but sections of both fine-grained granite (25.6%) and Småland Granite (12.1%) are encountered.

A total of 285 apparently open fractures are mapped in KA2858A, the majority of them in the interval 0–10 m. Only 19 of them are considered to be potentially flowing fractures. They intersect the borehole with orientation N20E and have fracture coatings of epidote and chlorite. The core in this interval is partly strongly foliated, the minerals are chloritised wallrock.

At 40.17 m borehole length, there is a sub-parallel fracture with orientation N65W, which is with certainty characterized as a flowing fracture. The fracture coating is calcite, chlorite and iron hydroxide. This fracture is followed by a group of calcite- and chlorite-coated fractures, in the interval 40.9–41.4 m, with the same orientation.

The last part of the core, exceeding 58 m borehole length, is strongly foliated with epidote-, chlorite- and iron hydroxide-filled fractures orientated N20E. One of these is parallel to the core in the interval 58.10–58.50 m. Oxidation, chloritisation and hematite alteration is noted in the interval 58–59.7 m.
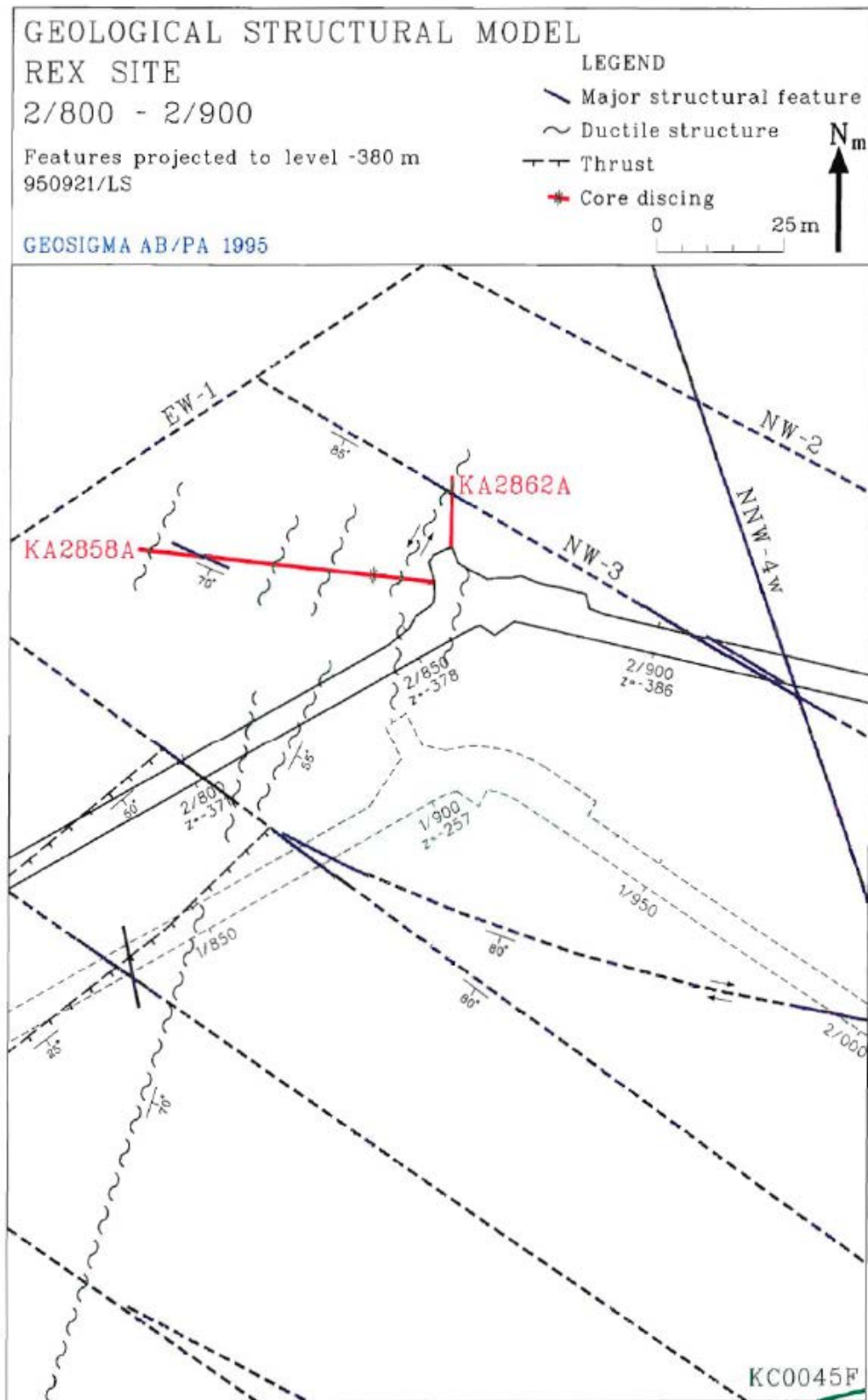
Figure 1-1. *Structural geological model of the REX Block.*

2 SWIW tests

2.1 Basic principles

In a SWIW (Single-Well Injection-Withdrawal) test, water with one or several tracers is injected into a rock formation and later pumped back. The tracer breakthrough during the pump-back phase (recovery phase) may then provide information about solute transport properties of the rock formation.

A SWIW tracer test may consist of all or some of the following phases:

1. Injection of fluid to establish steady state hydraulic conditions.

2. Injection of one or more tracers.

3. Injection of chaser fluid after tracer injection is stopped, possibly also label the chaser fluid with a different tracer.

4. Waiting phase.

5. Recovery phase with back-pumping of the previously injected tracer.

The injection of chaser fluid has the effect of pushing the tracer out as a "ring" in the formation surrounding the tested section. One advantage of employing a chaser fluid is that when the tracer is pumped back, a complete recovery breakthrough curve with a rising part, a peak and a decreasing part is obtained. During the waiting phase there is no injection or withdrawal of fluid. The purpose of this phase is to increase the time available for time-dependent transport-processes so that these may be more easily evaluated from the resulting breakthrough curve.

A schematic illustration of resulting breakthrough curve during a SWIW test, with and without a chaser injection phase, is shown in Figure 2-1.
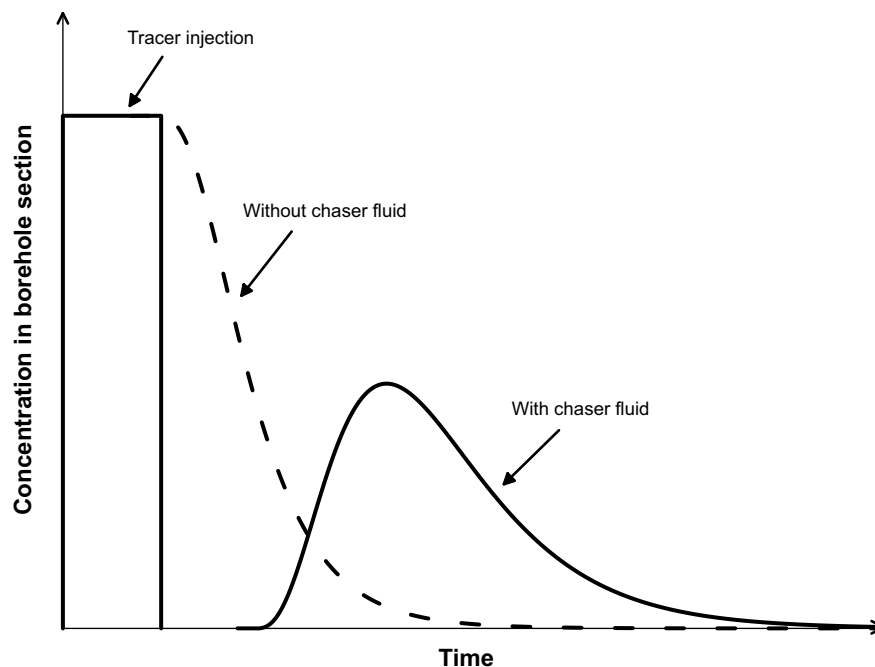

Figure 2-1. *Schematic tracer concentration sequence during a SWIW test, showing tracer recovery curves with and without chaser fluid injection.*

SWIW tests differ significantly in several ways from cross-hole tracer tests. Cross-hole tracer tests generally involve more extensive planning and supporting field tests than SWIW tests. SWIW tests are therefore less costly and may be employed in a larger number of borehole sections. The experimental scale in each method represents a major conceptual difference. In SWIW tests, only the rock volume adjacent to the borehole section is involved. The extent of the tested volume is given by how far the injection water has travelled along conductive features out into the formation before the beginning of the recovery pumping phase. However, this cannot be determined without additional borehole sections sufficiently close to the SWIW section. In cross-hole tests, it is reasonable to expect that the tested domain is comprised of connected transport paths between injection and pumping sections.

Perhaps the most significant attribute of a SWIW experiment compared to a cross-hole test, is the reversibility of the flow field. Thus, under ideal conditions, an injected tracer moves away from the borehole section and then back again along the same flow path(s). The flow reversibility that occurs in a SWIW test affects the interpretation of transport processes. For example, unlike for cross-hole tests, advective attributes such as fracture aperture (or porosity) and longitudinal dispersivity may not be determined independently from a SWIW test because of the unknown tracer travel distance (Becker and Shapiro 2003). Even if the porosity (or e.g. aperture) is independently known, dispersivity values evaluated from SWIW tests should be expected to be different from values evaluated from other types of tracer tests because the reversal of the flow field obscures the dispersion resulting from flow paths with different velocities (Gelhar et al. 1992).

A few basic theoretical properties of a SWIW experiment are presented below in this section. Further theoretical aspects under slightly more complicated conditions are provided in connection with analysis of results in Chapter 6.

During injection of water with a flow rate Q_{inj} [L^3/T] in a borehole section located in a homogenous planar fracture with aperture δ [L], and assuming negligible background flow, the velocity v(r) [L/T] as function of radial distance r [L] is given by:

$$v(r) = \frac{Q_{inj}}{2\pi r\delta}$$

(2-1)

The radial distance, measured from the borehole centre, an injected particle travels for a given volume of injected water, V_{inj} [L], is given by:

$$r = \sqrt{\frac{V_{inj}}{\pi\delta} + r_w^2}$$

(2-2)

where r_w is the borehole radius [L].

Because the volume which the water travels through (i.e. the aperture) during a SWIW test is not known, the radial travel distance cannot not be determined (unless other observation wells are present). However, a plausible travel distance range is illustrated in Figure 2-2 for a range of apertures from 0.0001 to 0.01 m and a total injected volume of 30 L (approximately the injected volumes in the synthetic SWIW tests described in this report). Figure 2-2 indicates that a radial travel distance (i.e. the outer edge, in the absence of dispersion, of the injected tracer volume at the end of the injection phase) is in the range of a few metres up to about 10 metres.

Effects of dispersion are expected to be significantly smaller in SWIW tests than in cross-hole tracer tests. Variability in travel times along transport paths in cross-hole tests cancels out in SWIW tests because of the flow reversal.
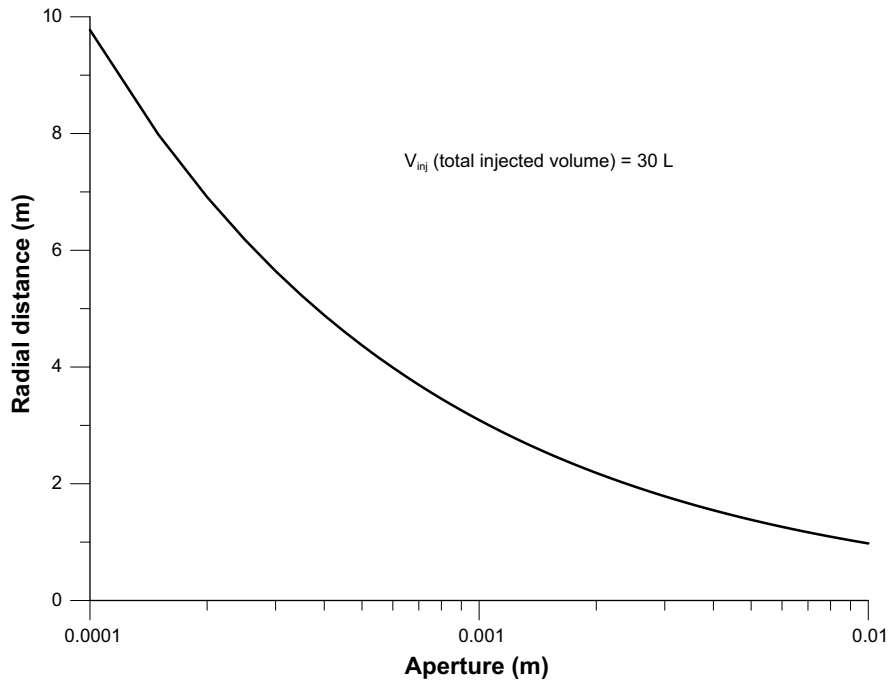
Figure 2-2. *Advective radial travel distance as a function of fracture aperture.*

Assuming that the dispersion effect can be described with a constant dispersivity a_L [L] and that molecular diffusion is negligible the governing equation for radial solute transport with advection and dispersion as the only transport processes may be written as (Lee 1999):

$$R_f \frac{\partial C}{\partial t} = -\frac{B}{r}\frac{\partial C}{\partial r} + \frac{a_L B}{r}\frac{\partial^2 C}{\partial r^2}$$

(2-3)

where $B = Q/2\pi\delta$ and R_f is the fracture retardation factor [–].

Considering only the processes of advection and dispersion in a homogenous system, the shape of the breakthrough curve is determined by a single parameter, herein called φ, given by Becker and Shapiro (2003) and Gelhar and Collins (1971):

$$\varphi = \frac{\delta a_L^2}{V_{inj}}$$

(2-4)

where V_{inj} is the total injected volume [L^3]. The aperture may alternatively be expressed as the product of porosity and thickness. In a homogenous radial flow system with advection and dispersion as the only transport processes, this single effective parameter determines the shape of the SWIW breakthrough curve.

The synthetic groundwater injected in the SWIW experiment described in the present report is made up by adding tracers as well as removing tracers (i.e. dissolved chemicals present in the native groundwater). Simulated SWIW recovery breakthrough curves for added and removed tracers, respectively, are shown in Figure 2-3 for varying values of the dispersion parameter, φ. The simulations are made using SUTRA with a one-dimensional radial flow and transport system, i.e. with the radial distance as the only space coordinate. The innermost nodes are located at the borehole radius. The tracer injection is simulated by a constant inflow with a specified concentration in the inflowing water. Immediately following the injection period, the water is pumped back. The example is for a case without a waiting phase, but in this case a waiting phase would give identical results, only with a translation in time.
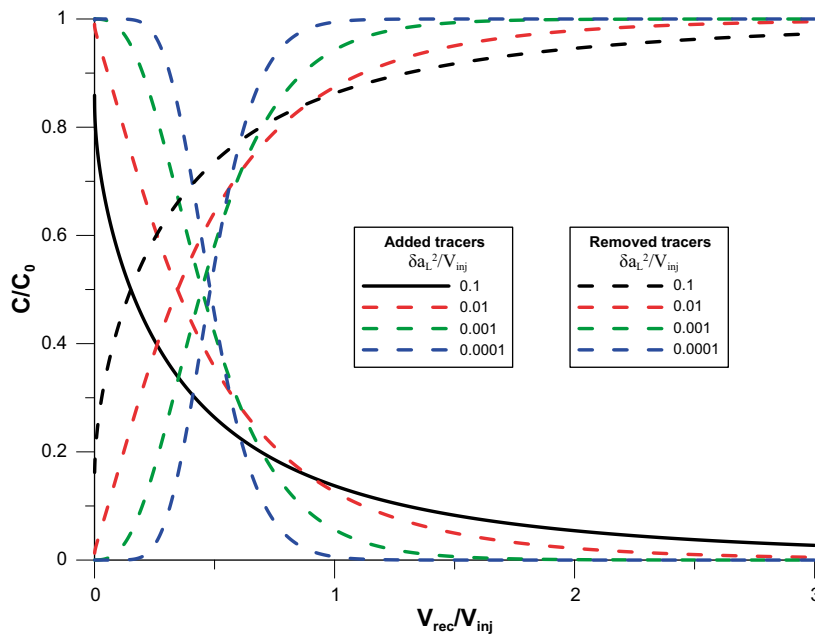
Figure 2-3. *Theoretical recovery breakthrough curves for added and removed tracers, respectively, assuming homogenous radial transport with advection and dispersion as the only transport processes.*

To what extent dispersion processes contribute to the shape of the recovery breakthrough curve in a SWIW experiment is not entirely clear. In a cross-hole tracer experiment, a large component of the dispersive effects is usually attributed to velocity variations among individual flow paths, which may be partly or fully independent, connecting the injection and sampling sections, respectively. In a SWIW experiment, this effect would not occur because of the flow reversibility. Tracers injected into fast as well as slow flow paths, and assuming that the flow paths are independent, would return to the SWIW section at the same time, contrary to a cross-hole test.

In individual flow paths, which is here taken to mean a continuous flow domain of arbitrary dimension, some dispersive spreading would also be expected to occur. In laminar flow between two parallel plates, a parabolic cross-sectional velocity profile develops. Combined with molecular diffusion, this mechanism causes so called Taylor dispersion. A thorough analysis of the effects of various forms of Taylor dispersion on SWIW tests in fractures is given by Neretnieks (2007).

Another mechanism that may add to dispersion is heterogeneity in fluid velocities within a flow path, caused by variation of fracture aperture and/or fracture roughness. In this case, the dispersive effect depends on the geometrical characteristics of the fracture plane within the flow path. Becker and Shapiro (2003) consider heterogeneous advection in a multiple flow paths that gives effects on SWIW recovery curves because of different dispersion characteristics within each flow path.

These dispersion mechanisms would be expected to occur simultaneously and not be reversible during a SWIW experiment. Thus, some dispersive effects would be expected to influence the recovery curve in a SWIW tests, although the effect would be expected to be smaller than in cross-hole tracer experiments.

The effect of linear equilibrium sorption, expressed through the fracture retardation factor R_f in Equation 2-3, is somewhat trivial as the effect may not be distinguished from the effect of dispersion (Figure 2-4). Thus, the retardation factor for a sorbing tracer may only be determined if non-sorbing tracer is used simultaneously, which is analogous to evaluation of sorbing tracers in cross-hole tests (Schroth et al. 2001).

Further generic simulations are presented in connection with discussion of results in Chapter 6.
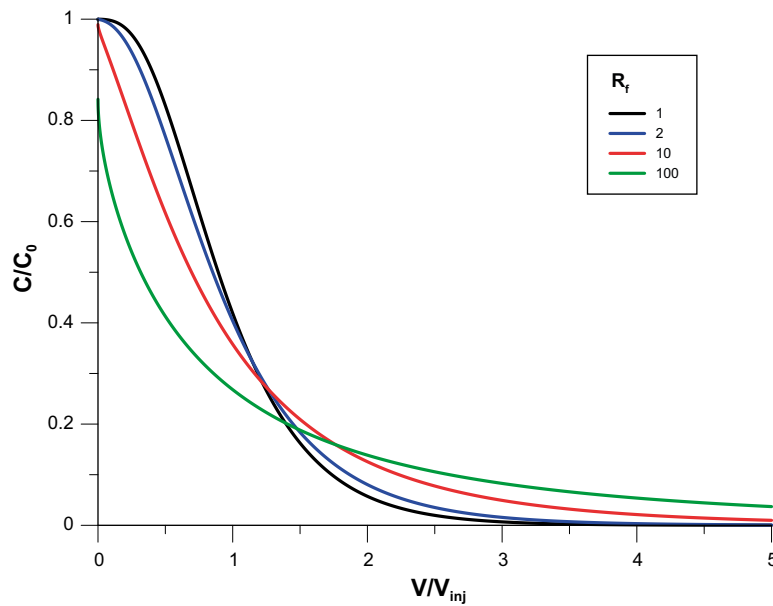
Figure 2-4. *Theoretical SWIW recovery breakthrough curves (added tracers) for varying fracture retardation factors, assuming a radial advection-dispersion transport model.*

2.2 Previous SWIW experiments in fractures

SWIW experiments were first developed and employed within the oil industry to estimate residual oil saturation in the rock (e.g. Tomich et al. 1973). Early developments of the single-hole tracer testing in the field of hydrogeology concerned estimation of advective parameters such as porosity and dispersivity. Methods to estimate longitudinal dispersivities from SWIW tests have been presented by Gelhar and Collins (1971). Extensions to single-well tracer tests in stratified aquifers with layers of different hydraulic conductivity, which would correspond to two or more conductive fractures in the same isolated borehole section, were presented by Pickens and Grisak (1981), Güven et al. (1985), and Molz et al. (1985). Advective heterogeneity in fractured rocks was accounted for by applying a channeling concept to Mirror Lake SWIW test data (Becker and Shapiro 2003).

SWIW tests have, in hydrogeological studies, also been used to study other processes than advection and dispersion. Schroth et al. (2001) provides a discussion of the determination of sorption attributes for a few simple cases of equilibrium and non-equilibrium sorption in a radial flow system. Drever and McKee (1980) used the Langmuir isotherm to evaluate adsorption parameters in a uranium formation from SWIW test data.

There are a number of studies of particular interest for the synthetic SWIW experiment, and for investigations concerning disposal of nuclear waste in fractured rock in general, that investigate time-dependent solute processes using SWIW tests. Tsang (1995) studied matrix diffusion effects and possibilities to identify this process in the presence of spatial heterogeneity by a comparison of SWIW tests, radially converging tracer tests, and dipole tracer tests. Haggerty et al. (2000, 2001) applied more elaborate models of multiple-rate mass transfer between mobile and immobile zone models for SWIW test data. Solute exchange with immobile regions during SWIW tests was also investigated by Gouze et al. (2008).

Background hydraulic gradients, and thereby a background groundwater flow through the borehole section, across the tested rock volume may be a disturbing factor for a SWIW test. Such background flow may cause the injected tracer to drift away during the duration of the test. A significant gradient may make it difficult to pump back all, or any, of the tracer during the recovery phase. Lessoff and Konikow (1997) present a numerical simulation study of the combined effect of several factors on the interpretation of SWIW tests. They studied how the combination of heterogeneity, natural gradient and hydrodynamic dispersion affects the possibilities of identifying/quantifying matrix diffusion. Their

results suggest that the combination of heterogeneity and existing natural gradient may disturb the theoretical reversibility of SWIW tests. Altman et al. (2002) extended this by including matrix diffusion, heterogeneity, and gradient in a single simulation model and suggested that difficulties in interpreting SWIW tests increase with combinations of low porosity, high gradient and high heterogeneity.

Within the Swedish site investigation program, a number of SWIW experiments have been performed at Oskarshamn and Forsmark (Nordqvist et al. 2012b, Nordqvist 2008). The purpose of these was to determine solute transport properties in fractures or fracture zones at typical repository depths (300–700 m) and with moderately high transmissivity values (10^{-8}–10^{-6} m^2/s). The selection of experimental borehole sections was made with the intention to test a variety of geological environments: single fractures, multiple fractures, or fracture zones. Selection of borehole sections for SWIW experiments were based on extensive geological, geophysical, and hydraulic investigations in each borehole.

A total of 12 SWIW experiments (six at each site) were carried out within the site investigation programs. The tests were typically carried out with a 1–2 hour tracer injection period followed by a 10–20 hour period of chaser fluid injection. Total injected water volumes ranged approximately between 100 to 340 L. The length of the test sections varied between 1 and 5 m. In each test, Uranine was used as a non-sorbing tracer, and cesium and rubidium (except in three of the tests) as sorbing tracers.

In general, the SWIW tests within the site investigations showed high tracer recovery. Although recovery pumping usually did not continue long enough for the breakthrough curves to reach background values, it was concluded that full recovery generally would have been obtained with continued recovery pumping.

The background groundwater flow in connection with site investigation SWIW tests were estimated using dilution tests. The background flow rates were generally low, especially in comparison with the experimental injection and pumping flow rates.

The results from SWIW tests within the site investigation program have also been analysed (Cvetkovic and Cheng 2011) and three of the tests have been analysed by Doughty and Tsang (2009).

Two SWIW tests were also performed at the TRUE-1 site at the Äspö HRL (Nordqvist et al. 2012a). The original experimental plan for these tests included the use of sorbing and radioactive tracers. However, because of very low tracer (Uranine) recovery in the preparatory tracer tests, radioactive/sorbing tracers were never used. Despite this, an interesting set of data was obtained including tracer breakthrough curves in four peripheral boreholes sections as well as in the central SWIW section. The observations of tracer response in the surrounding borehole sections are of considerable interest as observations in adjacent borehole sections have not been possible for the SWIW tests carried out within the site investigation programs (described above). The TRUE SWIW test results are therefore somewhat unique in this respect and provide evidence of tracer spreading during a SWIW test. The results from the observation sections demonstrate the heterogeneous nature of the radial solute spreading during the water injection phase. Tracer residence times as well as peak tracer concentrations in the various observation sections vary by at least one magnitude.

A possible explanation of the low recovery in the TRUE-1 SWIW tests is the presence of a highly conductive feature in the influence area of the tests that may have transported the tracer too far away from the test section before the pumping phase. The proximity of the experimental feature at the TRUE-1 site to the tunnel wall may have contributed to the low recovery in the tests.

3 Execution and equipment

As no previous hydraulic characterisation has been made of borehole KA2858A, some tests were carried out in order to determine the suitability of the site for the planned SWIW tests with synthetic groundwater. First, a hydraulic capacity test was performed and the flow was logged in a HMS channel. Further, the background groundwater flow was determined using dilution measurements. Water samples were collected during the process in order to characterise the water chemistry of the section, and also to characterise possible variations in time. A re-instrumentation of the borehole was performed to decrease the section volume and to shorten measurement times. Three preparatory SWIW tests were carried out, one without waiting period between injection and re-pumping and two with a waiting period (48 and 91 hours, respectively). Finally, the main SWIW tests with synthetic groundwater were performed, one with and one without a waiting phase. The main experimental events are summarized in Table 3-1.

Table 3-1. Main experimental events.

Event	Start date	Stop date	SKB sample number
Capacity test	2010-01-27 10:00	2010-01-29 12:00	
Groundwater flow measurement 1 (natural conditions)	2010-02-02 12:00	2010-02-09 13:59	
Groundwater flow measurement 1 (stressed conditions)	2010-02-09 14:12	2010-02-15 13:00 *	
Chemical sampling (3 samples)	2010-01-27	2010-01-29	20069, 20070, 20071
Re-instrumentation	2010-03-15 13:20	2010-03-15 19:12	
Groundwater flow measurement 2 (natural conditions)	2010-03-31 10:17	2010-04-07 09:28	
SWIW 1	2010-04-07 13:31	2010-04-19 11:35	
SWIW 2	2010-04-26 21:40	2010-05-19 12:55	
Chemical sampling (4 samples)	2010-03-15	2010-04-26	20106, 20107, 20108, 20109
Groundwater flow measurement 3 (natural conditions)	2010-09-09 08:42	2010-09-15 13:38	
SWIW 3	2010-09-16 11:36	2010-09-27 08:34	
SWIW 4	2010-11-02 21:24	2010-11-24 16:01	
SWIW 5	2010-11-25 10:40	2010-12-20 18:00	
Chemical sampling (5 samples)	2010-10-26	2010-12-20	20447, 20448, 20449, 20450, 20451
Groundwater flow measurement 4 (natural conditions)	2010-12-21 09:43	2010-12-29 08:00	

* The measurement was stopped due to a power failure, the exact time is not known.

3.1 Supporting tests in KA2858A

3.1.1 Capacity test

The capacity test was carried out with a flow period lasting for 48 hours. The flow rate from the test section was kept constant at 23.5 mL/min using a flow meter with a regulation unit. The flow rate was logged in a HMS-channel. The basic test data is shown in Table 3-2.

During the test, the pressure responses were registered in the borehole section as well as in surrounding boreholes. For boreholes connected to the HMS-system within 100 m from KA2858A, the plan was to increase the logging frequency to be able to detect very fast responses. Pressure data from borehole sections within 300 m were checked for responses from the capacity test.

Table 3-2. General test data for the capacity test in KA2858A, section 39.77–40.77 m.

Start flow period	2010-01-27 10:00:28
Stop flow period	2010-01-29 10:10:12
Stop recovery period	2010-01-29 12:00:00
Duration flow period (min)	2,890
Duration recovery period (min)	110
Q_m (mL/min)	23.5
Q_p (mL/min)	23.6
P_i (kPa)	3,124.03
P_p k(Pa)	2,933.33
P_f (kPa)	3,121.57
dP ($P_i - P_p$) (kPa)	190.69
S (m)	19.43

3.1.2 Groundwater flow measurements

Determination of the background groundwater flow through the experimental section was made using dilution tests at four occasions during the experimental program. A principal drawing of the experimental setup is shown in Figure 3-1. The tracer dye Uranine (50 ppm) was used in one of the measurements, whereas in the other three, Amino-G Acid (100 ppm) was used.

During the time period required to circulate one section volume the tracer was injected with a flow rate corresponding to 1/100 of the circulation flow rate. This implies a dilution of about 1/100 of the tracer solution, and that the theoretical initial concentration in the section should be about 0.5 ppm (Uranine) or 1.0 ppm (Amino-G Acid). Injection times and flow rates are presented in Table 3-3.

Continuous sampling was carried out during circulation by extracting a constant small flow (constant leak). The samples were collected using a fractional sampler. Depending on the sampling interval used, the sampling flow rate was adjusted so that a suitable sample volume (c. 6 ml) was collected in each sample tube. The sampling intervals and sample flow rates are found in Table 3-4.
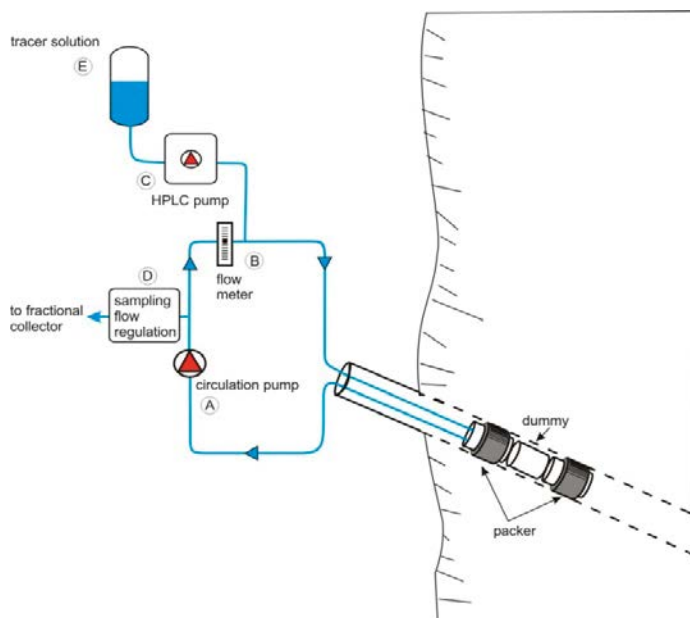

Figure 3-1. *Principal drawing of the experimental setup of groundwater flow measurements with the dilution technique.*

Table 3-3. Injection data for dilution tests 1–4 in KA2858A, 39.77–40.77 m.

	1	2	3	4
Volume (section + hoses) (L)	2.51	0.95	0.95	0.95
Circulation flow (L/h)	10	10	7	10
Injection flow (mL/min)	1.67	1.67	1.67	1.67
Injection time (min)	15	11	15	11
Start injection	2010-02-02 12:00	2010-03-31 10:17	2010-09-09 08:42	2010-12-21 09:43
Stop injection	2010-02-02 12:15	2010-03-31 10:28	2010-09-09 08:57	2010-12-21 09:54
Tracer	Uranine	Amino-G	Amino-G	Amino-G
Wanted initial conc. in section (ppm)	0.5	1.0	1.0	1.0
Injected volume (mL)	26.3	18.4	25	18.4
Injected mass (mg)	13.2	1.84	2.44	1.84

Table 3-4. Sampling intervals and flow rates.

Test	Sampling flow rates (mL/h)	Sampling intervals (min)
1	1.5	120
1	3.5	60
2	3.3	120
3	3.5	120
4	1.5	120

Groundwater flow measurement 1

The measurement period was about one week and the sampling interval was generally 120 minutes. After measuring the groundwater flow under natural conditions during one week, the adjacent borehole KA2862A was opened and the measurements continued for another week in order to check whether the groundwater flow in the test section was affected by the hydrological disturbance caused by the flow out (about 800 mL/min) from borehole KA2862A. No automatic regulation equipment was used; instead the flow rate was manually adjusted and measured using a watch and a measurement cylinder. The flow rate was relatively constant during the whole period. The drawdown in KA2858A was 153 m (1,530 kPa). During the first days of the measurement period the sampling flow rate for the dilution measurement was set to 60 minutes (in order to ensure enough data in case of very quick dilution) and thereafter 120 minutes. In the test section KA2858A, a small pressure response of 1.5–2 kPa occurred at the opening of KA2862A.

Groundwater flow measurement 2

The measurement period was about one week and the sampling interval was 120 minutes. Due to problems with the sampling equipment, data is missing from one part of the measurement period. However, this did not significantly affect the evaluation of the test.

Groundwater flow measurement 3

During the third dilution measurement the equipment was incorrectly connected, which led to too high concentrations in the samples. On the circulation line, the samples were extracted before the labelled water was allowed to circulate through the borehole section, just after the injection. This also implies that there is a risk that concentrated tracer solution has been leaking (diffusing) into the withdrawn samples during the whole measurement period and increased the concentration in the samples. In this case the measured dilution will be slower than the actual dilution, and the interpreted ground water flow rates will be underestimated.

Groundwater flow measurement 4

The measurement period was about one week and the sampling interval was 120 minutes. Due to problems with the equipment, the sample flow rate varied a lot and some sampling tubes were even found to be empty. The data points are more scattered, which leads to greater uncertainty in the interpreted flow rate.

3.1.3 Water sampling

The only information prior to the synthetic SWIW experiment about the water chemistry conditions in borehole KA2858A was from 1995. Series of water samples were collected during the various experimental phases. Dates, times and sample numbers for all samples are presented in Table 3-5.

Table 3-5. Water sampling occasions in KA2858A, 39.77–40.77 m.

Date	Start	Stop	SKB nr	Pumped volume (L)
2010-01-27	11:05	13:00	20069	1.83
2010-01-28	09:25	10:49	20070	33.6
2010-01-29	08:45	10:04	20071	65.9
2010-03-15	10:25	12:45	20106	0.52
2010-03-16	08:50	09:22	20107	0.76
2010-03-29	19:07	19:29	20108	1.7
2010-04-26	16:58	17:28	20109	674
2010-10-26	11:54	13:22	20447	13.2
2010-11-03	11:00	12:10	20448	8.2
2010-11-24	10:10	11:20	20449	1,517
2010-11-29	21:36	23:10	20450	9.4
2010-12-20	16:00	17:15	20451	1,505

The first series of three samples were collected during the capacity test (just after start of the flow period, in the middle of the flow period and at the end of the flow period, respectively). The objectives were to collect information about the water chemistry conditions necessary for preparing a synthetic groundwater and also to check the stability of the chemical composition with time. The samples were analyzed according to SKB class 3 with the additional parameters Cs and Rb.

The second series consist of four samples taken in conjunction with the re-instrumentation and the first preparatory SWIW test. The objectives were to control the stability of water chemistry with time, appraisal of the risk for microbial growth when adding large amounts of nitrate (using the sulphide concentration as an indicator), and to determine background levels for components planned to be used in the synthetic groundwater (i.e. Cs and Rb). The samples were analyzed according to SKB class 3 with the additional parameters Cs, Rb, nitrate and sulphide.

During the main tests a series of five samples according to SKB class 3 (with additional parameters Cs, Rb, nitrate, sulphide and microbiological analysis) were collected. The aim was to monitor the water chemistry during the test which might give supportive information when evaluating the main SWIW results. The first sample was taken just before the start of SWIW test 4, the second after about 3 hours recovery pumping and the third just before ending SWIW test 4. The fourth sample was collected after three hours of recovery pumping in SWIW test 5 and the last one just before SWIW test 5 was ended.

3.1.4 Re-instrumentation

In order to minimize the experimental volume (section and hoses), a dummy was installed in the experimental section and the dimension of tubing was changed from 6/4 (outer diameter [mm]/inner diameter [mm]) to 4/2. The existing equipment that was removed from the borehole (and subsequently partly replaced and complemented with new equipment) was in good condition and not corroded. Some oxides were present but in no remarkable amounts. The left photograph in Figure 3-2 shows

the section between the packers a few minutes after the equipment was removed from the borehole. The largest amounts of oxides were present in the upper part of the borehole (near the tunnel wall), as shown in Figure 3-3 but since the whole equipment passed through that sector when it was removed from the borehole it is somewhat difficult to know exactly the amounts of oxides present between the packers prior to the synthetic SWIW experiments.

The right photograph in Figure 3-2 shows the section between the packers after installation of a dummy.

Figure 3-2. *The left photograph shows the section between the packers a few minutes after the equipment was removed from the borehole and prior to the dummy installation.The right photograph shows the same section with the dummy installed.*

Figure 3-3. *The upper part of the existing equipment (near the tunnel wall) when it was removed from the borehole. The white coating is oxide.*

3.2 Synthetic groundwater and tracers

The chemical composition of the synthetic groundwater was prepared by substituting some of the naturally occurring ions with other ions, while maintaining the ionic strength of the groundwater in the formation around the experimental borehole section. The following substitutions were made:

- Na^+ was replaced by Li^+
- Ca^{2+} was replaced by Mg^{2+}
- Cl^- was replaced by NO_3^-
- K^+ was replaced by Rb^+ and Cs^+

In addition, Uranine was added and the synthetic water is also radon free. Thus, the injected synthetic groundwater may be characterized by Na, Ca, Cl, K and radon as removed tracers and Uranine, Li, NO_3, Mg, Cs and Rb as added tracers. The synthetic groundwater also contained ions of Sr, Br and SO_4 but these were not utilized as tracers (i.e. analysed during the recovery pumping phase). The composition of the synthetic groundwater is summarized in Table 3-6 (see Appendix 2 for comparison with the chemical composition of the ambient formation groundwater).

The synthetic groundwater was prepared at CLAB (SKB's interim storage facility for spent nuclear fuel), where large quantities of distilled water of high quality are available. About 70 litres of the synthetic water was prepared by mixing various salts, nitric acid and Uranine in distilled water. The synthetic water was stored and shipped in 10 L plastic containers.

Table 3-6. Composition of the synthetic groundwater.

Species	Theoretical (mg/l)	Analysis (mg/l)
Cl^-	0	< 0.2
Na^+	0	1.4
Ca^{2+}	0	< 2
K^+	0	< 4
NO_3^-	24,000	
Li^+	1,010	1,018
Mg^{2+}	2,990	3,150
Rb^+	27.5	29.6
Cs^+	4.76	4.87
Uranin	5.0	6.2
Sr	94	–
Br	109	106
SO_4^{2-}	615	–

– Not analysed.

3.3 Preparatory SWIW tests

3.3.1 General

Three preparatory SWIW tests were carried out in order to test the suitability of the selected experimental borehole section and to test the feasibility of the planned experimental injection and flow rates. Another important purpose was to provide information for deciding what waiting time to use between the injection and the pumping in the main test.

The first test was made with the tracer Uranine and no waiting time, while the second was made with the tracer Amino-G acid and 48 hours between injection and re-pumping. A third test was added based on the results from the first two, this time with Uranine and a 91hours long waiting time. The general principles of equipment and performance are described below. Any variations from these are explained in connection with each test description.

The initial strategy was to inject 15 L of tracer solution during 10 hours using a flow rate of 25 mL/min and then pump the water back using the same flow rate and with continuous sampling of the pumped water. The water was injected and pumped back through both the upper and the lower end of the section simultaneously. No circulation was applied. Pressure and flow rates were measured using the HMS.

The equipment consisted of pressurized tracer storage tanks for tracer injection, flow regulation equipment with flow meter, sampling equipment, manometer, plastic tubes and ball valves, see Figure 3-4 and Figure 3-5. The same flow meter and regulation unit was used for injection and withdrawal and the direction of the water was altered by adjusting the positions of the ball valves. No sampling was made during the injection period or the waiting period. The magnetic valve sampler was only used in the first of the preparatory SWIW tests.

The tracer injection was accomplished by applying an overpressure with nitrogen gas (N_2) on two connected pressure tanks (Figure 3-6) instead of using a pump. The tracer solution was pushed into the borehole section through the regulation unit/flow meter where the tracer injection flow rate was regulated.

Two different sampling systems were available: one fractional sampler (collecting a sample over a period of time) and one magnetic valve sampler (collecting momentary samples). Due to problems with the magnetic valve sampler it was only used in the first SWIW test. The samples from the fractional sampler were used for all tests. Samples were taken during the whole pumping period, more frequently in the beginning.

A web camera was installed and used for supervising the test and alarm functions for power failure or large variations in the system pressure. A power supply (UPS) was also connected to ensure operation of the most important equipment parts (sampler and regulation unit) in case of a power failure.
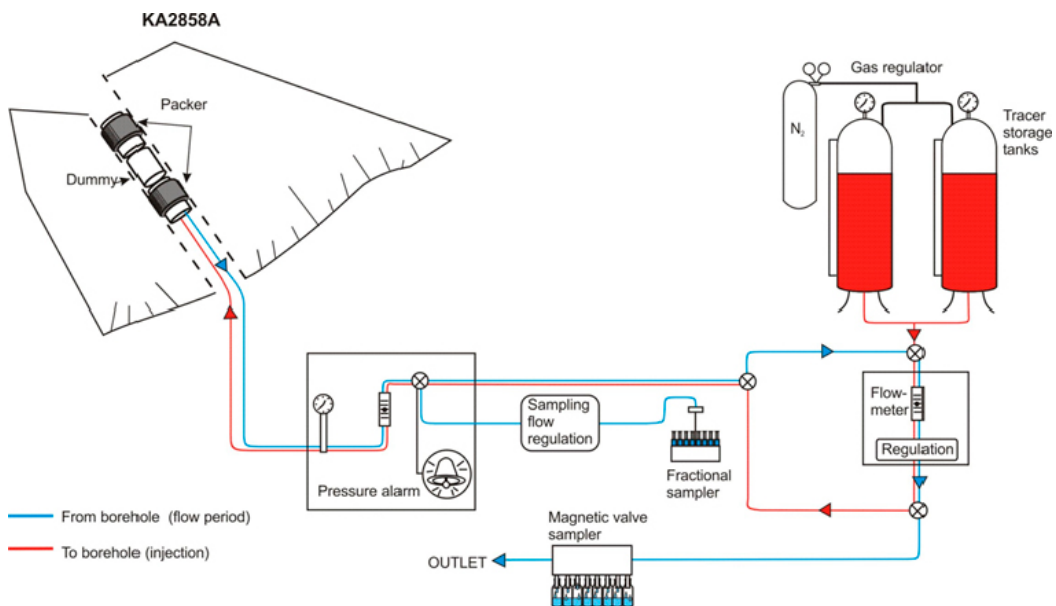

Figure 3-4. Schematic drawing showing the experiment during the preparatory SWIW tests (SWIW 1, SWIW 2 and SWIW 3). The ball valves were used to alter the flow direction allowing the water to flow either according to the red lines, or according to the blue lines.
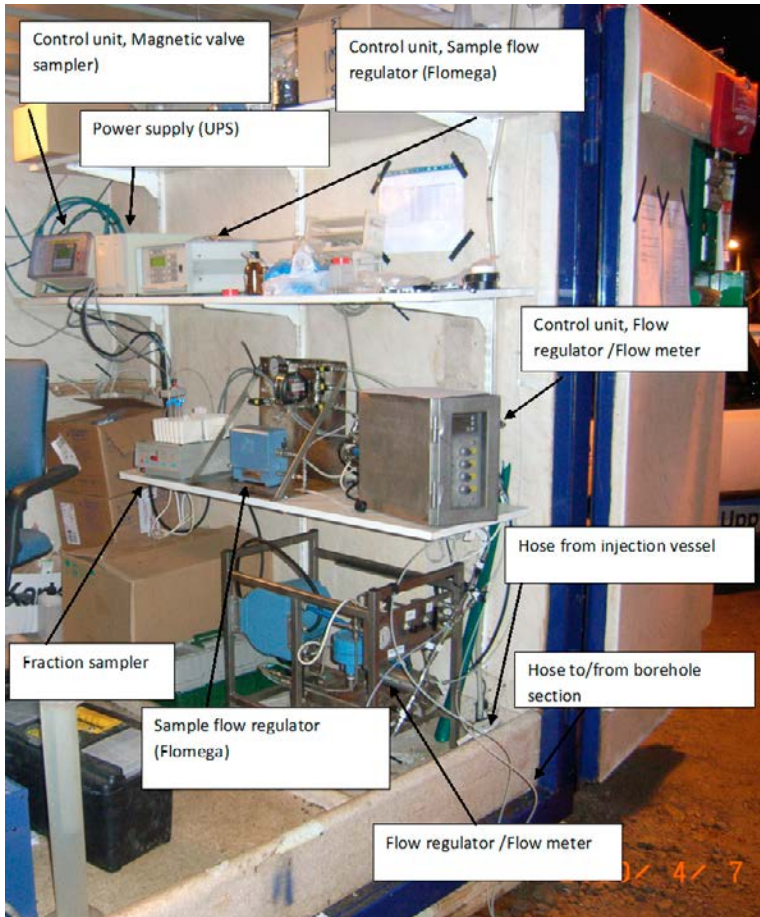
Figure 3-5. *Overview of the equipment used in the SWIW tests.*

Figure 3-6. *Pressurized tracer tanks and gas tube (N₂) used during tracer injection.*

General test data and pressure data during the preparatory SWIW tests are found in Table 3-7 and Table 3-8.

3.3.2 SWIW test 1

The actual flow rates, injection times and tracer concentrations used in the first SWIW test is presented in Table 3-8. After the injection period the flow direction was immediately reversed (no waiting period applied).

General test data and pressure data during SWIW test 1 are found in Table 3-7 and Table 3-8. The flow rate and pressure registrations are shown in Figure 3-7. Sampling intervals and sampling flow rates are given in Table 3-9.

Table 3-7. Pressure data for preparatory SWIW tests.

	Unit	SWIW 1	SWIW 2	SWIW 3
P (before injection start)	kPa	3,120	3,120	3,126
P (at stop of injection)	kPa	3,280	3,220	3,246
dP (pressure increase)	kPa	160	100	120
P (normal pressure in section)	kPa	3,120	3,120	3,128
P (end of flow period)	kPa	2,950	2,870	2,955
dP(pressure decrease)	kPa	170	250	173

Table 3-8. General test data for preparatory SWIW tests.

|	SWIW 1 Uranine	SWIW 2 Amino-G Acid	SWIW 3 Uranine
Start injection	2010-04-07 13:31	2010-04-26 21:40	2010-09-16 11:36
Stop injection	2010-04-07 23:31	2010-04-27 07:40	2010-09-16 21:36
Injection flow rate, start (mL/min)	–	29.5	28.3
Injection flow rate, stop (mL/min)	–	26.0	28.9
Injection flow rate, mean (mL/min)	28.4	28.5	28.5
Injection time (h)	10	10	10
Waiting time (h)	0	48	91
Theoretical initial concentration, C0 (ppm)	5.00	10.0	5.00
Measured initial concentration C0 (ppm)	5.02	9.6	4.92
Injected volume (water) (L)	15.6	16.3	16.9
Injected mass (tracer) (g)	0.078	0.157	0.082
Start withdrawal, sampling	2010-04-07 23:31	2010-04-29 08:00	2010-09-20 16:42
Flow rate (flow period) (mL/min)	29	Varying, then 29	28
Stop measurement.	2010-04-19 11:35	2010-05-19 12:55	2010-09-27 08:34
Length sampling period (h)	276	475	160
$C_{backgrund}$ (tracer) (ppb)	3	6	10.5
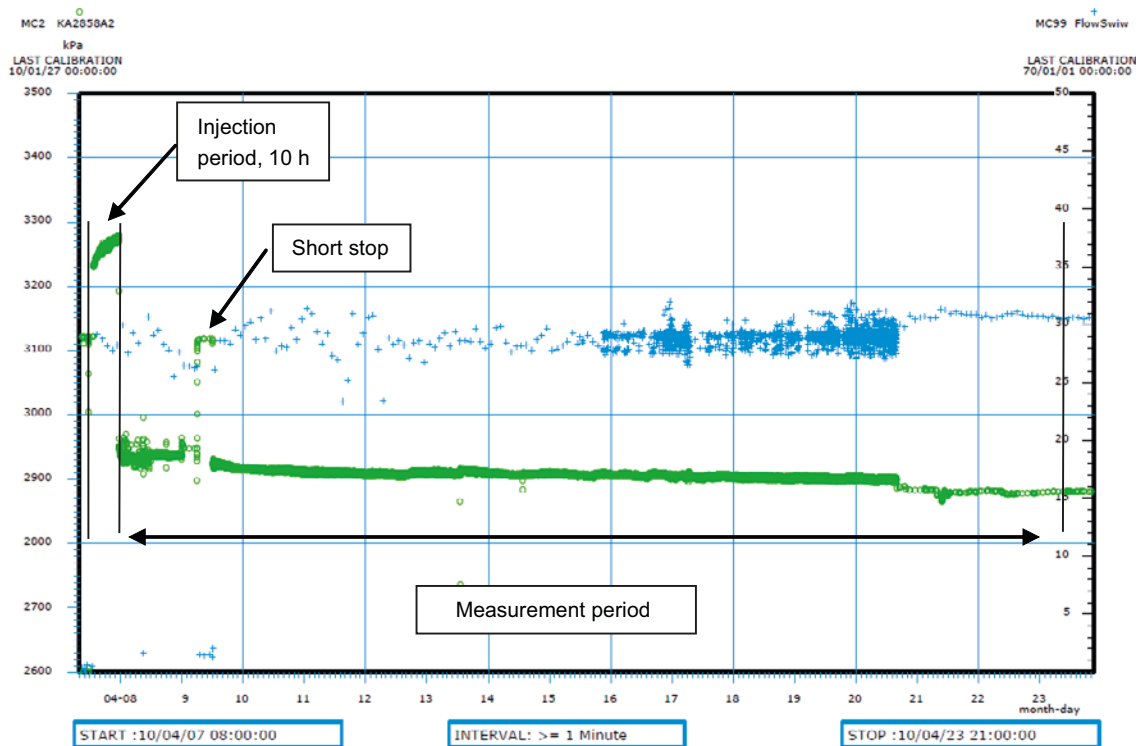
Figure 3-7. Pressure (green o) and flow rate (blue +) during SWIW test 1.

Table 3-9. Sampling intervals and sampling flow rates during SWIW test 1.

Time after flow period start	Sampling flow rate Fractional sampler	Sampling interval Fractional sampler	Sampling interval Magnetic valve sampler
0–12 h	18 mL/h	15 min	30 min
12–160 h	4.48 mL/h	60 min	6 h
160–275 h	2.4 mL/h	120 min	6 h

3.3.3 SWIW test 2

The second SWIW test was carried out in the same way as the first, except that a waiting period of 48 h was added between the injection and the withdrawal period and that the tracer was Amino-G Acid instead of Uranine. Before the injection started, the whole system (hoses and equipment) was filled with tracer solution, which was different from SWIW test 1 when the system was initially filled with formation water. The details of flow rates, injection times and flow rates are found in Table 3-8.

General test data for SWIW test 2 are found in Table 3-8. The flow rate and pressure registrations are shown in Figure 3-8, Figure 3-9 and Figure 3-10. Table 3-10 shows the sampling intervals used during the test.

The injection flow rate was slowly decreasing despite the use of an automatic regulation unit (see Figure 3-8). Due to problems with the regulation unit the flow rate varied a lot during the first six hours. After that the flow rate was slowly decreasing as no automatic regulation was used. Manual regulation was made using a needle valve.
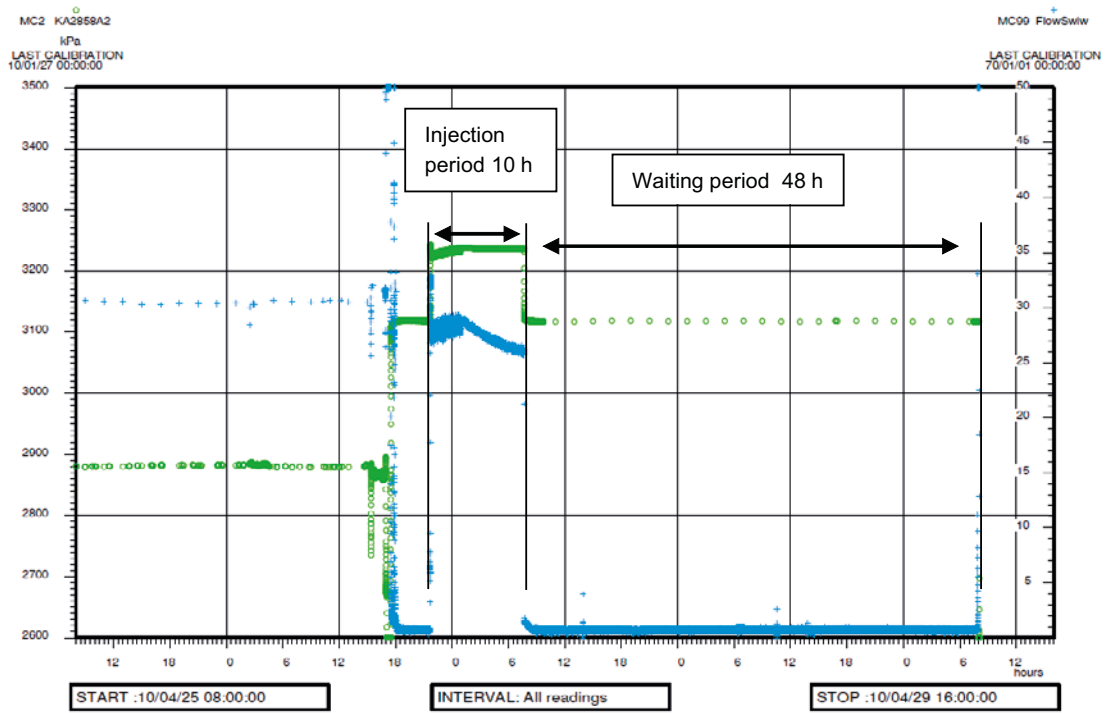
Figure 3-8. Flow rate (blue +) and pressure (green o) at the time just before injection, during the injection period and waiting period in SWIW test 2.
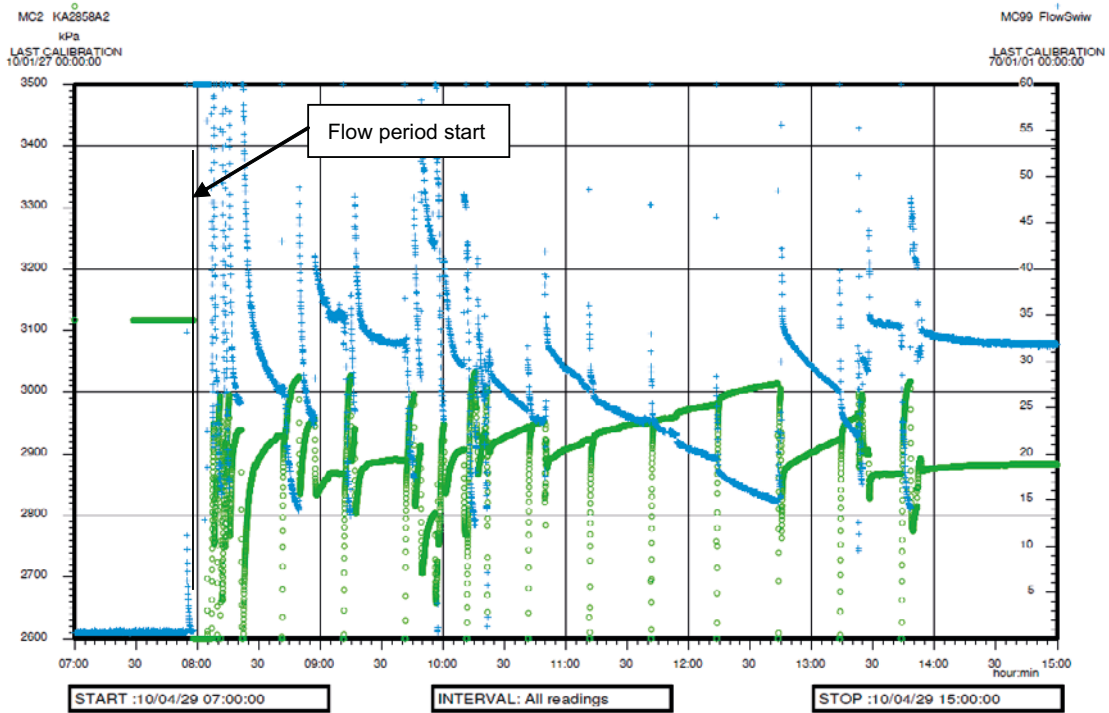

Figure 3-9. Flow rate (blue +) and pressure (green o) at the time just after start of the withdrawal period during SWIW test 2 when the regulation was not functioning.
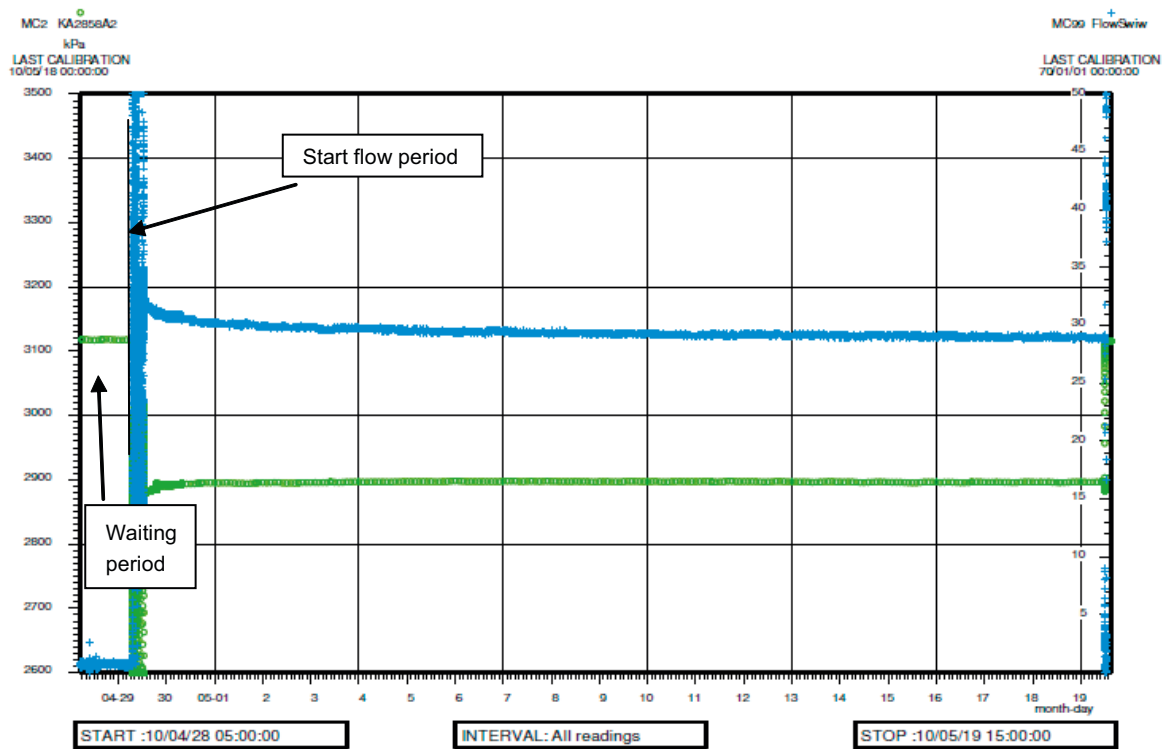
Figure 3-10. *Flow rate (blue +) and pressure (green o) during the waiting period and the whole withdrawal period during SWIW test 2.*

Table 3-10. Sampling intervals and sampling flow rates during SWIW test 2.

Time after flow period start	Sampling flow rate Fractional sampler	Sampling interval Fractional sampler
0–12 h	42 mL/h	10 min
12–24 h	13.6 mL/h	30 min
24–100 h	7.5 mL/h	60 min
100–475 h	3.0 mL/h	120 min

3.3.4 SWIW test 3

The third SWIW test was carried out in the same way as SWIW test 2, but the waiting period was longer, 91 h. The tracer was Uranine. Before the injection started, the whole system (hoses and equipment) was filled with tracer solution. General test data during SWIW test 3 are found in Table 3-11. The flow rate and pressure registrations are shown in Figure 3-11, Figure 3-12 and Figure 3-13.

During the first part of the withdrawal period the flow rate varied (between 20 and 40 mL/min), but a constant (i.e. no trend) mean flow rate at 28 ml/min was maintained. During a few hours on the second test day, some flow variations occurred again but after a while it was back to normal. There is no explanation for this behaviour.

Table 3-11. Sampling intervals and sampling flow rates during SWIW test 3.

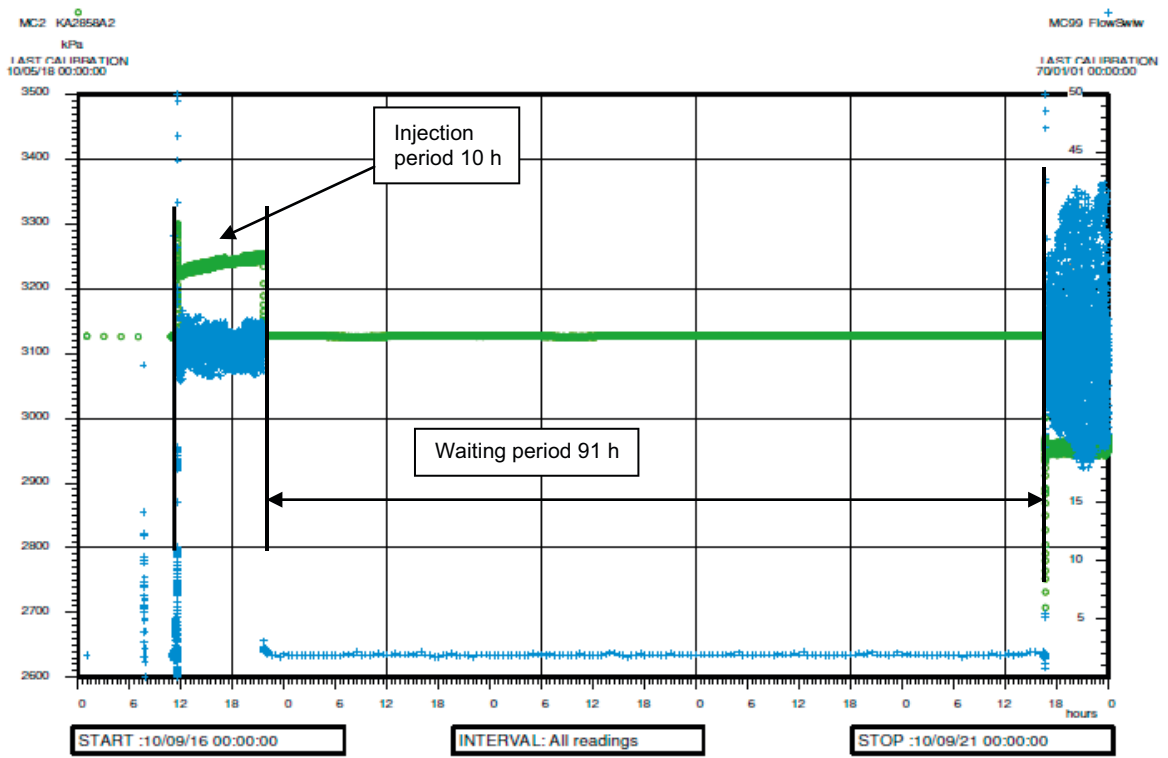| Time after flow period start	Sampling flow rate Fractional sampler	Sampling interval Fractional sampler
0–6 h	45 mL/h	10 min
6–12 h	12 mL/h	30 min
12–60 h	6.8 mL/h	60 min
60–160 h	3.5 mL/h	120 min

Figure 3-11. *Flow rate (blue +) and pressure (green o) at the time just before injection, during the injection period and waiting period in SWIW test 3.*
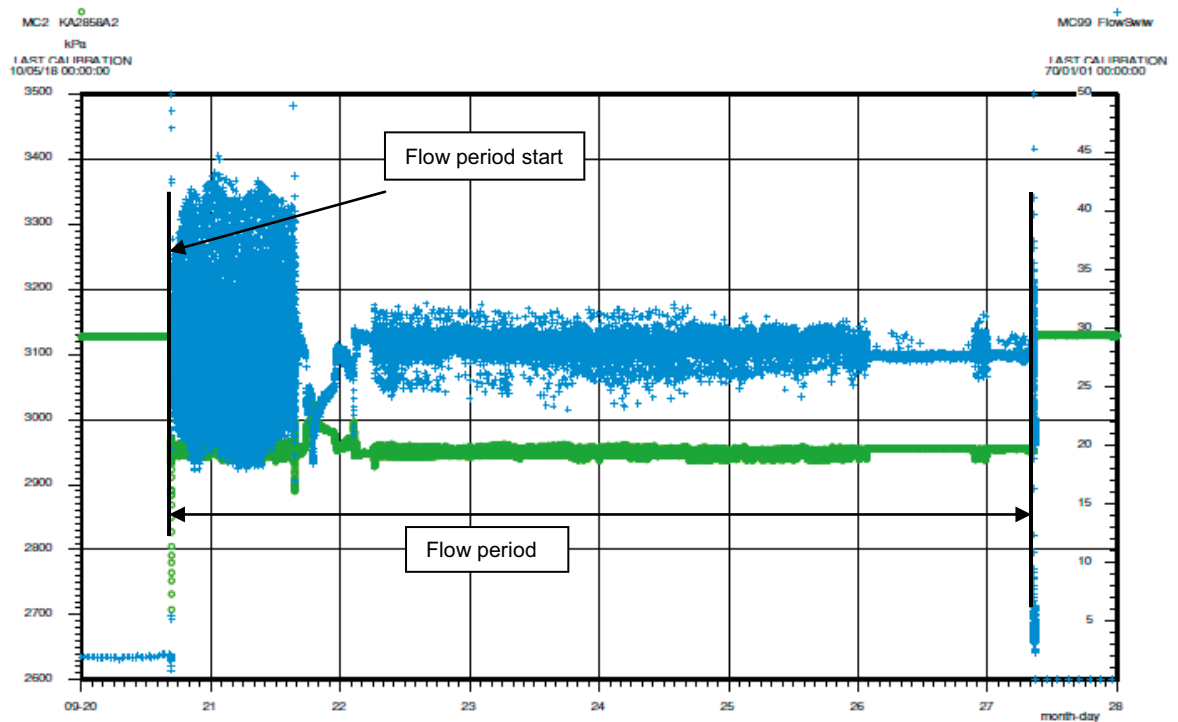

Figure 3-12. *Flow rate (blue +) and pressure (green o) during the flow period in SWIW test 3.*
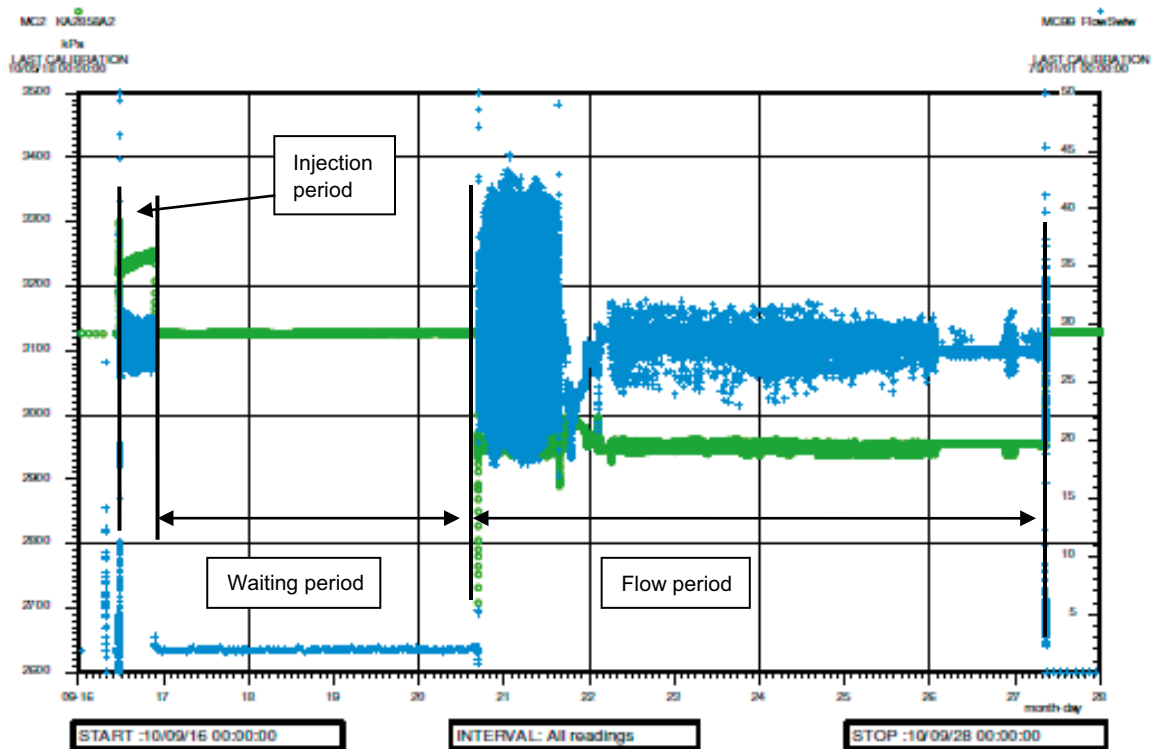
Figure 3-13. Flow rate (blue +) and pressure (green o) during the whole test period in SWIW test 3.

3.4 Main SWIW tests

The results from the three preparatory SWIW tests were used for the final design of the main SWIW tests. This process is discussed in more detail in Section 5.2, but the main experimental adjustments can be summarized as follows:

- The same waiting time as in SWIW test 3 (although the actual waiting time eventually turned out to be 93 hours instead of 91 hours).

- A doubling of the injection volume.

The injection- and pumping flow rates were doubled so that the test strategy was to inject 30 L tracer solution during 10 hours using a flow rate of 50 mL/min and then pump the water back using the same flow rate and continuously sample the pumped water. Before the injection started the whole system (hoses and equipment) was filled with synthetic groundwater. Prior to the actual tracer injection (increasing the pressure in the section) an exchange period without excess pressure where tracer solution was injected through one section end and water was withdrawn through the other end (ideally this would not cause any pressure changes in the section). The exchange was made during the time it takes to exchange the section volume three times (in this case just less than an hour). The water withdrawn from the section was collected for volume measurement and samples were collected every 10 minutes. After the exchange the water was circulated and the actual tracer injection into the tested rock feature was started. Samples were taken during the injection period using a fractional collector. During the recovery pumping phase the procedure was the same as in the preparatory tests; water was simultaneously withdrawn from the upper and the lower end of the section without any circulation.

3.4.1   Equipment and experimental setup

The equipment consisted of three pressurized tracer storage tanks connected to a gas tube with a gas regulator, automatic regulation unit with flow meter, three separate sampling equipment sets (flow regulation units and fractional samplers), circulation pump, flow meter (for circulation flow and withdrawal during the exchange period), plastic tubes and ball and needle valves (Figure 3-14).

The valves were set in different positions allowing the water to flow either along the red lines (injection) or the blue lines (withdrawal). During the exchange procedure, valve A was closed and the sampling at point B was replaced with a flow meter. During the injection with circulation the valve was open as well as during the withdrawal phase when water was withdrawn from both ends of the sections.

A web camera was used for monitoring the test and alarm functions for power failure or large variations in system pressure. A power supply (UPS) was also connected to ensure operation of the most important equipment parts (sampler and regulation unit) in case of a power failure.

The tracer injection was accomplished by applying an overpressure with nitrogen gas (N_2) on two connected pressure tanks (Figure 3-15) instead of using a pump. The tracer solution was pushed into the borehole section through the regulation unit/flow meter where the tracer injection flow rate was regulated.
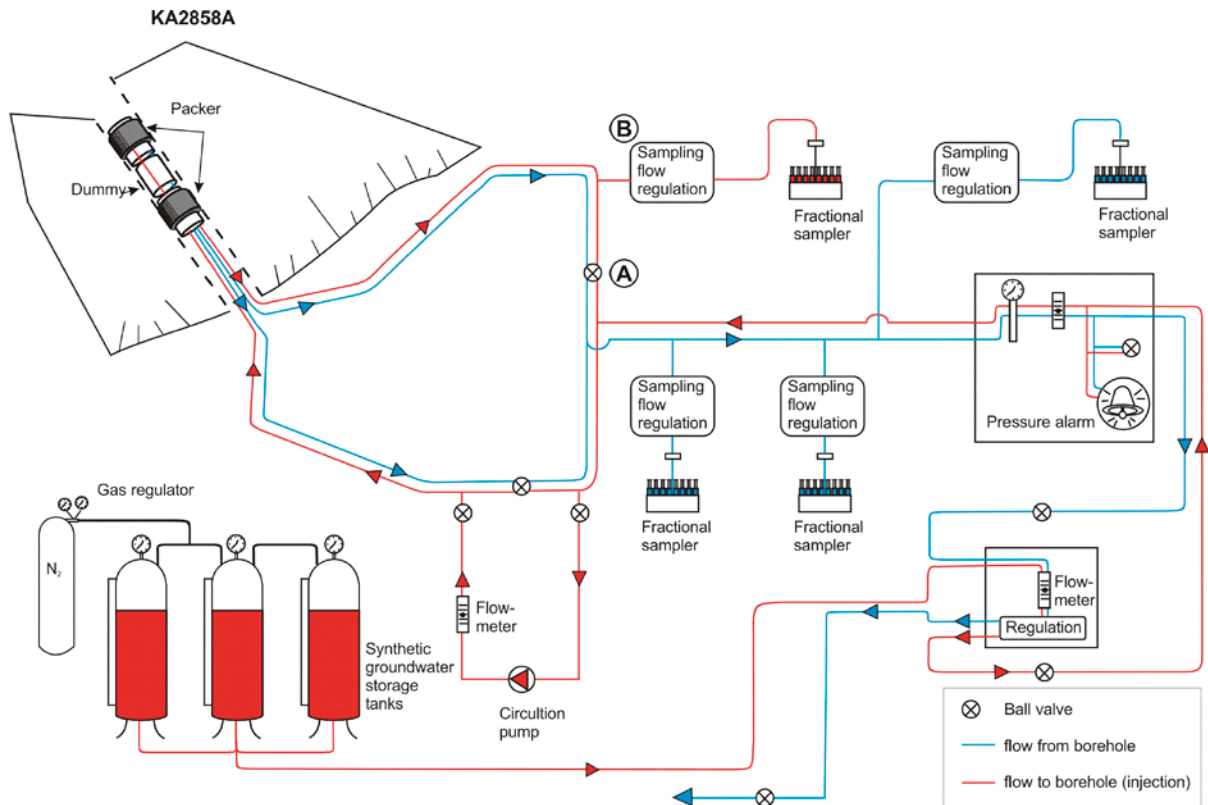

Figure 3-14. *Overview of the experimental setup and the equipment used in the main SWIW tests. The valves were set in different positions allowing the water to flow either along the red lines (injection) or the blue lines (withdrawal). During the exchange procedure the valve A was closed and the sampling at point B was replaced with a flow meter.*

Figure 3-15. *Pressurized tracer storage tanks and gas tube (N_2) used for injection of synthetic groundwater during the main SWIW tests (SWIW 4 and SWIW 5).*

3.4.2 Withdrawal and sampling

After 10 hours of injection the flow direction was reversed (immediately for SWIW 4 and after a waiting period for SWIW 5) and sampling begun. The automatic continuous sampling was made using three samplers (fractional samplers) connected to sample flow rate regulators (Flomega). Samples were also collected manually; some for analysis of radon and some were kept as spare samples in case additional analysis would be necessary. Samples were collected more frequently during the beginning of the tests.

The tubes in one of the samplers were intended for analysis of Uranine and they were prepared with buffer solution. The samples in the other two were intended for analysis with respect to cations (Na, Ca, K, Li, Rb, Cs) and chloride and nitrate respectively.

Laboratory gloves were used when handling the samples to avoid risk of contamination. The lids were stored in clean containers when not used and the time when the sample tubes were open was minimized by visiting the site every day (not on weekends) and placing lids on to the filled tubes.

The fractional samplers were placed before the flow meter/flow regulator which means that when the samplings flow rate was decreased the total flow rate from the section also decreased, without this being registered by the flow meter. In the final reporting of results, the flows from the fractional samplers were added to the flow meter data, in order to obtain accurate values for the total flow from the experimental borehole section.

General test data and pressure data from SWIW tests 4 and 5 are presented in Table 3-12 and Table 3-13.

Table 3-12. General test data for SWIW tests 4 and 5.

	SWIW 4	SWIW 5
Start exchange period	2010-11-02 21:24	2010-11-25 10:40
Stop exchange period	2010-11-02 22:20	2010-11-25 11:40
Volume in during exchange period (ml)	2,711	3,180
Volume out during exchange period (ml)	2,771	3,107
Start injection	2010-11-02 22:20	2010-11-25 11:40
Stop injection	2010-11-03 08:16	2010-11-25 21:40
Start flow period	2010-11-03 08:16	2010-11-29 18:28
Length waiting period (h)	0	93
Circulation flow rate during injection (mL/min)	168	168
Injection flow rate (mL/min)	50.0	53.0
Injection time (h)	10	10
Injected volume (L)	28.8	30.9
Flow rate (withdrawal) (mL/min)	50	50–61
Stop sampling	2010-11-24 16:01	2010-12-20 18:00
Length sampling period (h)	512	503

Table 3-13. Pressure data for SWIW tests 4 and 5.

	SWIW 4	SWIW 5
P (before inj. start)	3,120 kPa	3,120 kPa
P (at inj. stopp)	3,400 kPa	3,450 kPa
dP (pressure increase)	280 kPa	330 kPa
P (normal section pressure)	3,120 kPa	3,120 kPa
P (end of pumping)	2,785 kPa	2,810 kPa
dP (pressure decrease)	335 kPa	310 kPa

3.4.3 SWIW test 4 – main test without waiting period

A small pressure decrease of 5 kPa (from 3,121 kPa to 3,116 kPa) was noted during the exchange period, implying that the flow rate out from the section has been somewhat higher than the flow rate into the section. The flow rate registered by the flow meter was stable around a mean value of 50 mL/min. During a period (see Figure 3-16), the variations were large but with no apparent trends in the mean flow rate.

The pressure and flow rate was measured and registered during the whole test; see Figure 3-16, Figure 3-17 and Figure 3-18. Basic data for injected tracers are given in Table 3-14, which also presents calculated tracer recovery for each tracer. The recovery calculations are made by integration of flow-weighted breakthrough curves for each tracer. There appears to be some bias in the tracer recovery calculations, as over 100 percent or more recovery is indicated for all of the tracers. As this appears to be a systematic error, the reason might be some bias in determined pumping flow rates or injection flow rates.

Table 3-14. Concentration of added tracers SWIW 4.

	Uranine	NO_3^-	Li	Mg	Cs	Rb
Background (mg/l)	0.003	0.0026	3.8	34	0.0063	0.056
C0 (measured) (mg/l)	6.2	25,000	1,000	3,200	4.9	30
Injected mass (g)	0.18	730	29	90	0.14	0.85
Recovered mass (g)	0.18	967	32	94	0.15	0.89
Recovery (%)	100	132[*]	108	105	105	104

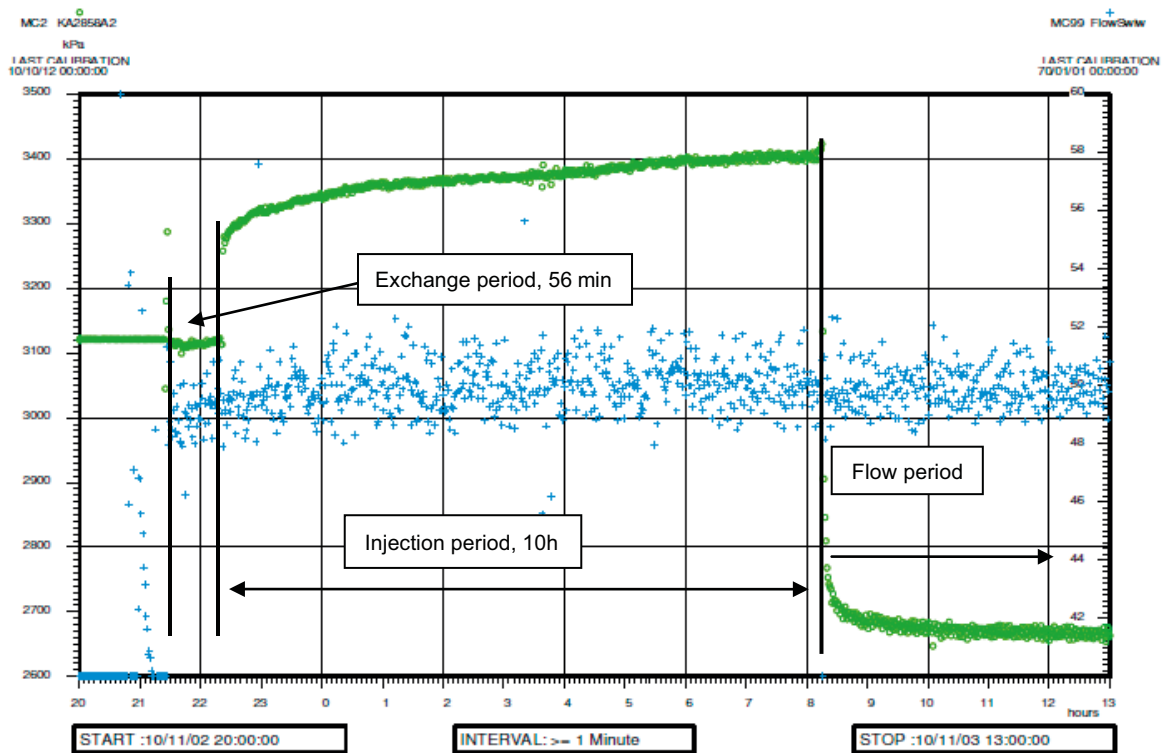* Uncertain estimate due to sparse and noisy data.

Figure 3-16. *Flow rate (blue +) and pressure (green o) at the time just before injection, during the injection period and start of flow period in SWIW test 4.*
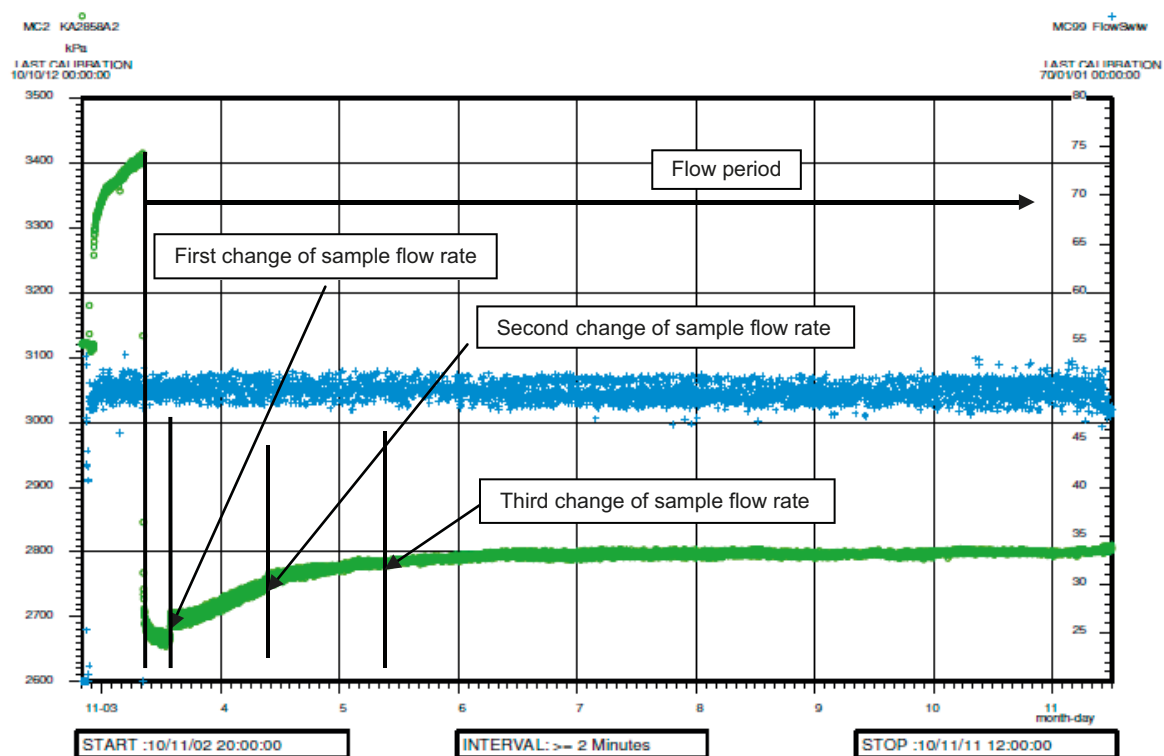

Figure 3-17. *Pressure (green o) and flow rate (blue +) during the beginning of the recovery pumping period for SWIW test 4. The occasions when the sampling flow rate was changed, affecting the total flow rate from the section, are marked in the figure.*
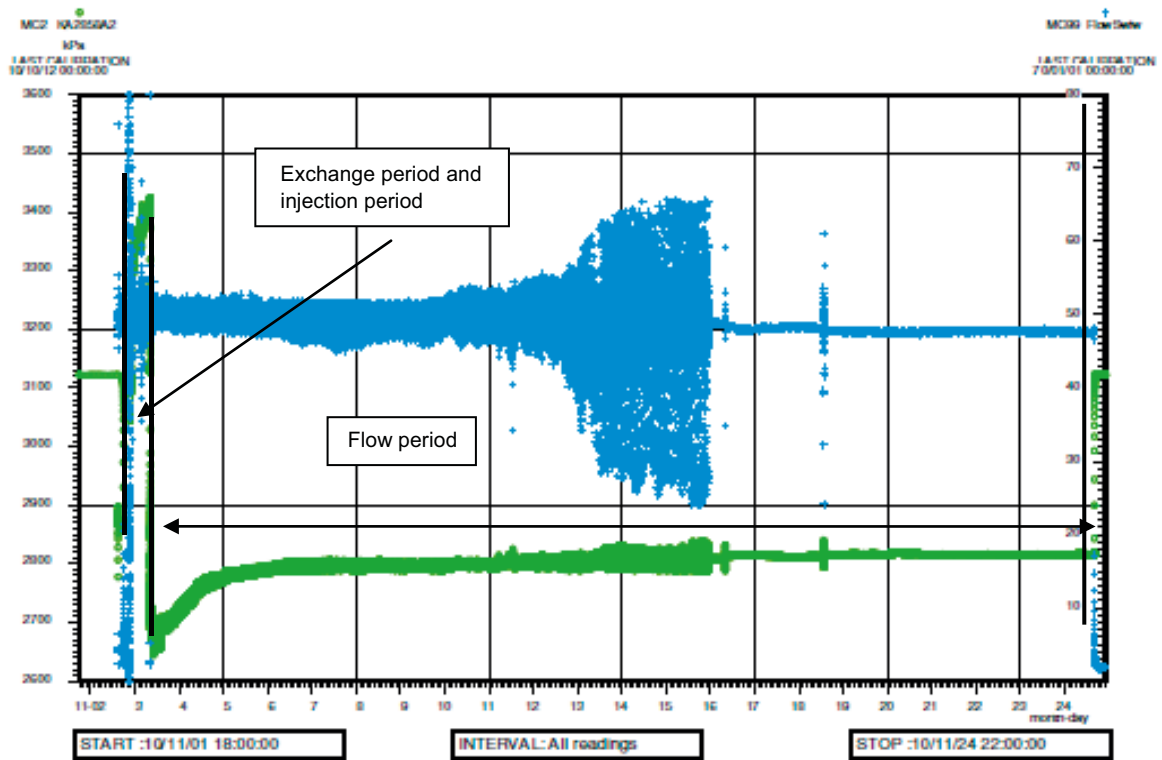
Figure 3-18. *Flow rate (blue +) and pressure (green o) during the whole test period in SWIW test 4.*

The samples were collected during the entire recovery pumping period, with short intervals at first, and longer intervals at the end, see Table 3-15. Borehole section pressure and flow rate during recovery are given in Table 3-16.

The manual sampling of radon continued for a week after start of recovery pumping. The manual sampling with larger volumes (165 ml) were maintained during the whole flow period.

Table 3-15. Sampling interval and flow rates for SWIW test 4.

Time after start	Sampling interval	Sample flow rate Sampler X	Sample flow rate Sampler Y	Sample flow rate Sampler Z
0–6 h	10 min	39 mL/h	95 mL/h	95 ml/h
6–24 h	30 min	13 mL/h	31 mL/h	33 ml/h
24–50 h	60 min	7.0 mL/h	15 mL/h	16 ml/h
50–512 h	120 min	3.4 mL/h	7.5 mL/h	8.4 ml/h

Table 3-16. Pressure and flow rates for SWIW test 4.

Normal section pressure 3,121 kPa

Time after start	Sampling interval	Time period from	Time period to	Pressure (kPa) at the end of the flow period	Average flow rate from section
0–6 h	10 min	2010-11-03 08:16	2010-11-03 13:54	2,670	54 mL/min
6–24 h	30 min	2010-11-03 13:54	2010-11-04 09:24	2,750	51 mL/min
24–50 h	60 min	2010-11-04 09:24	2010-11-05 10:18	2,785	51 mL/min
50–512 h	120 min	2010-11-05 10:18	2010-11-24 16:01	2,785	49 mL/min

3.4.4 SWIW test 5 – main test with waiting period

The second main SWIW test was carried out in the same way as SWIW test 4, but a waiting period was added between the injection and the withdrawal period. In addition, some equipment malfunctioning led to minor adjustments, although not affecting the experimental results, in experimental procedure.

The mean pressure during the exchange period was somewhat higher than the pressure in the undisturbed section, implying that the circulation flow rate out from the section was somewhat lower than the flow rate into the section. Pressure data are shown in Figure 3-19, Figure 3-20 and Figure 3-21.

Problems with the regulation and the flow meter caused flow rate variations during the exchange period as well as the injection period. The flow meter connected to the logger could not be used and regulation was made manually using a needle valve. However, the pressure registrations give good indications of how the flow rate varied. In the plot of section pressure during the exchange and injection period it is noted that the shape of the pressure curve is the same as in SWIW 4, in which the flow rate was constant (compare Figure 3-16 and Figure 3-19). However, a slightly larger pressure increase is noted, which implies a somewhat higher injection flow rate in SWIW test 5. The total injected volume during SWIW test 5, as well as during SWIW test 4, was calculated using both the estimated flow rate against time as well as measuring the volume in the tracer storage tanks before and after injection.
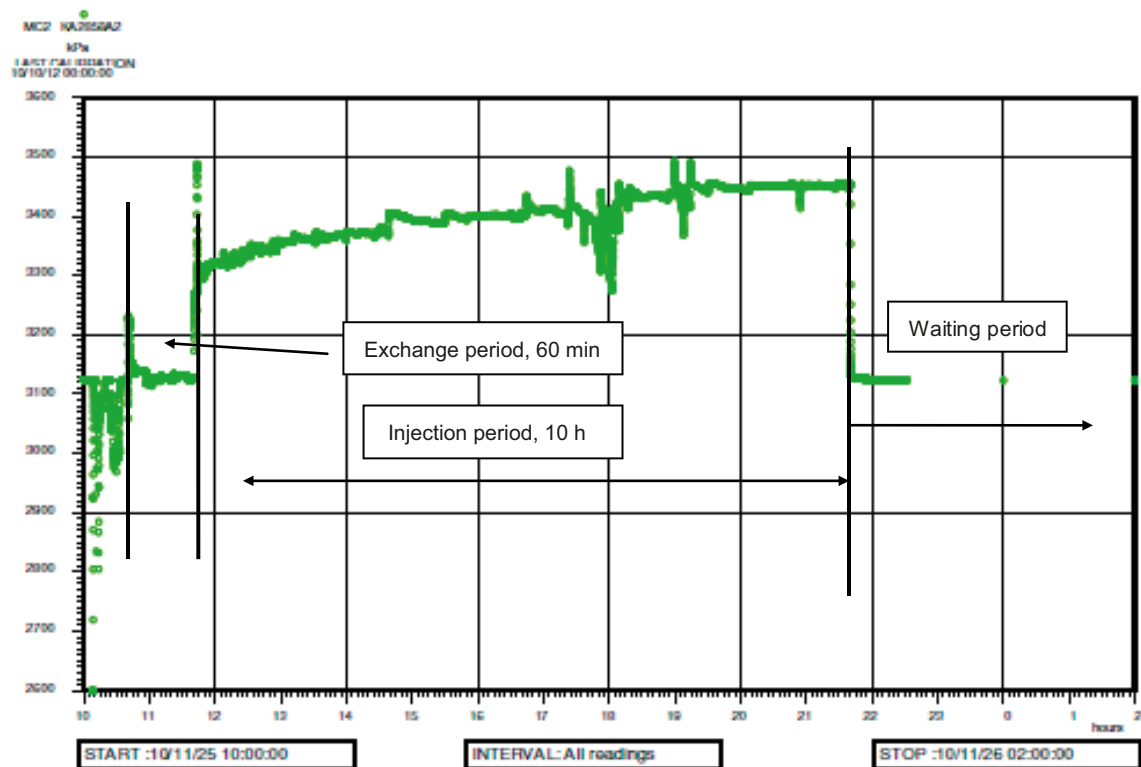

Figure 3-19. *Pressure at the time just before injection, during the injection period and start of waiting period in SWIW test 5.*
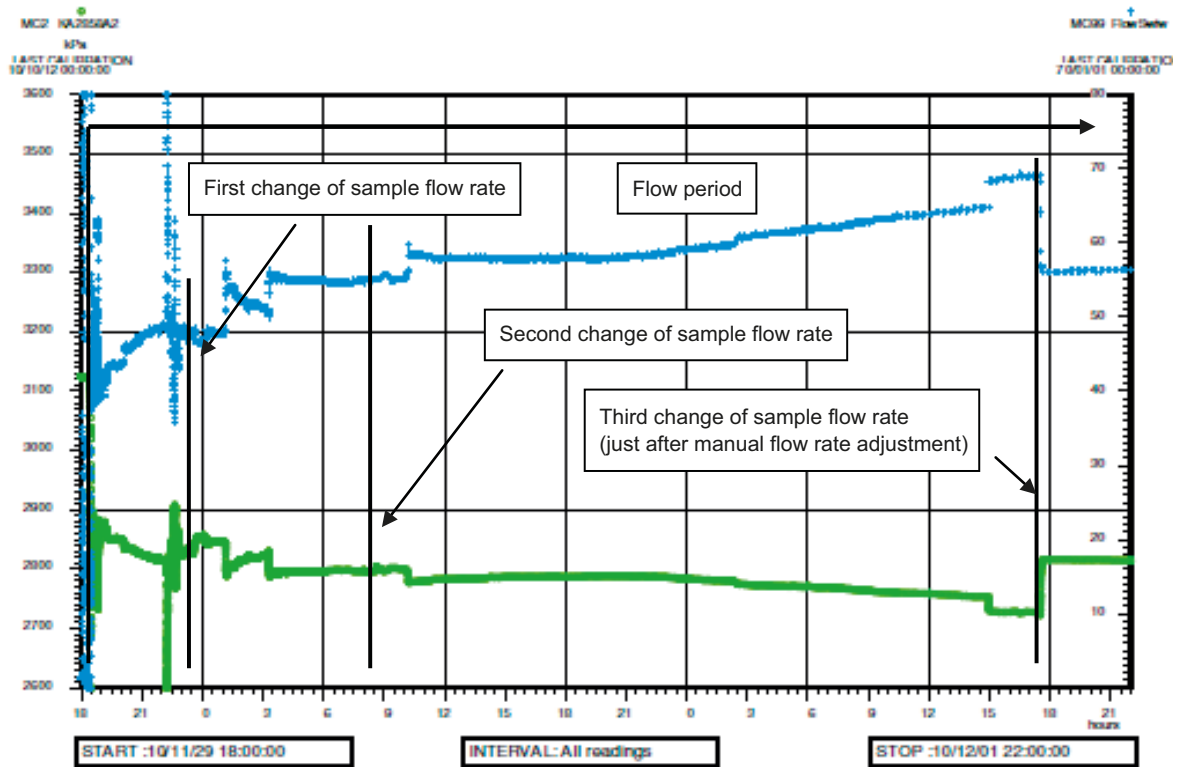
Figure 3-20. Pressure (green o) and flow rate (blue +) during the beginning of the flow period for SWIW test 5. The occasions when the sampling flow rate was changed, affecting the total flow rate from the section, are marked in the figure.
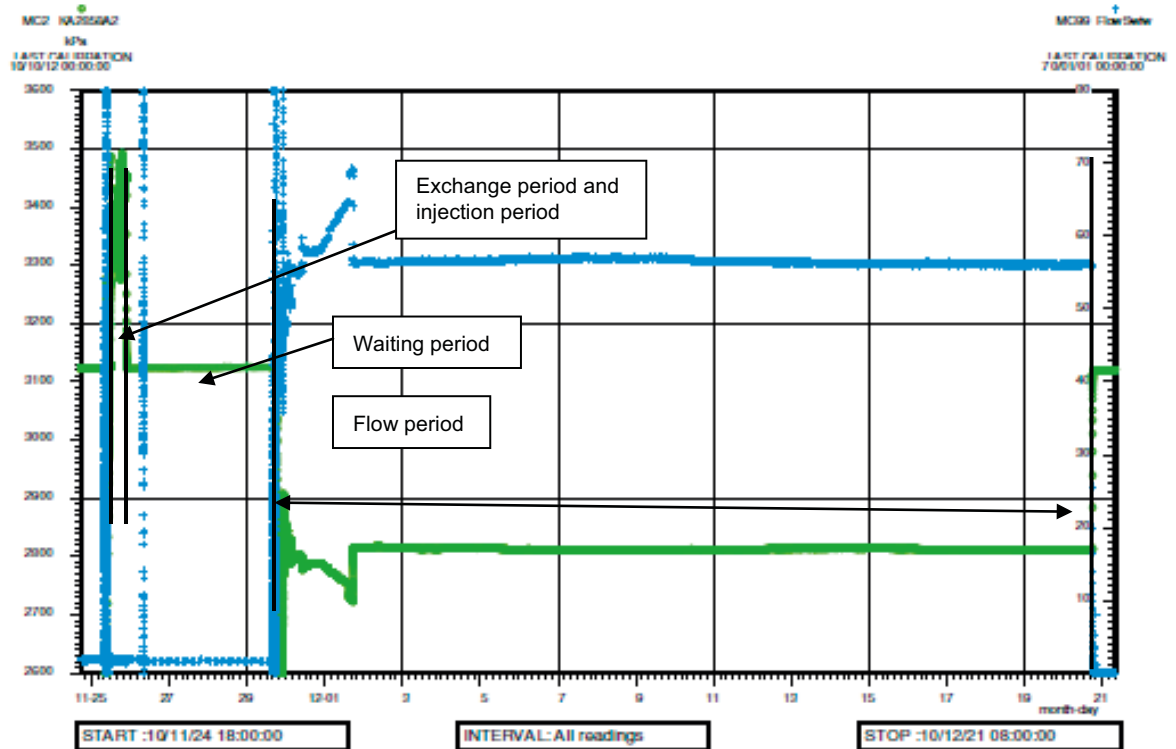

Figure 3-21. Flow rate (blue +) and pressure (green o) during the whole test period in SWIW test 5. Note that no flow rate was registered during the exchange and injection periods.

Basic data for injected tracers are given in Table 3-17, which shows that the tracer recovery at the end of the recovery pumping is generally somewhat smaller than in SWIW test 4. As discussed above, tracer recovery in SWIW test 4 appeared generally to be slightly overestimated. Whether this also applies to SWIW test 5 is not possible to say, but if that would be the case the recovery values may be a few per cent lower.

The samples were collected during the entire re-pumping period, with short intervals at first, and longer intervals at the end, see Table 3-18. Borehole section pressure and flow rate during recovery are given in Table 3-19.

Table 3-17. Concentration of added tracers in SWIW test 5.

	Uranine	NO_3^-	Li	Mg	Cs	Rb
Background (mg/l)	0.003	0.0026	3.8	34	0.0063	0.056
C0 (measured) (mg/l)	6.4	26,000	1,100	3,200	5.0	31
Injected mass (g)	0.20	790	33	100	0.15	0.94
Recovered mass (g)	0.17	736	29	88	0.15	0.87
Recovery (%)	89	93	89	88	95	92

Table 3-18. Sampling interval and flow rates for SWIW test 5.

Time after start	Sampling interval	Sample flow rate Sampler X	Sample flow rate Sampler Y	Sample flow rate Sampler Z
0–5 h	10 min	38	95	97
5–15 h	30 min	12	32	33
15–48 h	60 min	7.0	15	17
48–502 h	120 min	3.5	7.7	8.5

Table 3-19. Pressure and flow rates for SWIW test 5.

Normal section pressure 3,123 kPa					
Time after start	Sampling interval	Time period from	Time period to	Pressure (kPa) at the end of the flow period	Average flow rate from section
0–5 h	10 min	2010-11-29 18:30	2010-11-29 23:36	2,831	50 mL/min [1]
5–15 h	30 min	2010-11-29 23:36	2010-11-30 08:38	2,796	54 mL/min [1]
15–48 h	60 min	2010-11-30 08:38	2010-12-01 17:41	2,742	61 mL/min [1]
48–502 h	120 min	2010-12-01 17:41	2010-12-20 18:00	2,811	57 mL/min

[1] Varying flow rate.

4 Analyses and interpretation methods

4.1 Supporting tests in KA2858A

4.1.1 Capacity test

The capacity test was evaluated using the software AQTESOLV (version 4.5, HydroSOLVE, Inc.) using Moench' model for a leaky aquifer (pseudo-spherical flow) including skin and wellbore storage (Moench 1985).

4.1.2 Groundwater flow measurements

Dilution test is a common method for determining the flow rate through a borehole section (Gustafsson and Morosini 2002). The principle is to inject a tracer solution into a continuously mixed borehole section and then monitor the decrease in tracer concentration over time as illustrated in Figure 4-1. Dilution tests were carried out at several occasions during the synthetic SWIW experimental program.

Assuming that the background concentration is negligible, the dilution in a well-mixed borehole section, starting at time t = 0, is given by:

$$\ln(C/C_0) = -\frac{Q_w}{V} \cdot t \qquad (4\text{-}1)$$

where C (e.g. mg/m³) is the concentration at time t (s), C_0 is the initial concentration, V is the water volume (m³) in the test section and Q_w is the volumetric flow rate (m³/s) through the borehole section. Since V is known, the flow rate may be determined from the slope of the line in a plot of ln (C/C_0), or ln C, versus t.

A typical result from a tracer dilution experiment is illustrated in Figure 4-2.

As described in Section 3.1.2, the tracer concentration in the borehole section was monitored by withdrawal of small volumes of water at regular intervals. The sampling flow rate does in itself cause dilution of tracer and when the background groundwater flow rate through the borehole section is small, the sampling flow rate may affect the evaluation of the dilution test. For the dilution tests reported herein, correction for sampling is simply made by subtracting the sampling flow rate from the rate estimated from the dilution curve. The uncertainties connected with this procedure are further discussed in Section 5.1.2.
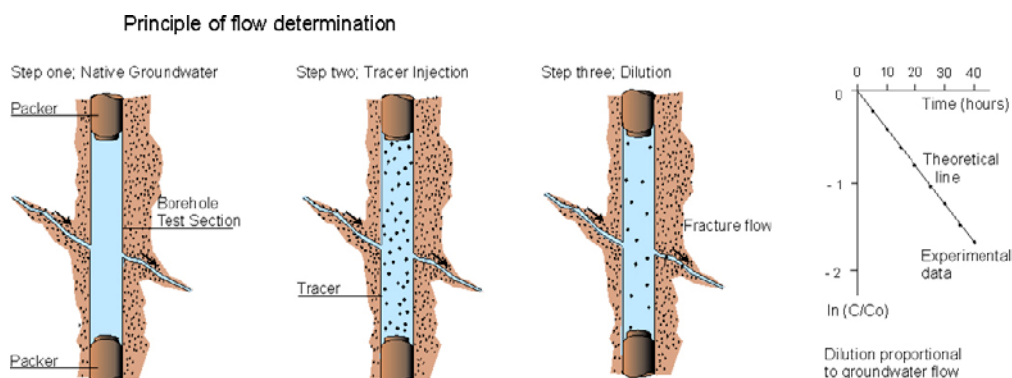

Figure 4-1. *General principle of the dilution method.*

Äspö HRLGroundwater flow measurement 2KA2858A (39.77–40.77 m)
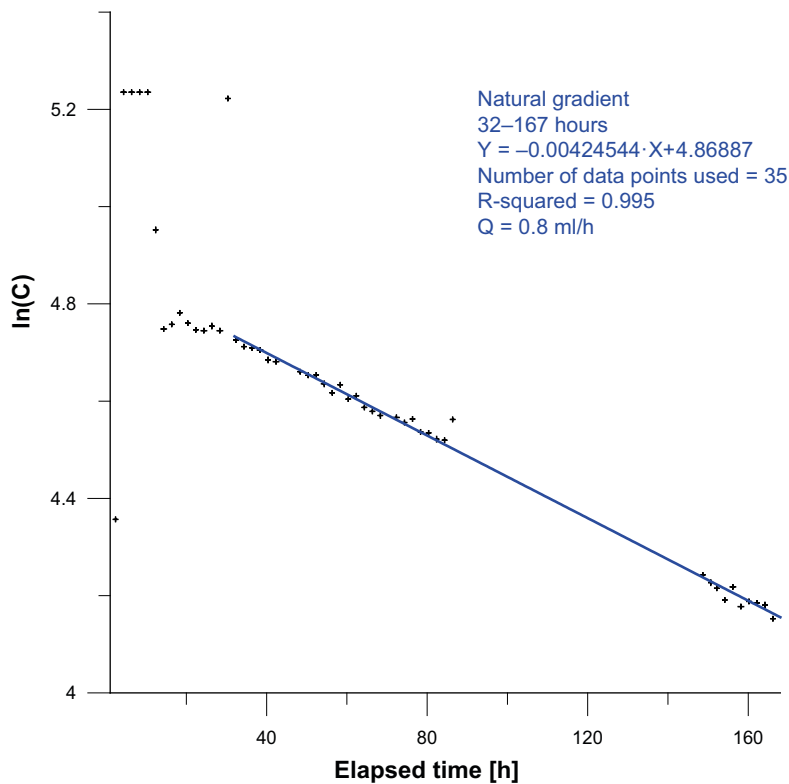

Figure 4-2. Example of a plot for evaluation of a dilution test.

4.2   Chemical analyses

Several laboratories were involved in the sample analyses.

Cl: Was analysed by both Eurofins and Äspö. Eurofins used the methods IC and Kone while Äspö used IC and Mohr-Titration. Evaluation of the lab results resulted in that Äspö laboratory was used for further analysis and evaluation.

NO$_3$: Was analysed by Eurofins in Linköping and ALS in Täby. Eurofins used the methods Kone, TRACCS och IC while ALS only used IC. Evaluation of the lab results resulted in that the Eurofins laboratory was used for further analysis and evaluation.

Na, K, Ca, Mg, Li, Cs, Rb: Was analysed by ALS Scandinavia in Luleå using ICP-MS and ICP-AES.

Radon: Analyses were performed at CLAB.

Abbreviations and definitions:

IC	Ion chromatograph
ICP-AES	Inductively Coupled Plasma Atomic Emission Spectrometry
ICP-MS	Inductively Coupled Plasma Mass Spectrometry
Kone	Discrete Spectrometry
Mohr-Titration	Titration with silver nitrate
MS	Mass Spectrometry
TIMS	Thermal Ionization Mass Spectrometer
LSC	Liquid Scintillation Counting
LSS	Liquid Scintillation Spectroscopy
TRACCS	Technicon Random Access Automated Chemistry System

In total, 12 water samples for general water chemistry were taken during the project. The purposes of the sampling were:

- To determine if the chemistry in the section is stabile over time.
- To see if there risk of microbe growth is high or low when nitrate is added (indication gives from the sulphide content).
- To give an accurate determination of the background contents of the compounds that are planned to be used as tracers in the main test (e.g. Cesium (Cs) and Rubidium (Rb)).

The quality of the analyses was checked by calculating the relative charge balance errors according to the equation below. Relative errors within ± 5% are considered acceptable.

$$\text{Relative error } (\%) = 100 \times \frac{\sum cations(equivalents) - \sum anions(equivalents)}{\sum cations(equivalents) + \sum anions(equivalents)}$$

4.3 SWIW tests

4.3.1 Time adjustments and other basic calculations

Reported experimental times have been adjusted for residence times in the borehole section, tubing and other equipment. Thus, the reported time for a sample during the recovery pumping phase represents the time, as accurately as possible, when the water leaves the fracture and enters the section.

Background concentrations for tracers are determined from sampling prior to the main SWIW tests. In the results shown herein, the background concentrations have been subtracted.

The breakthrough curves presented in this report generally show normalized concentrations (C/C_0) for each tracer, in order to compare tracer with each other. The normalizing concentration, C_0, differs depending on whether the tracer is added or removed. When tracers are added, which is the "standard" method, C_0 is the injection concentration. It was found that the injection concentration could be fairly accurately determined from samples taken during the injection period.

For removed tracers, C_0 is the resident concentration in the fracture. Because all of the breakthrough curves for the removed tracers clearly reached steady-state concentrations, C_0-values for these were obtained by averaging values from the later part of the breakthrough curves.

The total mass of each injected tracer was calculated by the flow-meter registrations during the injection period and the known initial concentration of the tracer solution.

4.4 Modelling/Simulations

For modelling and SWIW test in this report, three basic simulation models have been used. All models are highly simplified and assume homogenous conditions. Results of model simulations are presented primarily throughout Chapter 6. The models are as follows:

1. Radial flow and advective-dispersive transport in a single fracture, with linear equilibrium sorption.
2. As above, but with a porous matrix on both sides of the fracture. The tracer may diffusive into the matrix and undergo linear equilibrium sorption in the matrix (no sorption in the fracture in this case).
3. A two-dimensional areal flow model with advection and dispersion. This was used in simulations used for analysis of effects from the background flow on the SWIW test results.

These models are described in more detail below.

4.4.1 Radial flow and advective-dispersive transport in a single fracture, with linear equilibrium sorption

The governing transport equation for this model is given by Equation 2-3 (Section 2.1) and the simulation examples given in Section 2.1 are obtained using this model. The model is run with steady-state groundwater flow but transient solute transport. The tracer transport for a non-sorbing tracer is in this case only dependent on the radial velocity distribution and longitudinal dispersion. Sorbing tracers are simulated assuming equilibrium linear sorption, which can be defined using a simple fracture retardation factor, R_f (see Equation 2-3). The retardation factor for a fracture may be defined on a surface-sorption basis by, for example:

$$R_f = 1 + A_r K_a \tag{4-2}$$

where K_a is the sorption distribution coefficient [L] and A_r is the surface area to volume ratio [L^{-1}]. In a cross-hole tracer test the retardation factor indicates how much a sorbing tracer is delayed in time compared to a non-sorbing tracer. In a SWIW test, however, there is no difference in arrival time in the breakthrough curve. In the absence of dispersion, a SWIW test can not distinguish between different retardation factors. However, in the presence of dispersion, a difference in the retardation factor will also result in a different recovery breakthrough curve, as shown in Figure 2-4.

This model is in a sense one-dimensional because there is only one spatial coordinate, the radial distance from the experimental borehole section, extending from the borehole radius to some distance sufficiently "far away" to not influence the simulated transport. The boundary condition at the borehole radius is specified flow; during the injection phase the concentration of the added water has to be specified as well. At the outer boundary, the boundary condition is specified head and specified concentration.

During the synthetic SWIW experiments, some tracers are added to the rock formation but some are also removed from the formation. The initial conditions depend on which of the two types tracers that are simulated. For added tracers, initial concentration is zero everywhere including in any water that enters the model through the outer constant head boundary. For removed tracers, initial concentration is set to a specified value throughout the model; this value must be specified for water entering through the outer boundary as well.

The model was run using the numerical finite-element simulation code SUTRA (Voss 1984). The radial transport system was simulated using 2,400 nodes in the radial direction with an outer boundary located at r = 25 m. The element closest to the simulated borehole section has very fine discretisation and increase in size with increasing distance from the borehole. The simulations are carried out in steps according to the various experimental phases.

4.4.2 Matrix diffusion model

The matrix diffusion model may be considered as an add-on to the model described in Section 4.4.1 above. All of the flow still takes place in a plane-parallel fracture but the fracture is lined on both sides by a hydraulically stagnant but porous matrix.

The simulations including matrix diffusion are carried out assuming a vertical section with radial symmetry. The simulated geometry approximately corresponds to a dual-porosity approach based on the assumption of parallel fractures and is schematically illustrated in Figure 4-3. A similar approach was used by Lessoff and Konikow (1997) for simulation of SWIW tests.

The same simulation code, SUTRA, was used also in this case. For the fracture, element sizes start very small closest to the borehole and expand with distance. In the vertical direction (i.e. away from the fracture), element sizes increase with distance from the fracture. The simulation mesh consists of 42,000 elements and 42,411 nodes.

Boundary and initial conditions are analogous with the basic single-fracture model described above; initial concentrations are specified throughout the matrix as well. Note that there are no particular boundary conditions at the fracture/matrix interface, as the fracture and the matrix form a continuous computational domain. The fracture/matrix interface is defined by a change in properties, mainly hydraulic conductivity and porosity. When properties change from a finite element to an adjacent one some averaging is made, which implies that the "sharpness" of the interface is somewhat limited
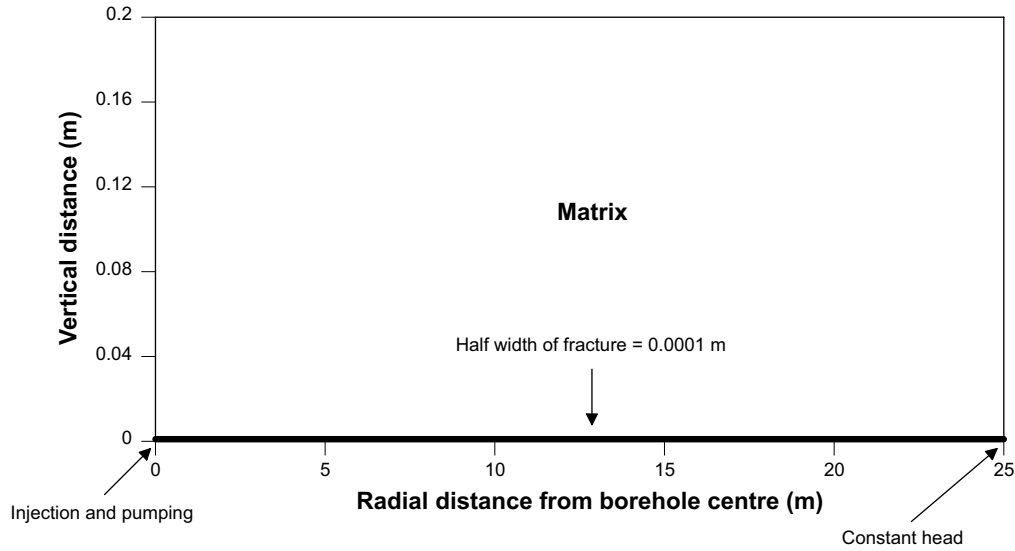
Figure 4-3. *Layout for simulation of SWIW test in a fracture with matrix diffusion.*

by the element sizes next to the interface. In the model used here, the thickness of the first matrix element away from the fracture is made very small ($8 \cdot 10^{-6}$ m) and thereafter increasing progressively away from the interface.

The code simulates solute transport with the standard advection-dispersion-diffusion model in two dimensions. However, with radial geometry and the matrix, what is effectively simulated is longitudinal dispersion in the fracture and only diffusion in the matrix.

The layout in Figure 4-3 represents a single plane-parallel fracture with an assumed width of 0.0002 m (half-width = 0.0001 m) having a porosity of 1.0. The matrix (simulated with a very low value of hydraulic conductivity) extends, on both sides of the fracture, to a distance of 0.2 m away from the centre of the fracture. The model extends 25 m in the radial direction, which is intended to be well beyond the distances that solute may travel during the simulated fluid injection. A porosity value is assigned to the smatrix (p_m) as well as a pore diffusivity value. The latter is less than diffusivity in water due to tortuosity and constrictivity effects. The pore diffusivity, D_p [L^2/T], is commonly defined as (Bodin et al. 2003):

$$D_p = D_W \frac{\delta_D}{\tau^2} \tag{4-3}$$

where D_W is the diffusivity in free water [L^2/T], δ_D is the constrictivity [–] and τ is the tortuosity [–].

Sorption of tracers is in this case considered only for the matrix (no sorption in the fracture). Sorption in the matrix is simulated assuming linear equilibrium sorption (K_d – sorption). One-dimensional transport of a sorbing tracer by diffusion may be described by:

$$\frac{\partial C_m}{\partial t} = \frac{D_p}{R_m} \frac{\partial^2 C_m}{\partial z^2} \tag{4-4}$$

where C_m is solute concentration in the matrix [M/L^3], z is a coordinate perpendicular to the fracture [L], and the matrix retardation factor, R_m, is given by:

$$R_m = 1 + \frac{\rho_s(1 - p_m)}{p_m} K_d \tag{4-5}$$

where ρ_s is the density of the solid [M/L^3], p_m is the matrix porosity [–] and K_d is the distribution coefficient for linear equilibrium sorption [L^3/M].

In the simulations herein with SUTRA, however, diffusion in the matrix is not strictly one-dimensional because the employed model is fully two-dimensional throughout the simulation domain.

A complete list of the various SUTRA model parameters that influence the computed breakthrough curve in the simulation model employed includes:

- fracture aperture,
- longitudinal dispersivity,
- matrix porosity,
- tracer diffusivity,
- solid density,
- linear sorption coefficient (K_d).

In addition, the total injected volume also influences the dispersion as described in Section 2.1.

Analogous to the effective dispersion parameter φ, the above listed matrix parameters can be combined into a group that effectively determines the shape of the breakthrough curve. The effective parameter group for matrix diffusion effect for a non-sorbing tracer (i.e. Uranine) may be written as (Moreno et al. 1983):

$$A = \frac{\delta}{2 p_m \sqrt{D_p}} \tag{4-6}$$

where δ is the fracture aperture [L].

For a sorbing tracer the combined parameter above extends to:

$$A_R = \frac{\delta}{2 p_m \sqrt{R_m D_p}} \tag{4-7}$$

4.4.3 Two-dimensional flow and transport model

This model is used only to analyze effects of the background flow on the experimental SWIW results; such effects may not be studied with a radial-symmetry model. The flow and transport is simulated in a 50·50 m areal domain; SUTRA is the simulation code also in this case (39,601 nodes, 39,204 elements). The outer boundary condition is specified head around all four sides of the model and the head values are specified so that a uniform background flow is obtained. The well (i.e. the SWIW borehole section) is placed at a node somewhat "upstream" the centre of the model domain (x = 20 m). The simulation mode is steady-state flow and transient solute transport.

4.4.4 Parameter estimation method

All of the models described above are in this report used both in a forward simulation mode as well as in an inverse (parameter estimation) mode. Non-linear least-squares regression was employed to fit the simulation models to experimental data, based on the Marquardt method for weighted non-linear regression (Marquardt 1963).

5 Results of preparatory tests and other supporting investigations

5.1 Tests of KA2858A

5.1.1 Capacity test

The flow rate was constant during the whole period except for two separate occasions when the flow rate was zero causing the pressure to increase for a short while. The first occasion was in the afternoon of January 27 and the second one during the night between January 27 and 28. During a period, the flow regulation did not function satisfactory, which led to relatively large oscillations around the mean flow rate, 23.5 mL/min. This variation is also reflected in the pressure registrations. However, the mean flow rate was still constant, so the oscillations are not considered to have affected the evaluation of the test, see Figure 5-1.

The capacity test was evaluated using the software AQTESOLV. Using Moench' model (Moench 1985) for a leaky aquifer (pseudo-spherical flow). The transmissivity (T) of the section was estimated to about $3.7 \cdot 10^{-8}$ m^2/s.

Responses in surrounding boreholes

Possible pressure responses in all sections connected to the HMS system and located within 300 m from the test section KA2858A was checked for by plotting the pressure data from HMS. No responses were detected apart from one possible, very weak response in KA2862A, which intersects the high-transmissivity zone NW-3. KA2862A is also the only borehole within 100 m distance. However, such judgements are very difficult to make due to the decreasing trend present at the time when the flow period starts (Figure 5-2 and Figure 5-3). No clear effect of neither the start or the stop of the flow period can be discerned. On the other hand, an effect of the short intense flow period on the day before when the equipment was tested is visible.
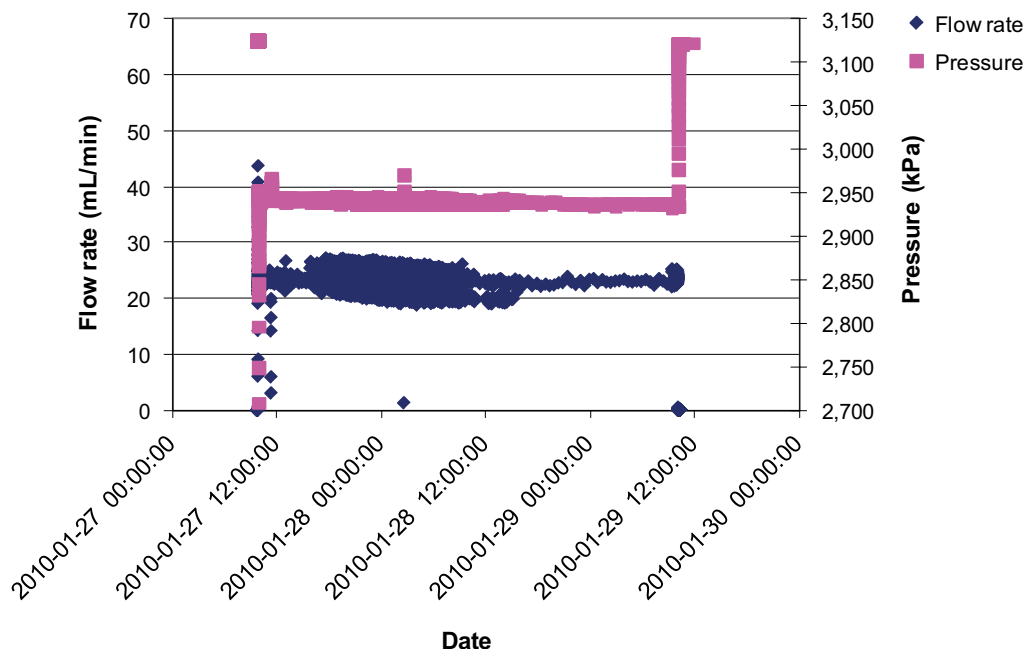

Figure 5-1. *Overview of flow rate and pressure in the test section during the capacity test.*
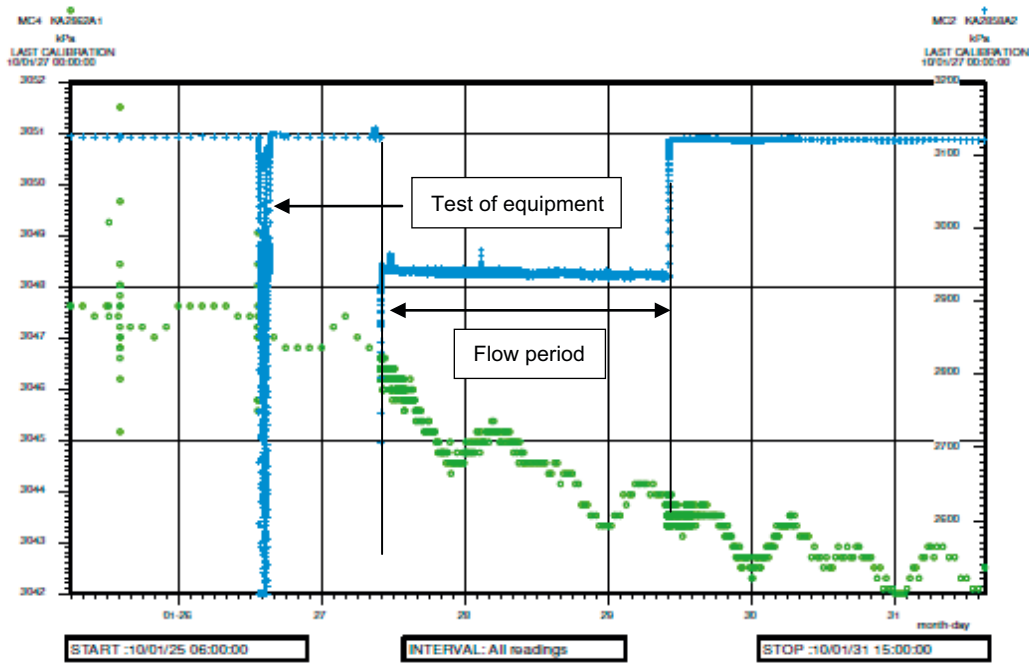
Figure 5-2. *Pressure data from the test section KA2858A:2 (blue +) and the observation borehole KA2862A (green o) during the capacity test from 2010-01-25 to 2010-01-31.*
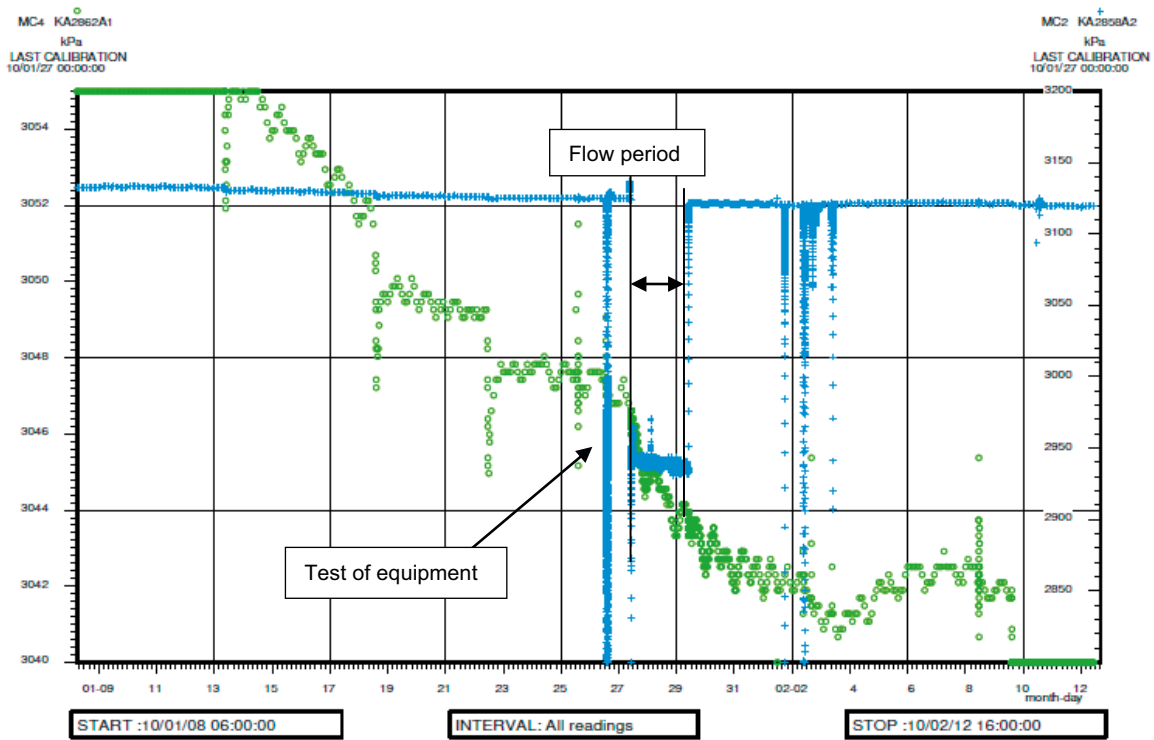

Figure 5-3. *Pressure data from the test section KA2858A:2 (blue +) and the observation borehole KA2862A (green o) during the capacity test from 2010-01-08 to 2010-02-12.*

Within the SELECT experiments, Winberg et al. (1996) interference tests including these two boreholes were carried out during 1995. An important difference compared the present test is that in 1995 a particular water-bearing section in KA2862A (15.02–15.98 m) was tested, whereas now the entire borehole (0–15.98 m) is tested. During these earlier tests a disturbance in KA2858A (flow rate 0.13 L/min) showed no significant responses in KA2862A. None of the other observation boreholes were affected either. Inversely, no significant responses were observed in KA2858A:2 when the flow rate in KA2862A (15.02–15.98 m) was 1.1 L/min. Hence, the results from these new tests are in accordance with the previously performed test in the SELECT campaign.

5.1.2   Groundwater flow measurements

The results from the four groundwater flow measurements are summarized in Table 5-1. Comments on the results for each test are listed below. The tracer dilution graphs and the pressure in the section during the measurement periods are presented in Appendix 1.

Generally, the estimated flow rates are low and of about the same magnitude as the sampling flow rates. When this happens, the evaluation of the groundwater flow rate through the borehole section is affected because the sampling flow rate causes additional dilution of the tracer. Thus, a high sampling flow rate results in a too high estimate of the groundwater flow, unless the sampling flow rate is compensated for. For evaluation of the dilution tests presented here, the sampling flow rate is simply subtracted from the rate given by the slope of the dilution graph. This correction is not entirely correct as it does not account for the effect on the hydraulic conditions around the borehole section, i.e. the sampling flow rate adds a small drawdown cone that is superimposed on the background flow. This results in uncertainty at low flow rates. For example, if the evaluated background flow is equal to the sampling flow rate, this means that all of the dilution in the borehole comes from the sampling flow. However, this does not mean that the background flow rate is zero (which would be the results when simply subtracting the sampling flow rate). Theoretically, all that one can say is that the background flow rate is between zero and about 2/3 of the sampling flow rate (assuming uniform flow in a homogenous plane with constant pumping).

Thus, the evaluated flow rates in Table 5-1 may be somewhat higher, especially the lower flow rates. The uncertainty due to the sampling flow rate decreases with increasing flow and the evaluated flow rate for test 1 (natural gradient) should be less uncertain. Overall, with consideration to uncertainty due to sampling, Table 5-1 indicates that the background flow rates vary approximately between 1–3 mL/h, possibly with the lower part of the range more representative for conditions during the main synthetic SWIW tests (tests 4 and 5).

Each dilution test is discussed in more detail following Table 5-1.

Table 5-1. Results from groundwater flow measurements in KA2858A.

Test number	1 Natural gradient	1 Stressed gradient	2 Natural gradient	3 Natural gradient	4 Natural gradient
Start injection	2010-02-02 12:00		2010-03-31 10:17	2010-09-09 08:42	2010-12-21 09:43
Start flow period in KA2862A		2010-02-09 14:22			
Start measurement	2010-02-02 12:15	2010-02-09 14:12	2010-03-31 10:28	2010-09-09 08:57	2010-12-21 09:54
Stop measurement	2010-02-09 13:59	2010-02-15 13:00 [1]	2010-04-07 09:28	2010-09-15 13:38	2010-12-29 08:00
Length measurement period (h)	170	165	166	149	190
Length of evaluated period (h)	118	70 (early), 60 (late)	134	104	166
Evaluated groundwater flow (mL/h)	3.1	5.4 (early), 2.6 (late)	0.8	0.1 [2]	1.0

[1] The sampling was interrupted by power failure. The exact stop time is unknown.
[2] Uncertain measurement result.

Groundwater flow measurement 1

This measurement is the only one performed prior to the re-instrumentation of the borehole equipment. The results indicate a low natural groundwater flow. There is some influence from the disturbance in KA2858A, but it is not very large.

Since two different sampling intervals was used during the period of stressed gradient, two different sampling flow rates were used since the sample volume is always 6 mL. During the first 3.5 days the sampling flow rate was 3.5 mL/h and during the following 3.5 days the sampling flow rate was 1.6 mL/h. Hence, the evaluation has to be divided into two different periods depending on how large the sampling flow rate was.

The evaluated groundwater flow during the later part of the disturbed period is even somewhat lower than the flow under natural conditions. However, as the flow rates are low there is uncertainty sue to the sampling flow rate, see above. In addition, it is in principle not inconceivable that the flow can decrease if the pumping in a nearby borehole causes a change in flow direction. However, the conclusion is that a hydraulic disturbance in zone NW-3 does not seem to have any major effects on the flow rates in KA2858A, which means that the planned SWIW test can be performed without risk of disturbance from other activities.

Ground water flow measurement 2

The results show a lower groundwater flow than measured prior to the re-instrumentation. The quality of the data appears to be good; hence the deviating results are surprising.

Ground water flow measurement 3

The result must be regarded as uncertain due to the incorrect experimental setup in this test (described in Section 3.1.2). There is a risk that the flow rate is underestimated if concentrated tracer has been leaking into the sampled water.

Groundwater flow measurement 4

During a major part of the measurement period the sample volume in the tubes varied, which means that the sample flow has varied. The reason for this is not known, but it can either be something wrong with the regulation unit, or that something has been partly clogging the thin hose to the sampler. During the last 54 hours of the measurement period the sample flow rate was constant, but there are nonetheless variations and uncertainties of the measured sample concentrations. It seems as the varying flow rate have caused uncertainties in the measured concentrations. The data points are more scattered than during the other measurements, which results in larger uncertainties of the interpretation of the groundwater flow. The evaluation is shown in Figure A1-8 in Appendix 1. The evaluated groundwater flow is 1.0 mL/h. The sampling flow rate varied, but the mean value was about 1.5 mL/h.

5.1.3 Chemical analyses

The results from the chemical analyses are presented in Appendix 2. The charge balance error was small ($< \pm 5\%$) for all samples except the ones taken during the beginning of the two main tests when the nitrate concentration is very high. Here, the charge balance error was very high due to problems with analyses of the high nitrate concentrations.

Ten of the twelve water samples taken during the synthetic SWIW project represent the natural water composition, i.e. background (or near background) concentrations. Only the samples taken during the beginning of the withdrawal periods in SWIW 4 and SWIW 5 represent water mainly consisting of synthetic water. Figure 5-4 shows the concentrations of Na, Ca and Cl in these ten samples, which shows that the concentrations are fairly stable over time. The pumped volume before the samples are taken varies between 2 and 1,500 L, which indicates that the background water composition is fairly homogenous around the borehole section.
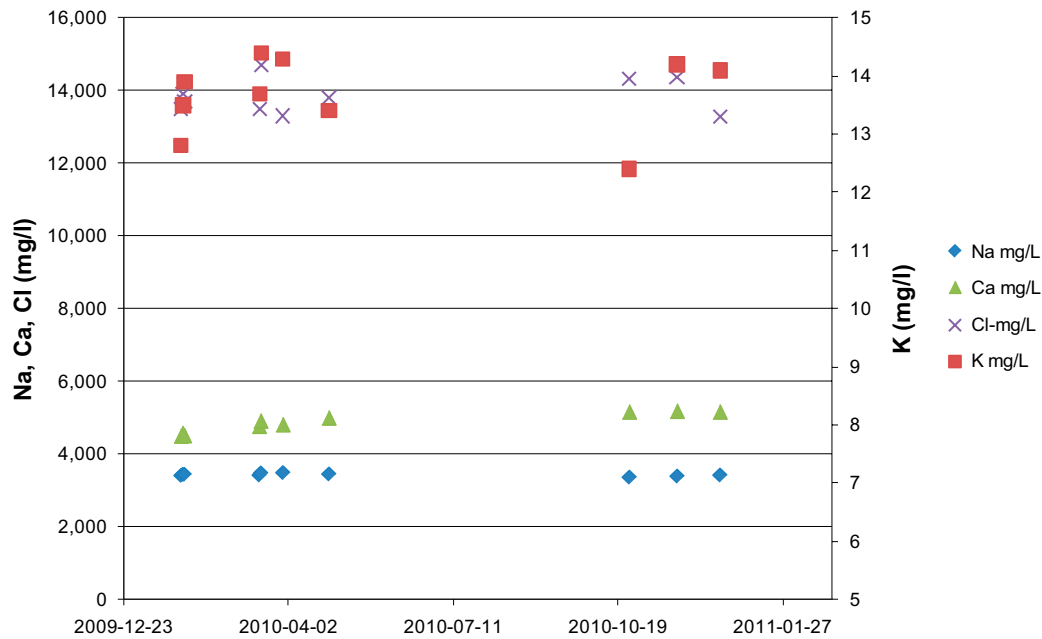
Figure 5-4. *Results of the ten samples taken during the whole synthetic SWIW project representing background conditions. Discharged volumes varies from 2 to 1,500 L.*

5.2 Preparatory SWIW tests

The performance of the three preparatory SWIW test is described in Section 3.3. A single tracer was used in each of the preparatory tests. Uranine was used in SWIW tests 1 and 3, while Amino-G acid was used in SWIW test 2. Both of these tracers are known to be reliable conservative tracers in this kind of rock environment. The reason for using Amino-G in SWIW test 2 was to avoid potential interference with any remaining Uranine from SWIW test 1. A summary of the main experimental features of the preparatory SWIW tests is provided in Table 5-2.

The resulting breakthrough curves from all three preparatory tests are shown in Figure 5-5, which is plotted with pumped volume/total injected volume on the x-axis in order to compare results from tests with different total injection volumes. These results were the main basis for planning and design of the main SWIW tests (test 4 and 5).

After completing SWIW test 1 and 2, it was found that the difference between the breakthrough curves were very small, despite that SWIW test 2 employed a waiting phase of 48 hours. In fact, it appears as if the curve for SWIW test 2 differs in the "wrong" way compared with SWIW test 1. However, some of these differences might also be attributed to the fact that different tracer injection procedures were employed in SWIW tests 1 and 2, respectively.

Based on the results from SWIW tests 1 and 2, it was decided to run an additional preparatory test (SWIW test 3), with a further increase of the waiting phase duration. This resulted in a significantly larger difference in the breakthrough curve, in the beginning of the curve (Figure 5-5) as well as in the late-time values at low concentration (Figure 5-6).

Table 5-2. Main experimental features of preparatory SWIW tests.

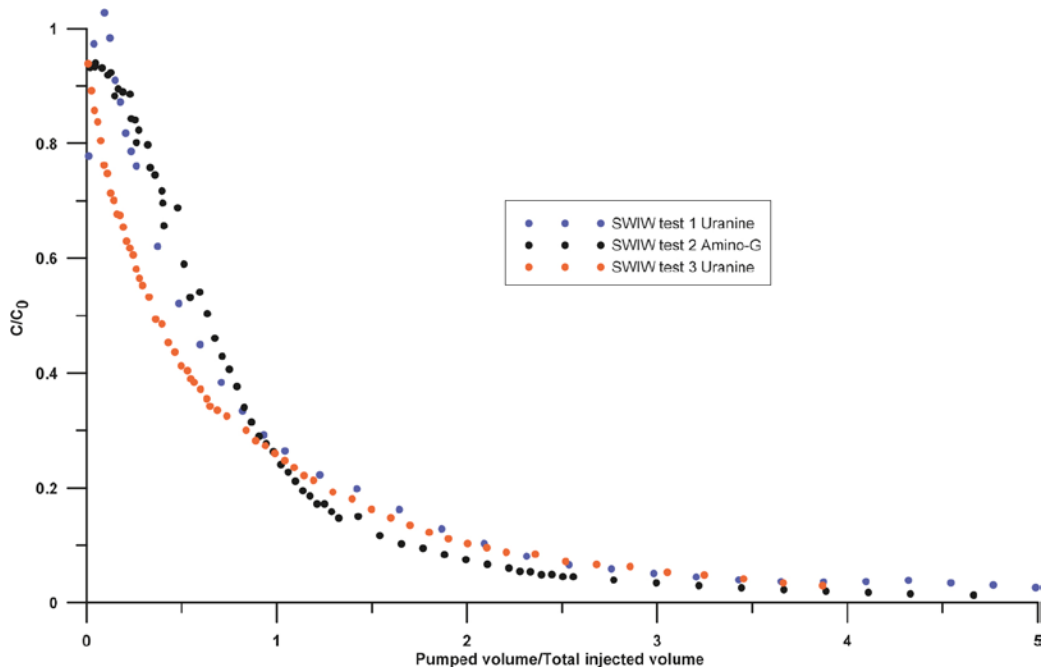| Test	Tracer	Total injected volume (L)	Waiting phase duration (hours)
SWIW 1	Uranine	15.6	0
SWIW 2	Amino-G	16.3	48
SWIW 3	Uranine	16.9	91

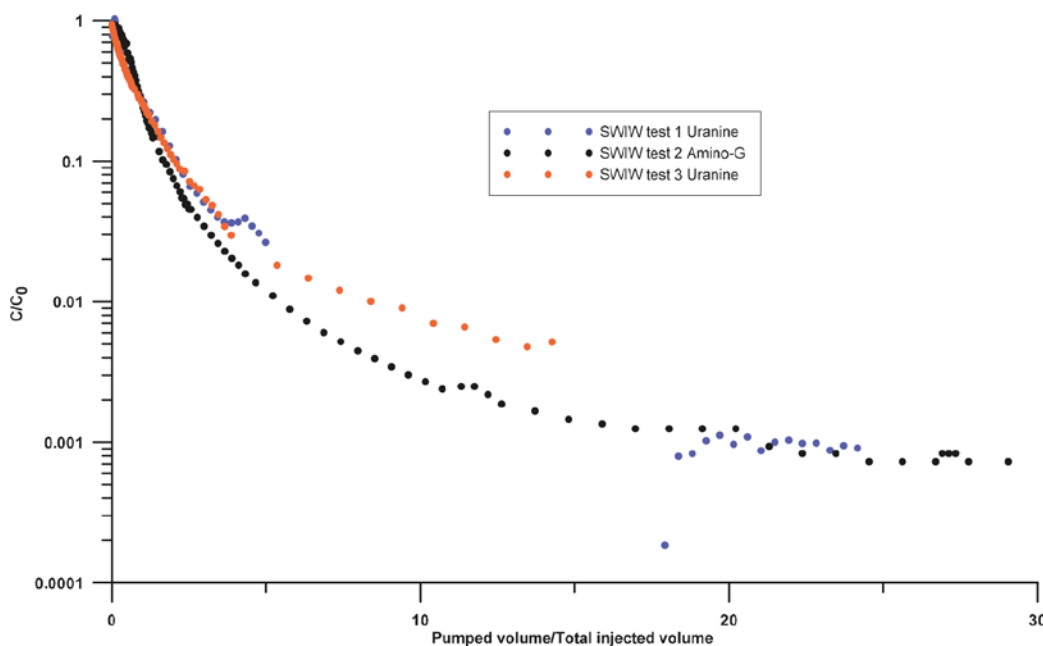***Figure 5-5.*** *Breakthrough curves for preparatory SWIW test 1, 2 and 3.*

Figure 5-6. *Semi-logarithmic plot of breakthrough curves for preparatory SWIW test 1, 2 and 3.*

In all three preparatory tests, the tracer recovery is very similar and approach complete recovery at the end the sampling. Based on this, in combination with the breakthrough results, it was decided to run the main synthetic SWIW tests with the longer waiting phase duration. Further, it was also decided to increase the total injected volume in order to possibly decrease the theoretical effective dispersion effect (see Equation 2-4), with the purpose of further increasing the possibility to distinguish differences between tests with and without a waiting phase.

The subsequent performance of the main SWIW tests (4 and 5) showed, however, that Uranine behaviour during all of the synthetic SWIW tests was highly uncharacteristic and not typical for a conservative non-sorbing tracer. Thus, much of the planning and design for the main tests was based on misleading information due to the anomalous behaviour of Uranine. This is analysed in more detail and further commented on in Section 6.1.4.

6 Results of main SWIW tests

6.1 Overview of results

6.1.1 SWIW test 4, without waiting period

An overview of the tracer breakthrough results for added and removed tracers are shown in Figure 6-1, which shows normalized concentrations plotted against elapsed time from start of the recovery phase. For added tracers, concentrations are normalized by the injection concentrations for each tracer, which are based on samples taken during the tracer injection. For removed tracers, values are normalized using the apparent steady-state plateau at later times. The time axis is shown in logarithmic scale in order to increase visibility.

Tracers generally behave as expected. Added and removed tracers are basically a mirror image of each other. Of the added tracers, i.e. the tracers starting at $C/C_0 = 1$ and then declining, a notable unexpected behaviour is observed for Uranine. Uranine was intended to be used a non-sorbing tracer and was also used in two of the preparatory tests (SWIW tests 1 and 3). Uranine would be expected to behave approximately as NO_3 or the possibly weakly sorbing tracers Li and Mg. However, Figure 6-1 shows that Uranine behaves more like the relatively strongly sorbing tracers Cs and Rb.

The early part of the breakthrough curve for potassium, K, is affected by a high detection limit.

A more detailed plot, with the intention of better visualizing differences between the various break-through curves, of added tracers is shown in Figure 6-2. For comparison purposes, a generic plot with simulated breakthrough curves with varying fracture retardation factors (i.e. no matrix) are shown in Figure 2-4. An obvious qualitative judgement that the results for Cs and Rb indicate relatively strong retardation, which also is expected, Figure 6-2 also highlights the anomalous behaviour of Uranine. The remaining tracers, Li, Mg and NO_3, show similar breakthrough, indicating that they all behave approximately as non-sorbing tracers.
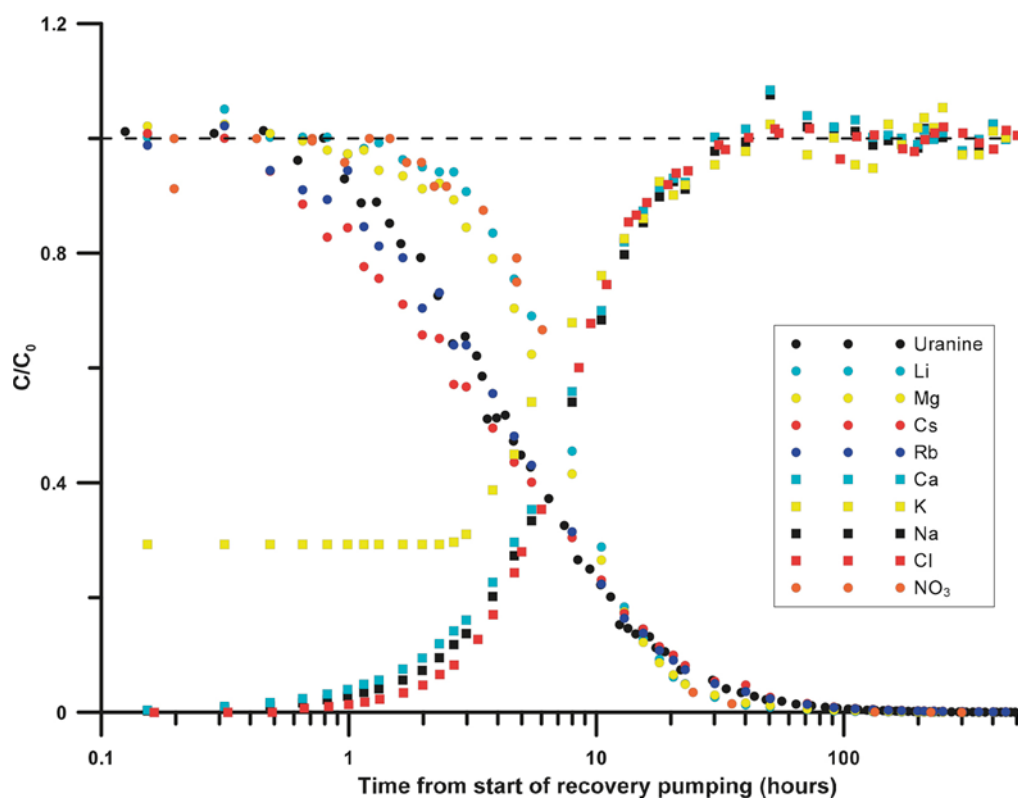

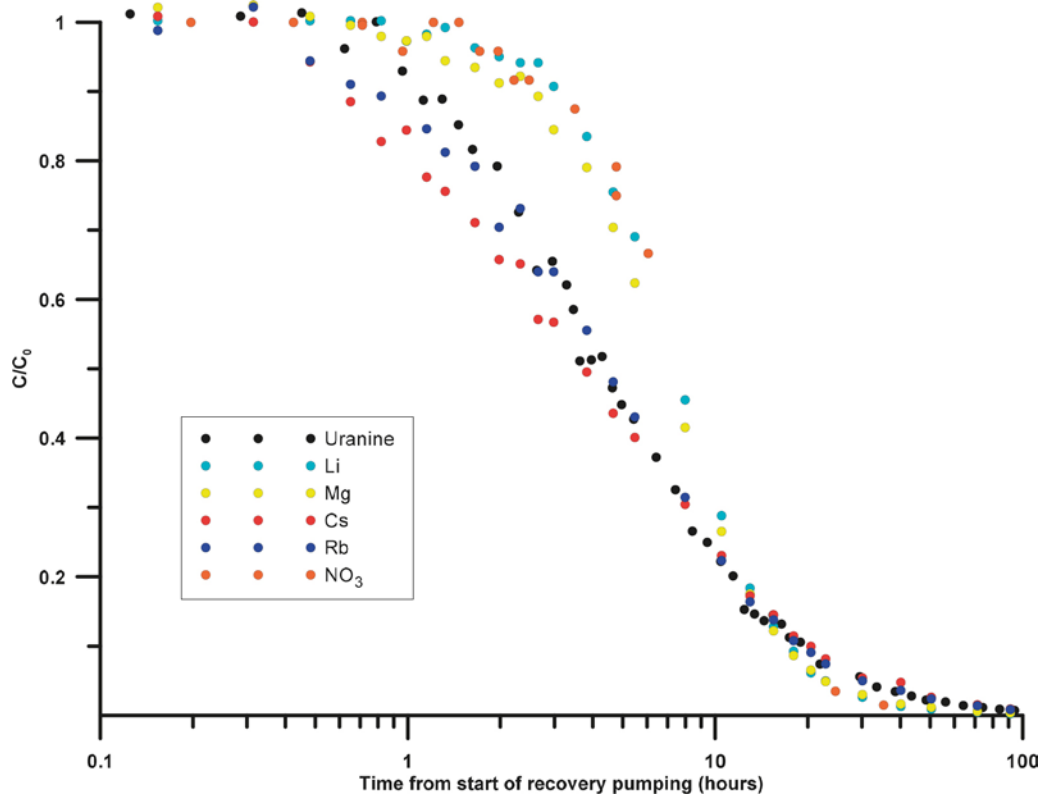*Figure 6-1.* *Overview of results from SWIW test 4.*

Figure 6-2. *Detailed plot of breakthrough curves added tracers in SWIW test 4.*

A more detailed plot of removed tracers is shown in Figure 6-3. The breakthrough curves for sorbing and non-sorbing tracers, respectively, may be expected to differ in an analogous way as for added tracers. Qualitatively, one may discern slightly different retardation among the removed tracers. Retardation seems to increase in the order of Cl, Na and Ca. Comparisons with K is more difficult because of the high detection limit, but from the data above the detection limit, K appears to be strongest sorbing removed tracer.

6.1.2   SWIW test 5, with waiting period

An overview of the tracer breakthrough results for added and removed tracers are shown in Figure 6-4, which shows normalized concentrations plotted against elapsed time from start of the recovery phase. For added tracers, concentrations are normalized by the injection concentrations for each tracer, which are based on samples taken during the tracer injection. For removed tracers, values are normalized using the apparent steady-state plateau at later times. The time axis is shown in logarithmic scale in order to increase visibility.

As for SWIW test 4, tracer breakthrough results are about as may be expected. The main difference compared with SWIW test 4 is that concentrations at early times differ more and the difference between sorbing and non-sorbing tracers appears to be more clearly visible. This is also expected as the purpose of the employed waiting time is to magnify differences among the tracers. A clear difference from SWIW 4 is that added tracers start at lower C/C_0 and removed tracers start at higher $C/C_0.$ This is consistent with prior expectations of what might happen during the waiting phase of the experiment due to diffusion effects.

6.1.3   Comparison of SWIW test 4 and SWIW test 5

Comparisons of individual tracers in lin-log plots are shown in Figure 6-5 for added tracers and Figure 6-6 for removed tracers, respectively. For each of the tracers, there is a clear difference between SWIW test 4 and SWIW test 5. The differences are qualitatively consistent with the prior hypothesis of diffusive mass-transfer during the waiting phase (Nordqvist et al. 2008). This is discussed further in sections 6.4 and 6.5.
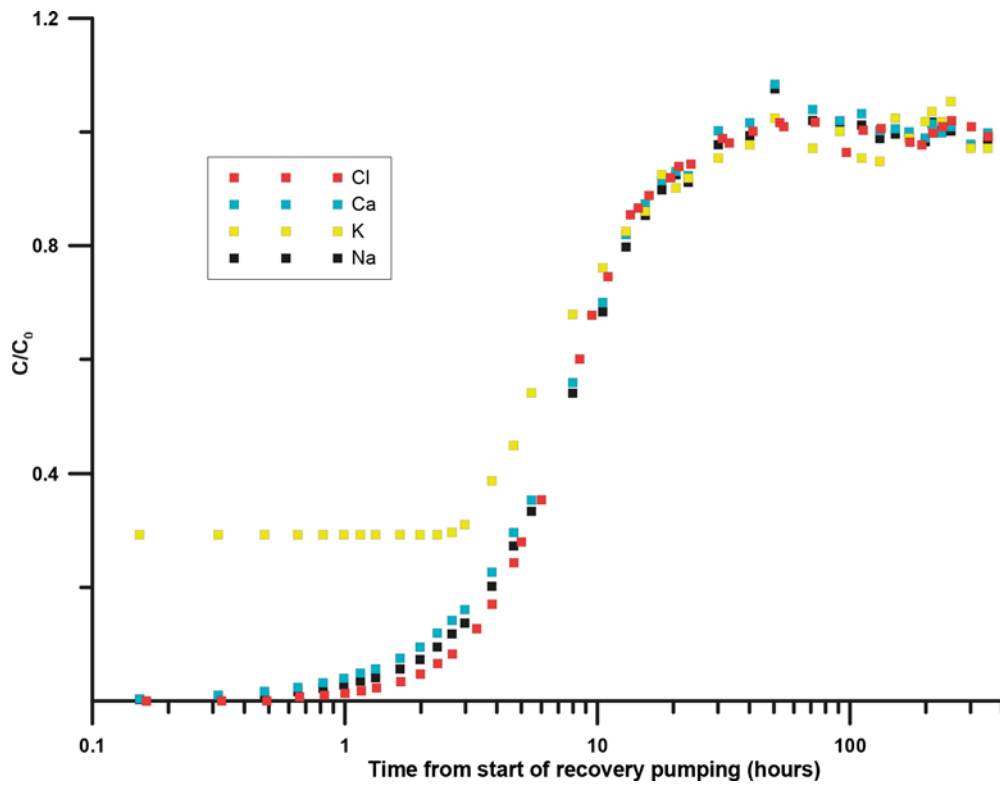
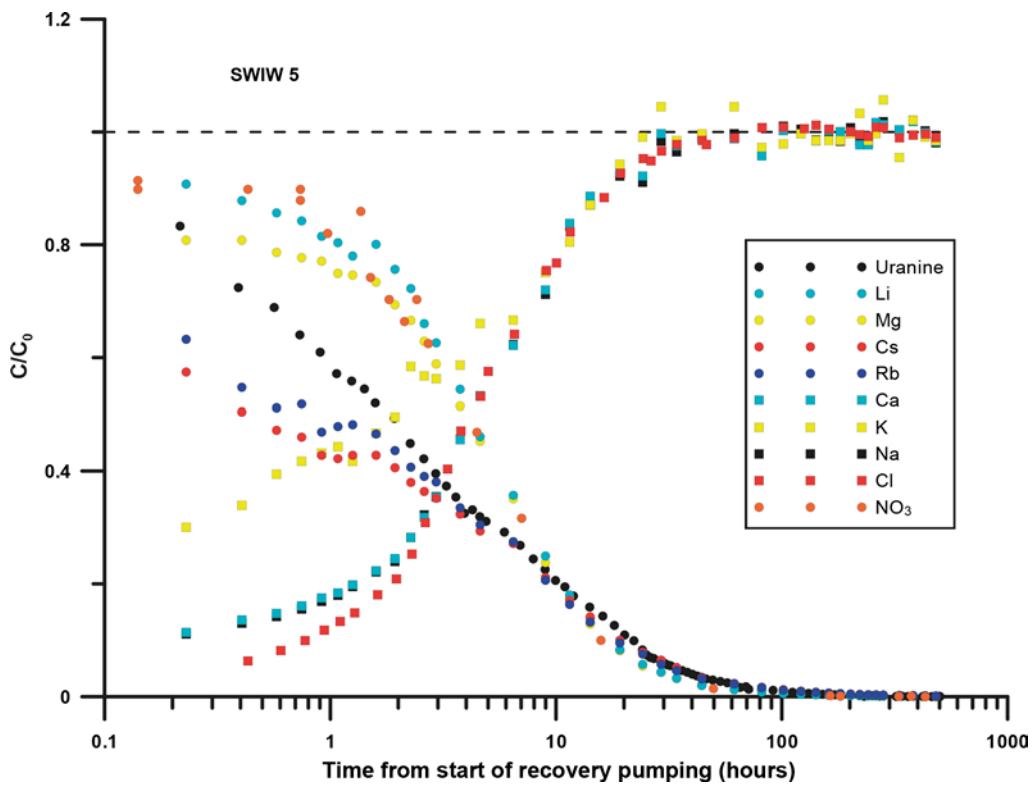**Figure 6-3.** *Detailed plot of breakthrough curves for removed tracers in SWIW test 4.*

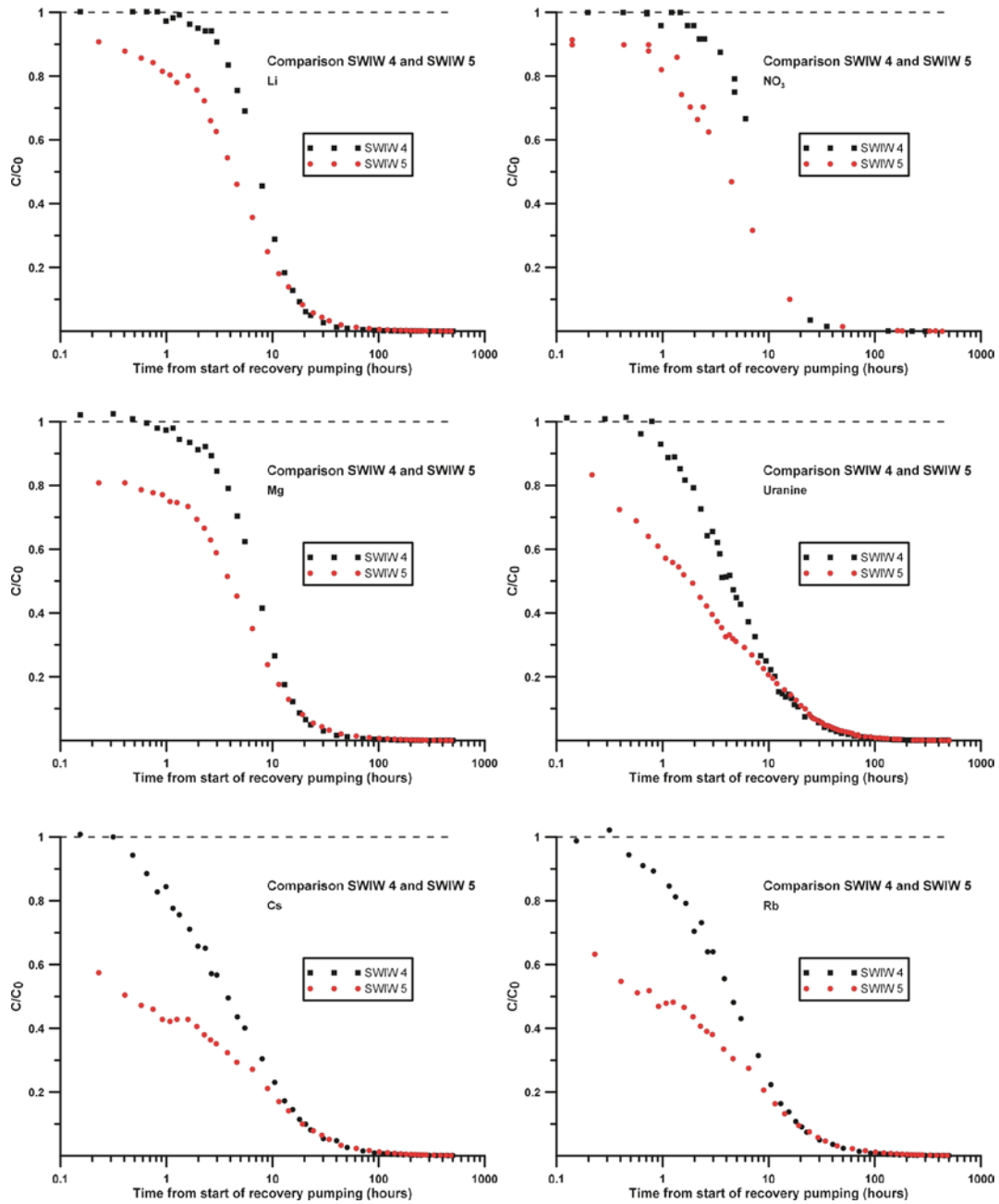**Figure 6-4.** *Overview of results from SWIW test 5.*

Figure 6-5. Comparison of SWIW 4 and SWIW 5 results for added tracers.

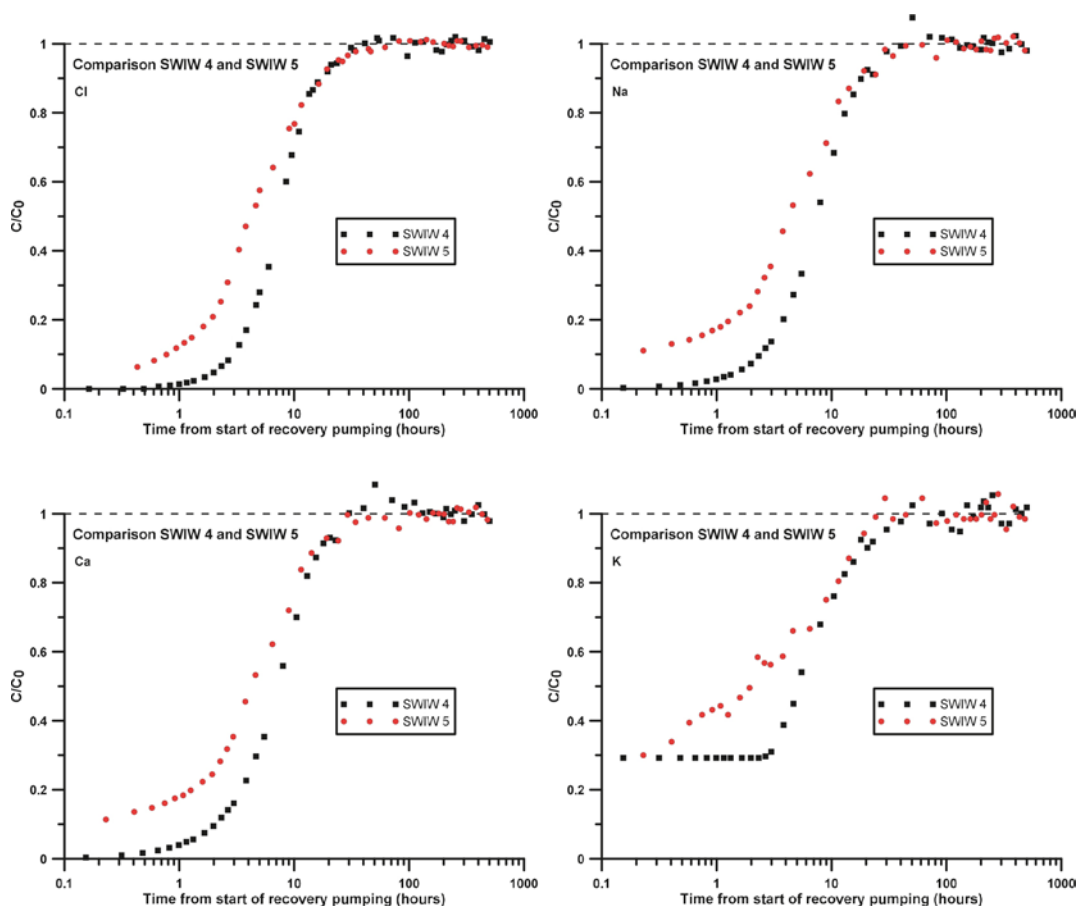***Figure 6-6.*** *Comparison of SWIW 4 and SWIW 5 results for removed tracers.*

6.1.4 Comparison of SWIW test 4 and SWIW test 5 with preparatory tests (SWIW test 1, 2 and 3)

The preliminary SWIW tests (preparatory tests) were carried out employing a single non-sorbing tracer in each of the tests. SWIW tests 1 and 3 used Uranine as a tracer while Amino-G was used in SWIW test 2. Because the anomalous behaviour of Uranine during the main SWIW tests, i.e. behaving approximately as a relatively strongly sorbing tracer, it is of considerable interest to compare Uranine results in the preparatory tests and main tests, respectively. Uranine is known to be a very reliable choice as a conservative tracer and has in other tracer experiment resulted in practically identical breakthrough curves as other conservatives or very weakly sorbing tracers, such as Li (Lindquist et al. 2008). Also in previous SWIW tests within the site investigation programme (Nordqvist 2008), there were no indications that Uranine would behave as a non-conservative tracer.

The unexpected behaviour of Uranine is apparently not specific for SWIW 4. A comparison of SWIW test 1 and SWIW test 4 (the only tests without a waiting phase) in Figure 6-7 shows very similar behaviour of Uranine in both of the tests. A small difference may be expected because SWIW test 1 and SWIW test 4 employ different injection volumes, which would give slightly different values of the dimensionless dispersion parameter, φ (see Section 2.1). However, it is difficult to discern any such differences between the breakthrough curves, especially as the beginning of the breakthrough curve for SWIW test 1 might be affected by the fact that a different injection procedure was used in SWIW test 1 than the other tests. Note that the x-axis is scaled in order to facilitate a direct comparison between the tests.

The cause for the uncharacteristic Uranine behaviour is at present not known. Checks were made of the spectrofluorometer calibration curves, which were found to be accurate. Further, the Uranine used in the various tests were prepared in different batches and originated from different containers. One possible environmental effect might be water chemistry conditions at the site. However, the uncharacteristic behaviour of Uranine is observed regardless of whether the injection solution is

prepared with native groundwater (SWIW tests 1 and 3) or with synthetic groundwater (tests 4 and 5). Another consideration regarding Uranine is that full complete recovery is indicated in all of the tests, which would suggest some kind of retardation (sorption) process rather than degradation of Uranine.

Because Figure 6-7 suggests that the behaviour of Uranine may somehow be related to site environmental conditions, it is of interest to re-examine the results of SWIW test 2, which was performed with the tracer Amino G acid. The preparatory tests (SWIW tests 1, 2 and 3) were carried out in order to optimize experimental procedures for the main SWIW tests. After the completion of SWIW test 2, an important result was a comparison of SWIW tests 1 and 2, the latter employing a waiting phase of 48 hours. The resulting breakthrough curves from these two tests showed very similar results, which was taken as an indication that the employed waiting phase was not sufficiently long to distinguish possible effects of diffusive mass transfer. This led to the decision to perform an additional preparatory test, with a waiting phase of 91 hours. In retrospect, with the knowledge of Uranine giving misleading results (as a conservative tracer), one may conclude that the comparison between SWIW test 1 and 2 was not relevant. Figure 6-8 shows a plot of the results of SWIW test 1 and SWIW test 2 (also shown earlier in Section 5.2) together with the breakthrough curve of Li from SWIW test 4. The breakthrough for a conservative tracer should have been much more similar to Li in SWIW test 4 than the actual Uranine curve from SWIW test 1. Figure 6-8 then indicates that the waiting period of 48 hours in SWIW test 2 indeed has a visible effect on the breakthrough curve during the recovery phase.

Although Uranine has been found to not act as conservative tracer, it should be possible to, at least qualitatively, compare Uranine results from different tests. Figure 6-9 shows that the difference between Uranine in test 1 (no waiting phase) and test 3 (91 hours waiting phase) is about as can be expected, assuming that diffusive mass transfer away from the fracture takes place during the waiting phase. However, the difference between SWIW 3 and SWIW 5 is not consistent with this interpretation. These tests employ about the same waiting periods (91 and 93 hours, respectively) and differ only in the total injected volume. The expected effect of this would be a decrease the dimensionless dispersion parameter, φ, which in turn should result in a slightly longer "plateau" in the beginning of the breakthrough curve followed by a slightly steeper descent, see Section 2.1. This would occur even in the presence of matrix diffusion and linear sorption. Instead of the afore-mentioned effect of decreased dispersion, the SWIW 5 breakthrough curve begins at an even lower level. A possible explanation for this might be that the background flow affects the breakthrough during the waiting phase.
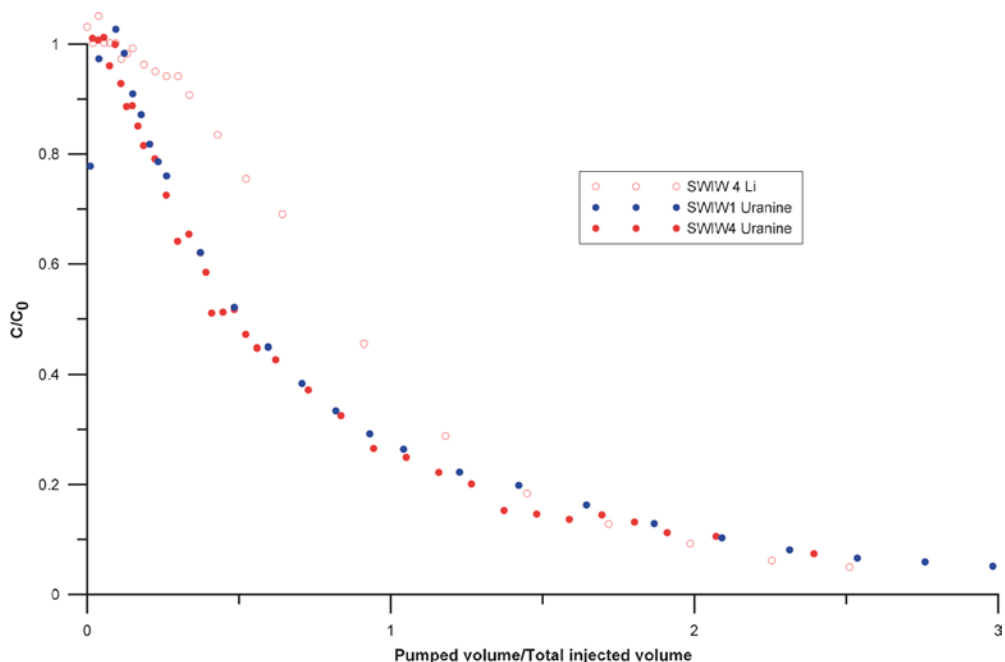

Figure 6-7. *Comparison of Uranine breakthrough in SWIW test 1 and SWIW test 4. Li from SWIW test 4 is shown as a reference representing a conservative tracer.*
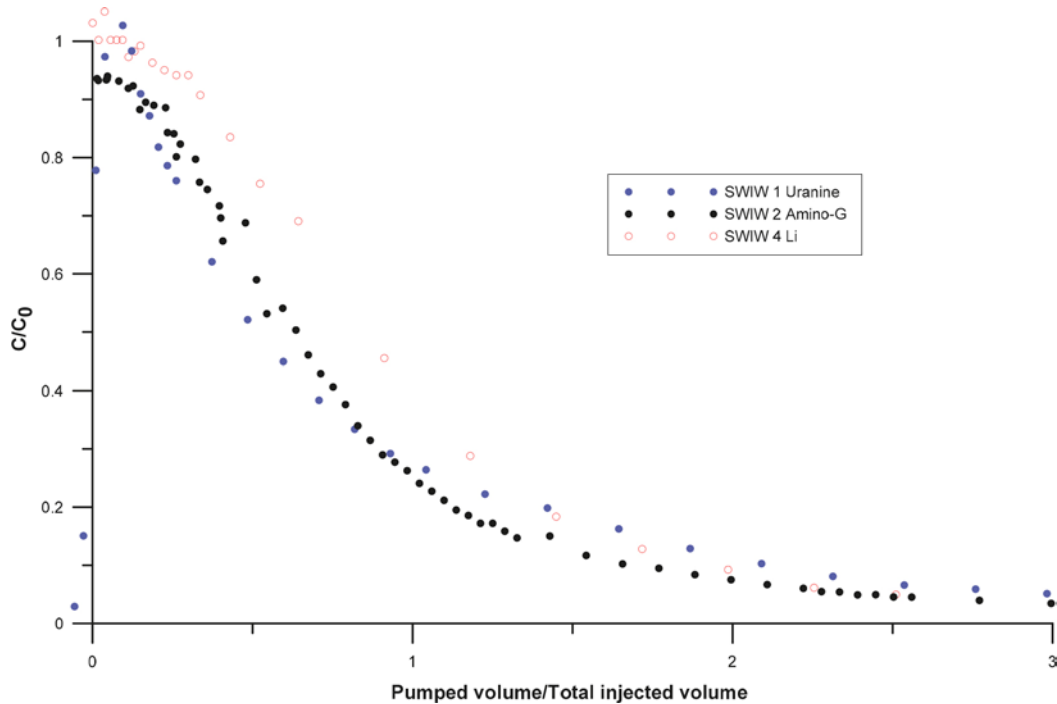
Figure 6-8. *Comparison of results from SWIW test 1 (Uranine), SWIW test 2(Amino-G) and Li from SWIW test 4. The latter is thought to better illustrate conservative tracer behaviour in SWIW test 1 than the actual results for Uranine.*
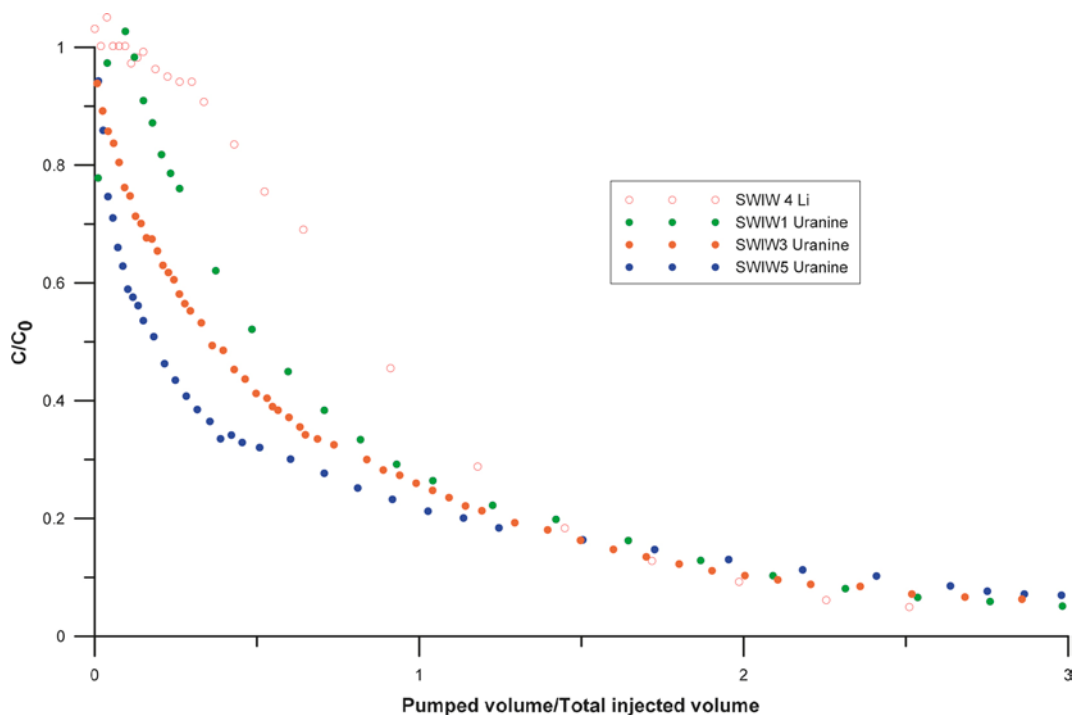

Figure 6-9. *Comparison of results for Uranine. The results of Li from SWIW test 4 is shown as a reference representing a conservative tracer without waiting phase.*

The results from the second preparatory test, SWIW test 2, may be compared with a conservative tracer (other than Uranine) from SWIW test 5. Figure 6-10 shows a comparison of Amino-G from SWIW test 2 and Li from SWIW test 5 (again Li from SWIW test 4 is included as a reference for a conservative tracer without a waiting phase). In this case it is more difficult to make a straight-forward comparison as the tests differ both in total injected volume as well as in the duration of the
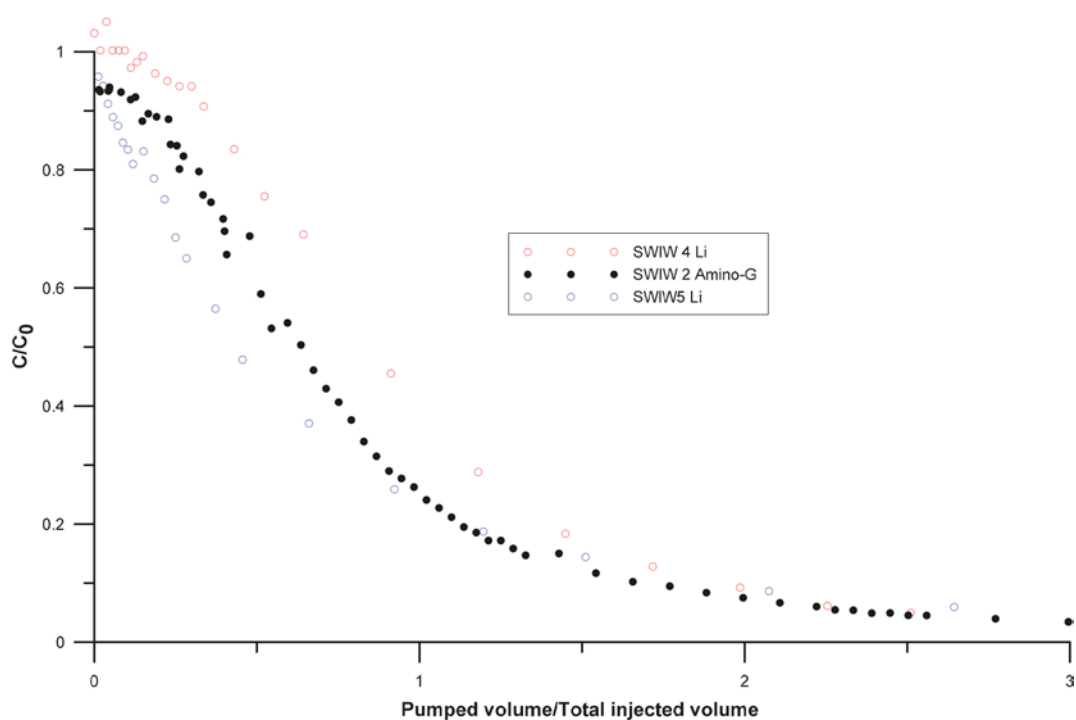
Figure 6-10. *Comparison of tests with a waiting phase and other conservative tracers than Uranine. The results of Li from SWIW test 4 is shown as a reference representing a conservative tracer without waiting phase.*

waiting period. In this case the results are approximately consistent with increasing time available for diffusive mass transfer. SWIW test 5 employs a larger injected volume but the effect of this is probably minor compared with the increased duration of the waiting period. However, the very beginning of the Amino-G recovery curve shows a plateau that does not appear to "fit" as a case in-between the other two curves in the plot. This might possibly be another indication that the background flow affects the tracer behaviour.

The comparison of preparatory SWIW test results (SWIW tests 1, 2 and 3) with the main SWIW tests (tests 4 and 5) has shown how the anomalous behaviour of Uranine resulted in misleading information for further experimental planning after the two first preparatory tests. In particular, the conclusion that the shorter waiting phase (48) was not sufficient for the waiting phase to have a visible effect on tracer breakthrough may have been different with a more "normal" Uranine behaviour. In retrospect, the additional SWIW test (test 3) might not have been necessary. On the other hand, experimental data from SWIW test 3 strengthen the speculation that the background flow has a notable effect on tracer breakthrough, especially during the waiting phase. If this is the case, it is very important for further and more detailed evaluation of the main SWIW test results. Section 6.3 further below deals more extensively with issues concerning the influence of background flow on the SWIW test results.

6.1.5 Radon results

Results from the radon measurements during SWIW test 4 (Figure 6-11) and SWIW tests 5 (Figure 6-12) are shown below. Although radon data is not further analysed herein, a preliminary comment is that it might potentially be useful in verifying that time-dependent processes are important for the results. The difference between Rn and Cl appears to be larger in SWIW 5, which would be consistent with the hypothesis of Rn production during the waiting phase. The early parts of the curves seem consistent with previous scoping calculations (Nordqvist 2009), but the later parts of the Rn breakthrough data in SWIW 4 seems questionable. The C_0-value is based on two samples before SWIW 4 injection. If instead the last Rn measurements are more representative (it is not inconceivable that they form a plateau but data are too few to be conclusive) for the background Rn (i.e. steady-state concentration in the fracture), then the curves would look more like expected.
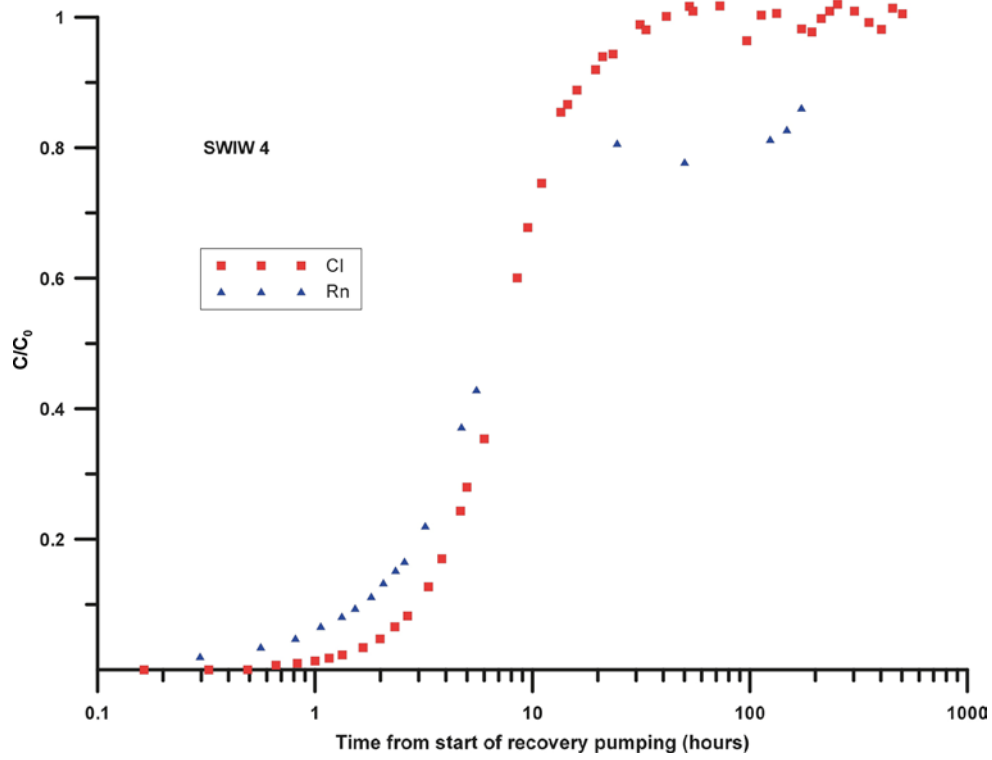
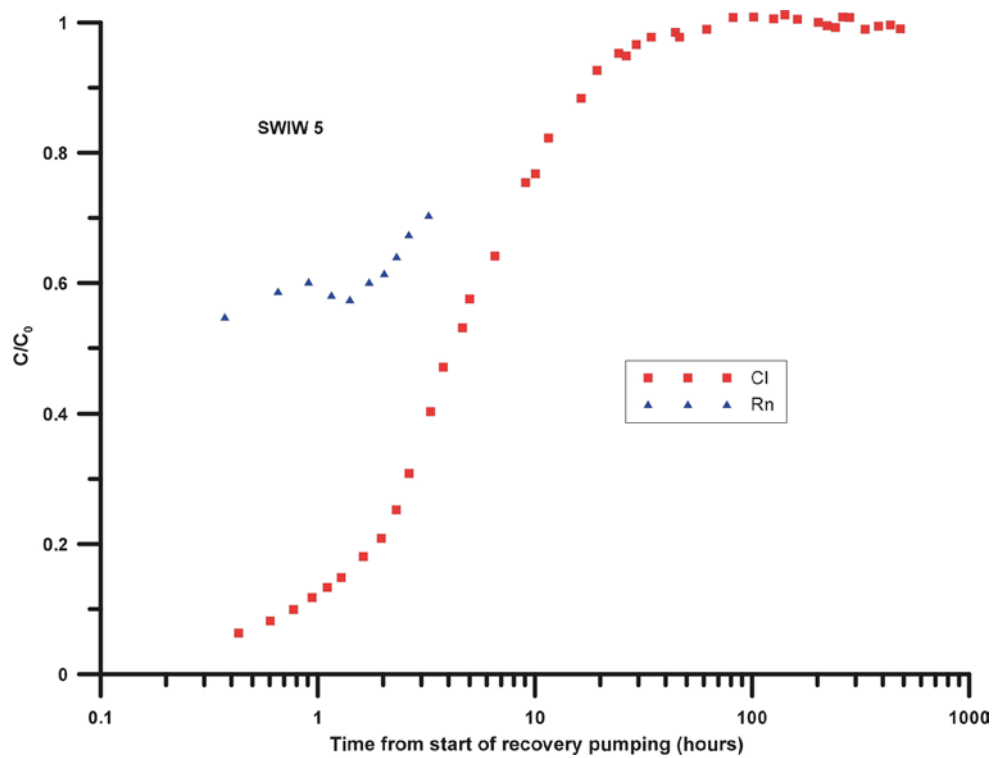*Figure 6-11.* *Experimental results for radon and chloride in SWIW test 4.*

Figure 6-12. *Experimental results for radon and chloride in SWIW test 5.*

6.2 Basic analysis without matrix diffusion

6.2.1 SWIW test 4

As was discussed in Chapter 2, if advection and dispersion are the only transport mechanisms, the breakthrough curve from a SWIW experiment may be described using a single parameter group comprising aperture, dispersivity and injected water volume. An obvious first step in the analysis of experimental results is to investigate how much of the data can explained solely by advection and dispersion. This was done for some of the tracers that may be considered conservative or very weakly sorbing (such as Li). Only data from SWIW test 4 was considered here because it is visually apparent from the experimental curves that additional transport mechanisms occur during SWIW test 5.

Best-fit modelling using an advective-dispersive transport model in a radial flow geometry (see Section 4.4) was carried out for Li, NO_3 (added tracers) and Cl (removed tracer). A single estimation parameter was considered, i.e. the effective dispersion parameter φ ($= a_L^2 \delta/V_{inj}$). In practise, this was accomplished by using a fixed value of simulation model aperture of 0.001 m and estimating the longitudinal dispersivity. The injected volume was given as input to the model and equal to the actual experimental injection volume.

The results of the purely advective-dispersive modelling of conservative tracers are shown in Figure 6-13 (NO_3), Figure 6-14 (Li) and Figure 6-15 (Cl).

Overall, model fit to experimental data in the preceding figures is very good. Estimated values for the product $a_L^2 \delta$ vary within $(5.2–5.7) \cdot 10^{-5}$ m^3 for all three tracers (Cl: $5.2 \cdot 10^{-5}$; Li: $5.5 \cdot 10^{-5}$; NO_3: $5.7 \cdot 10^{-5}$). For example, assuming an aperture value of 0.001 m results in a range in dispersivity values of 0.23–0.24 m, which means that all three tracers give almost identical values for the effective dispersion parameter. Thus, both added and removed non-sorbing tracers, in SWIW 4, give results that are consistent and to a large extent explained by simple radial advection and dispersion model. However, this is not true for the low concentrations at late-time breakthrough for the added tracers, which will be further discussed in Section 6.4.
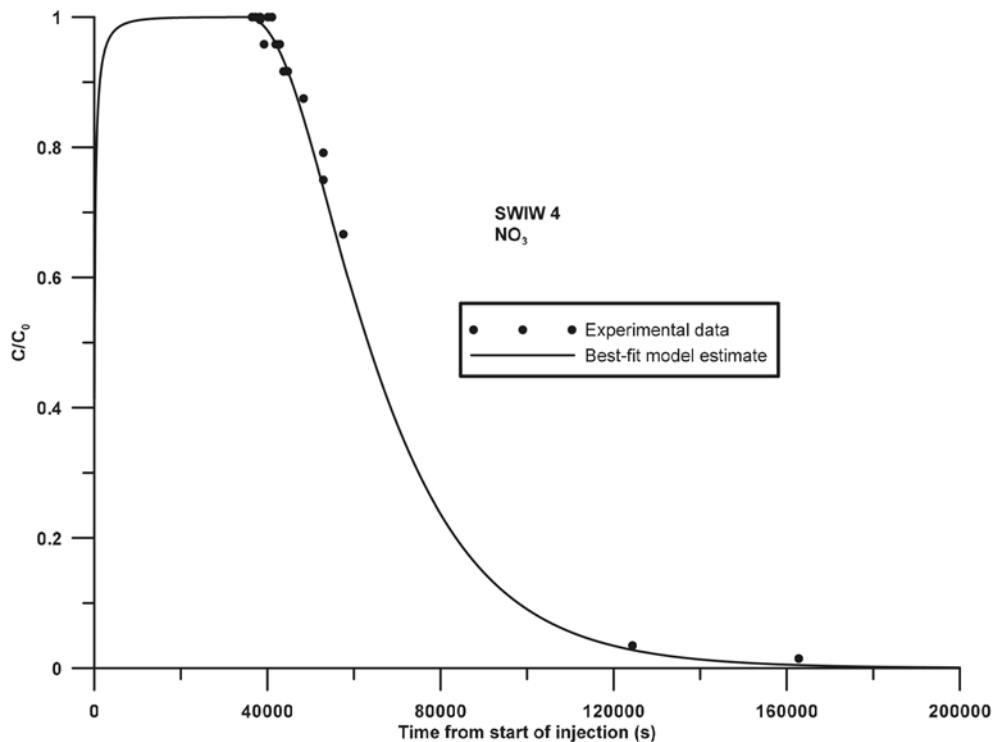

Figure 6-13. *Best-fit model estimate of NO_3 breakthrough in SWIW test 4.*
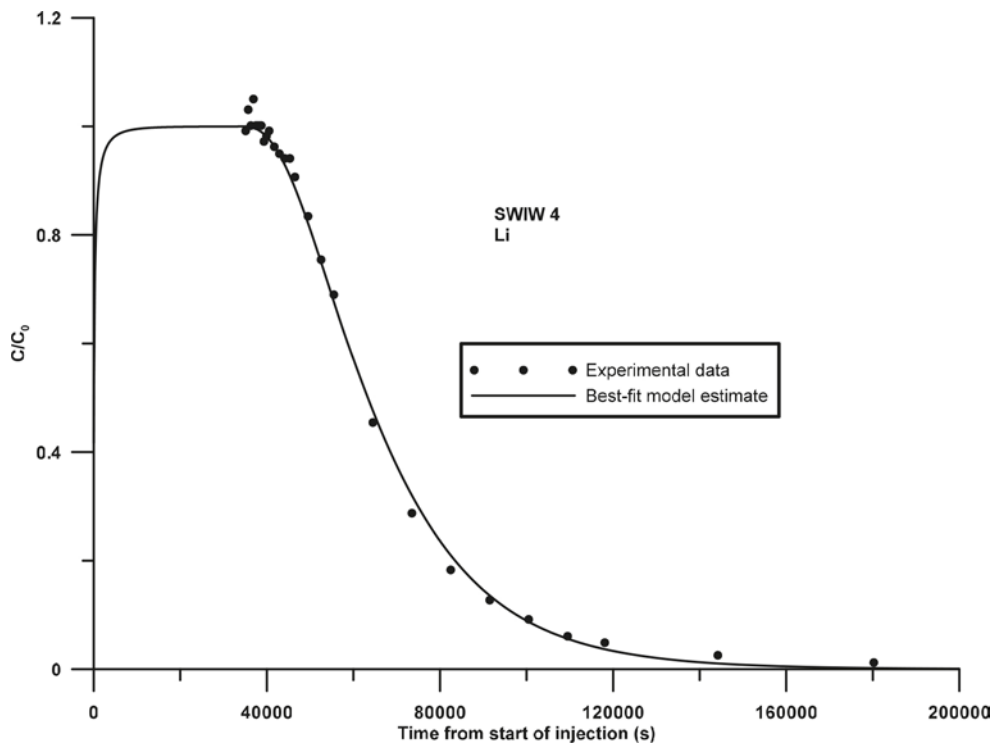
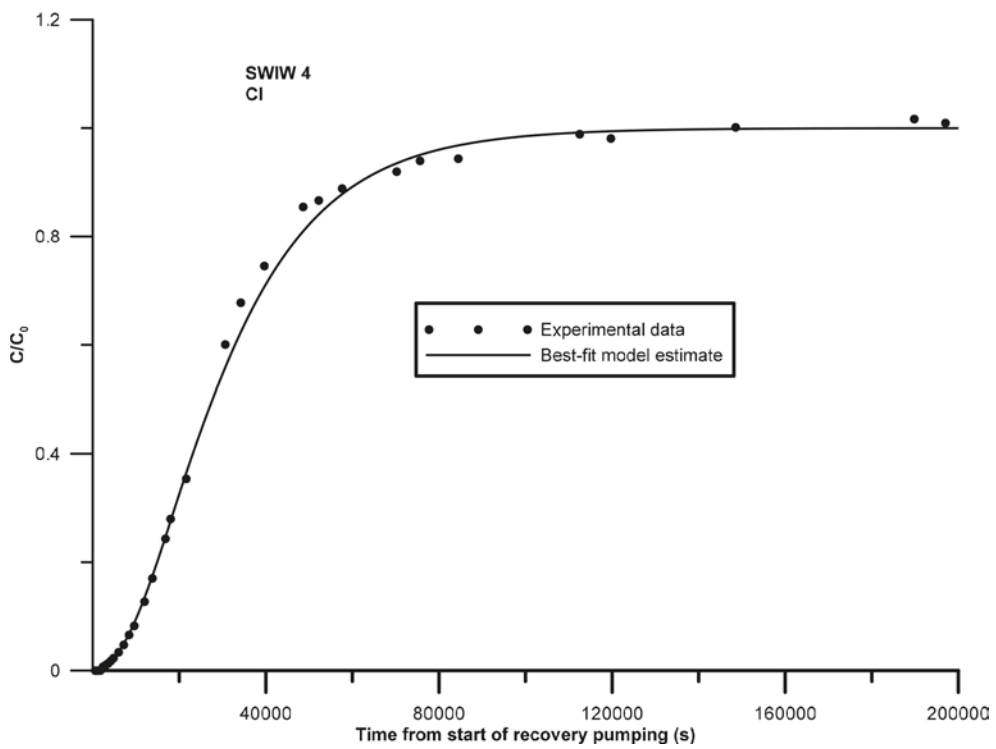**Figure 6-14.** *Best-fit model estimate of Li breakthrough in SWIW test 4.*

Figure 6-15. *Best-fit model estimate of Cl breakthrough in SWIW test 4.*

Because non-sorbing tracers are largely explained by a simple advection-dispersion model, a first approach would be to evaluate sorbing tracers in SWIW test 4 using the traditional linear equilibrium sorption added to the basic radial advection-dispersion model. This entails estimation of the fracture retardation factor, R_f, for each sorbing tracer.

Retardation factors may be estimated only in the presence of breakthrough data for a non-sorbing tracer. On this case, NO_3 was chosen as non-sorbing for the added tracers and Cl as non-sorbing for the removed tracers. The estimated retardation factors are thus a measure of how the other tracers are retarded relative to NO_3 and Cl, respectively.

Two estimation parameters were applied in each case: the effective dispersion parameter, φ, and the fracture retardation factor, R_f. The effective dispersion parameter was also evaluated for NO_3 and Cl individually.

The results are shown in the following six figures (Figure 6-16 to Figure 6-21). The first three figures show added tracers and the remaining three show removed tracers (Li was not considered to be a sorbing tracer in this case). The values of the estimated retardation factors are shown in Table 6-1, which indicates that Mg, Na and Ca are weakly sorbing tracers while Cs, Rb and K are relatively strongly sorbing. The tracers Cs and Rb were used in most of the SWIW experiments that were carried during the site investigation program and these tracers were in all tests found to be strongly sorbing but within a very large range. Evaluated retardation factors varied between approximately 10 – 1,000 for Cs and Rb in the site investigation SWIW tests (Nordqvist 2008). Thus, the evaluated retardation factors obtained here from SWIW test 4 (10.2 for Rb and 14.6 for Cs) are at the lower end (i.e. least sorbing) of the site investigation range.

The anomalous behaviour of Uranine has been commented on earlier, and its overall behaviour could be indicative of a sorbing tracer. However, retardation modelling of Uranine is not presented here because it, despite the evidence in experimental data, might be questioned as sorbing tracer. A regression simulation with Uranine, not shown here, gave a retardation factor of about nine.
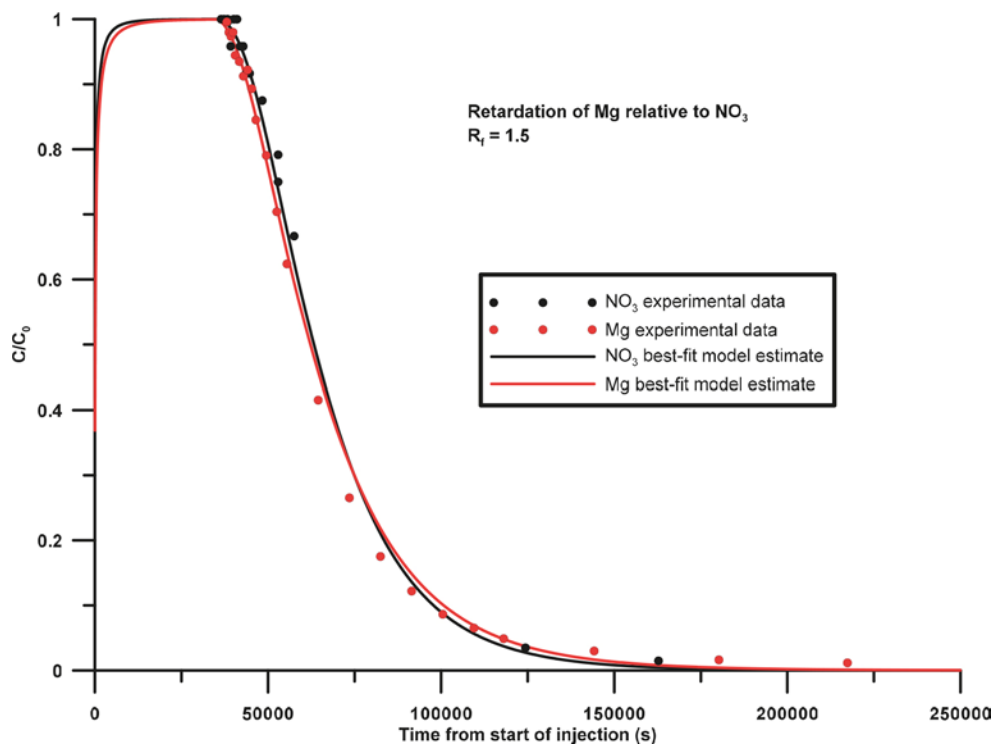

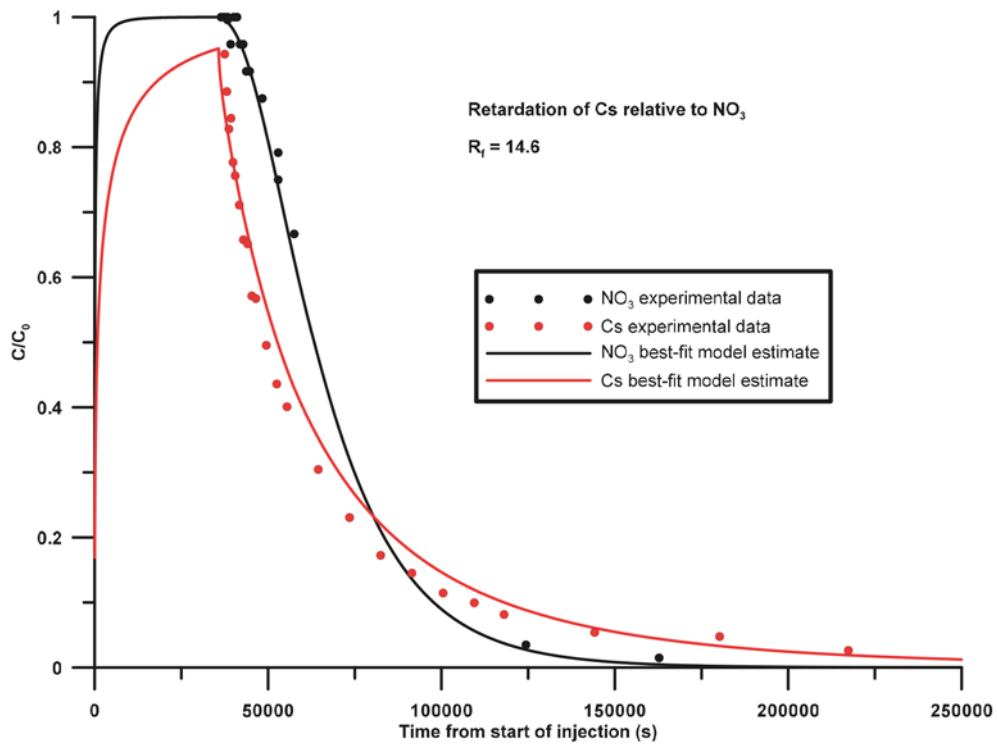***Figure 6-16.*** *Best-fit modelling results for retardation of Mg in SWIW test 4.*

Figure 6-17. *Best-fit modelling results for retardation of Cs in SWIW test 4.*

Figure 6-18. *Best-fit modelling results for retardation of Rb in SWIW test 4.*

Figure 6-19. *Best-fit modelling results for retardation of Na in SWIW test 4.*

Figure 6-20. *Best-fit modelling results for retardation of Ca in SWIW test 4.*

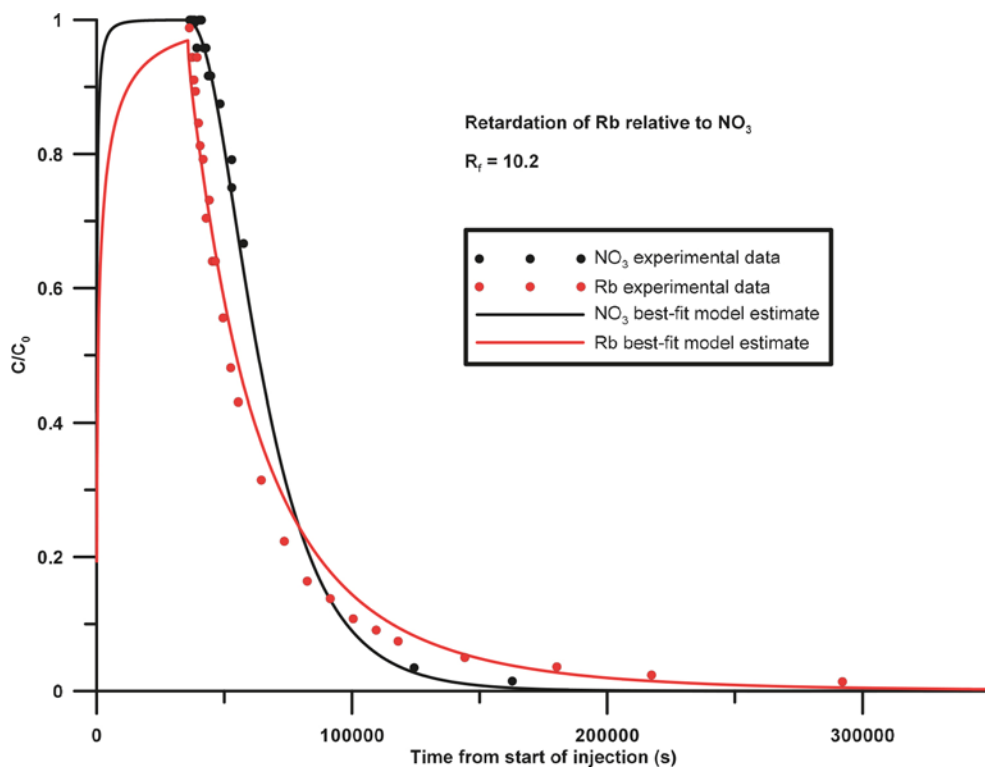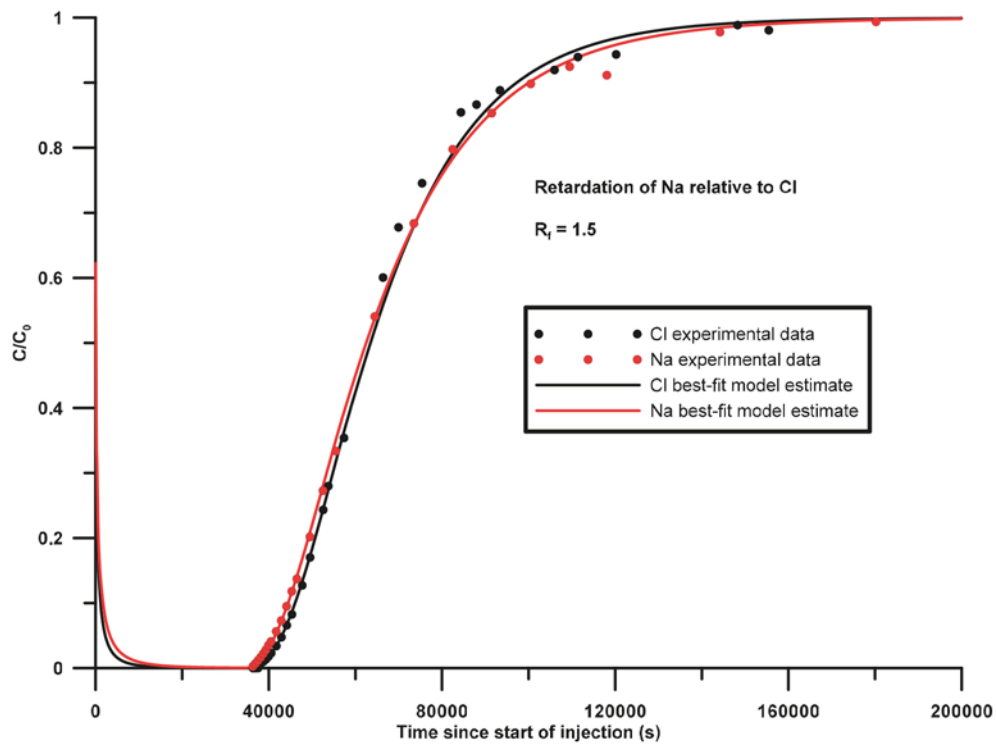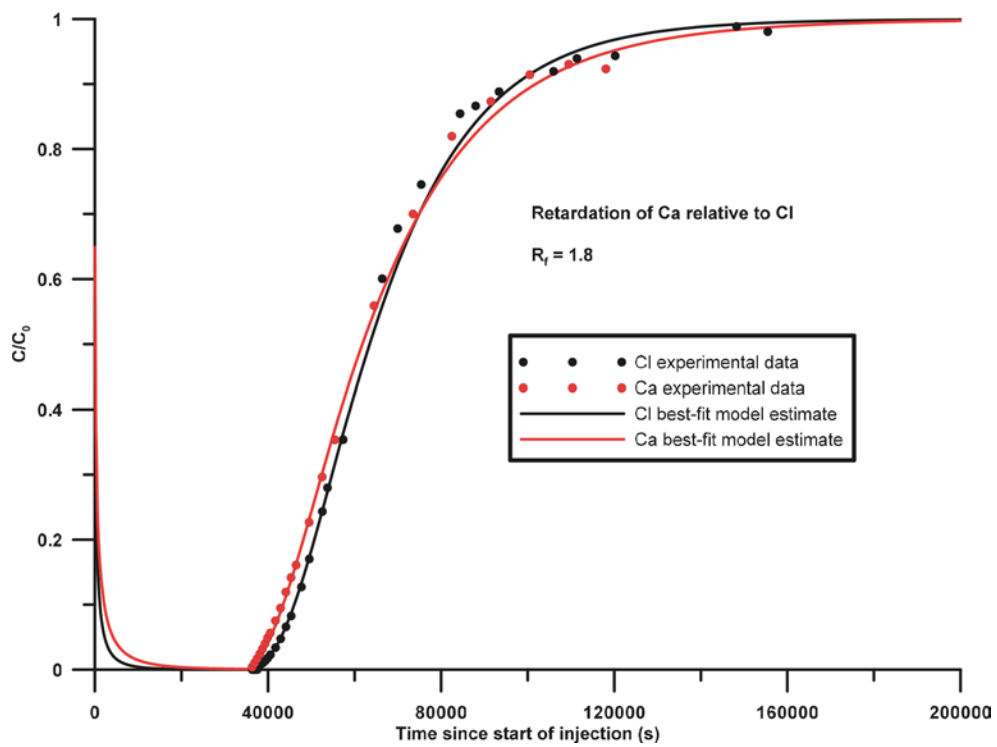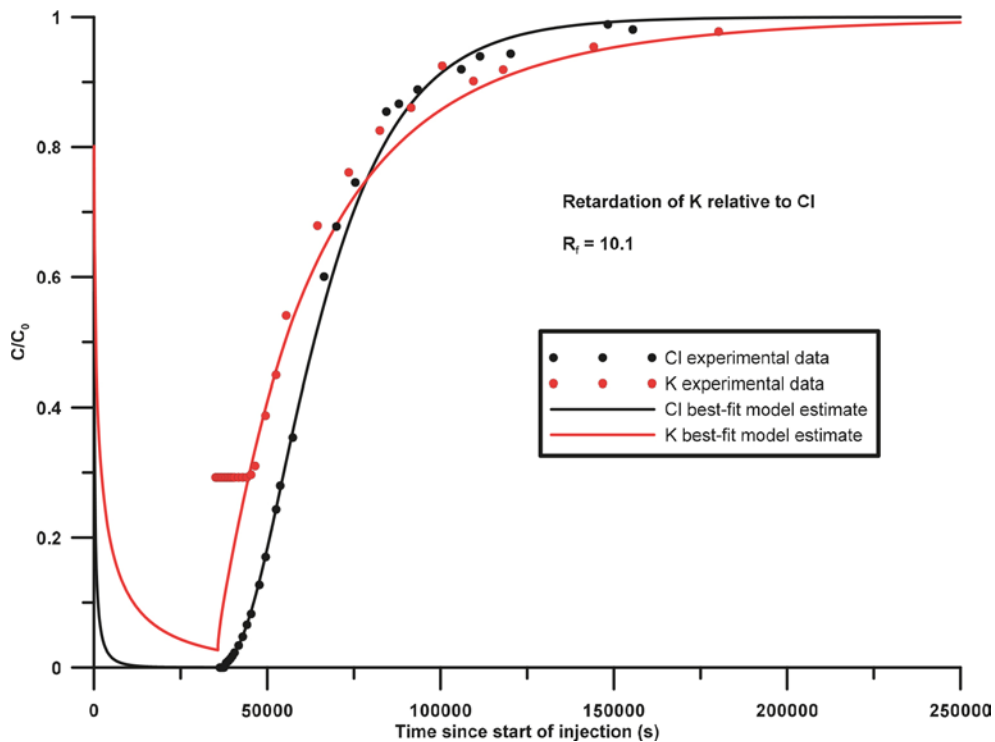**Figure 6-21.** *Best-fit modelling results for retardation of K in SWIW test 4.*

Table 6-1. Estimated fracture retardation coefficients in SWIW test 4.

Tracer	Retardation factor, R_f
Mg	1.5
Cs	14.6
Rb	10.2
Na	1.5
Ca	1.8
K	10.1

6.3 Influence of background groundwater flow

Experimental data from the preparatory tests and main test suggest that the influence of the background flow needs to be analysed in order to distinguish between diffusive and advective effects. The background flow was measured at several occasions using point dilution tests (see Section 5.1.2). The evaluated groundwater flow rates through the borehole section varied approximately between 1 and 3 ml/h. These values are very uncertain because the sampling flow rates during the dilution tests were on the order of magnitude as the apparent flow rates through the borehole section. In order to evaluate the "natural" flow rates, the sampling flow rates were simply subtracted from the apparent flow rates. However, this is not an entirely accurate method of compensating for large sampling flow rates, because the sampling flow affects the flow field around the borehole and superimposes a small drawdown. A more accurate compensation for large flow rates has not yet been developed.

This sub-section presents first an overview of some basic theoretical aspects of the flow pattern around a borehole section in a uniform flow field. Simulated examples all assume homogenous conditions; see Section 4.4 for a model description. Following this, some of the experimental results from the main SWIW test are examined with consideration taken to background flow effects.

A borehole section pumped with a constant flow rate in a uniform two-dimensional flow field, at steady-state conditions, results in a so called downstream stagnation point. The stagnation point represents the downstream limit of the capture zone of the pumped borehole section. The location of the stagnation point depends only on the pumping flow rate and the magnitude of the uniform flow. The distance d_{stag} to the stagnation point may be calculated as (Bear 1988):

$$d_{stag} = \frac{Q}{2\pi q_0} \qquad\qquad (6\text{-}1)$$

where Q is the pumping flow rate per unit thickness [L^2/T] and q_0 is the uniform flow rate per unit thickness and per unit width [L/T] (also called Darcy velocity). If water is injected in the borehole section, d_{stag} denotes the distance in the downstream direction from the borehole section. An illustration of the flow pattern resulting from a point sink (i.e. a pumped borehole section) in a uniform flow is shown in Figure 6-22.

The example in Figure 6-22 approximately corresponds to conditions during SWIW 4 and 5 with a background flow towards the lower end of the plausible flow range (as discussed in Section 5.1.2). Assuming homogenous conditions and a borehole convergence factor of 2, q_0 is related to the estimated flow through the borehole section, Q_{bh}, by:

$$q_0 = \frac{Q_{bh}}{2\phi_{bh} L_{bh}} \qquad\qquad (6\text{-}2)$$

where ϕ_{bh} is the borehole diameter [L] and L_{bh} is the length of the borehole section [L]. The uniform discharge rate in Figure 6-22 ($3.25 \cdot 10^{-9}$ m/s) then corresponds to a flow rate through the borehole section of about 1.3 ml/h.
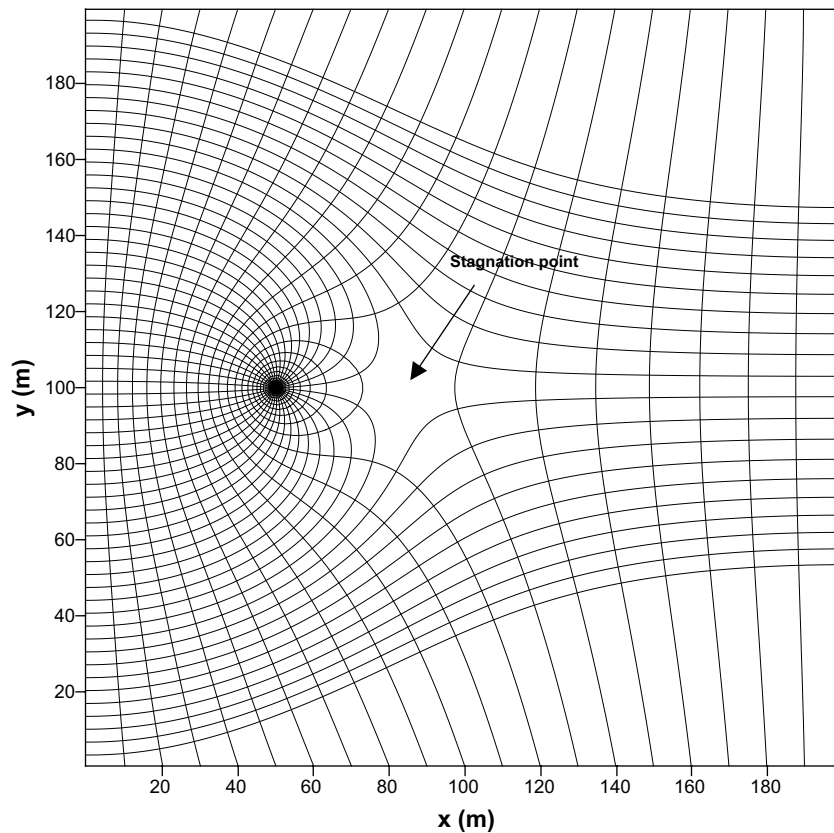

Figure 6-22. *Illustration of the flow field for a point sink in uniform flow in the x-direction. The example corresponds to a pumping flow rate of about $8 \cdot 10^{-7}$ m^2/s (per unit thickness) and a uniform discharge rate of $3.25 \cdot 10^{-9}$ m/s. The distance to the stagnation point (according to Equation 6-2) is about 30 m.*

As been discussed above, the estimated flow rates from the dilution measurements are associated with uncertainty because of high sampling flow rates. Further, it cannot be determined to what extent the evaluated flow rates are representative for the average specific discharge across the entire flowing feature. If it is assumed that the a plausible range for the background flow would correspond to 1–10 ml/h through a borehole section (Q_{bh}), then a plausible range for the distance to the stagnation point would be about 5 – 50 m. This is illustrated in Figure 6-23, which shows a plot based on Equation 6-1.

Downstream travel distance during injection in a uniform flow field

The discussion above about the distance to the stagnation point refers to steady-state conditions during either pumping or injection of water. During a SWIW test, the significance of the stagnation point is that during the injection phase, the injected water cannot travel further upstream than to the stagnation point. More importantly, during the recovery phase the recovery pumping cannot capture any of injected water that has travelled beyond the downstream stagnation point. It is therefore of interest to estimate the downstream travel distance during the tracer injection phase and to relate this to the distance to the stagnation point. The downward travel distance is, in addition to the injection pumping flow and the background flow, also dependent on the aperture/porosity of the flow system.

Calculation of the theoretical position of the advective front for a point source in uniform flow was described in Nordqvist and Gustafsson (2002), based on Bear (1988). As a special case of this, the front position along the flow direction can be calculated from:

$$\psi = \xi - \ln(1 + \xi) \qquad (6-3)$$

With the dimensionless variables τ and ξ defined as:

$$\psi = (\frac{2\pi q_0^2}{nQ})t \qquad \xi = (\frac{2\pi q_0}{Q})x \qquad (6-4)$$

where Q in this case in the injection flow rate per unit thickness [L^2/T], x is a coordinate in the downstream flow direction [L], t is time [T], and n is the porosity [–]. The notation follows Bear (1988), which describes a porous aquifer, but is equivalent with a plane-parallel fracture concept if one replaces the porosity with the fracture aperture per unit thickness.
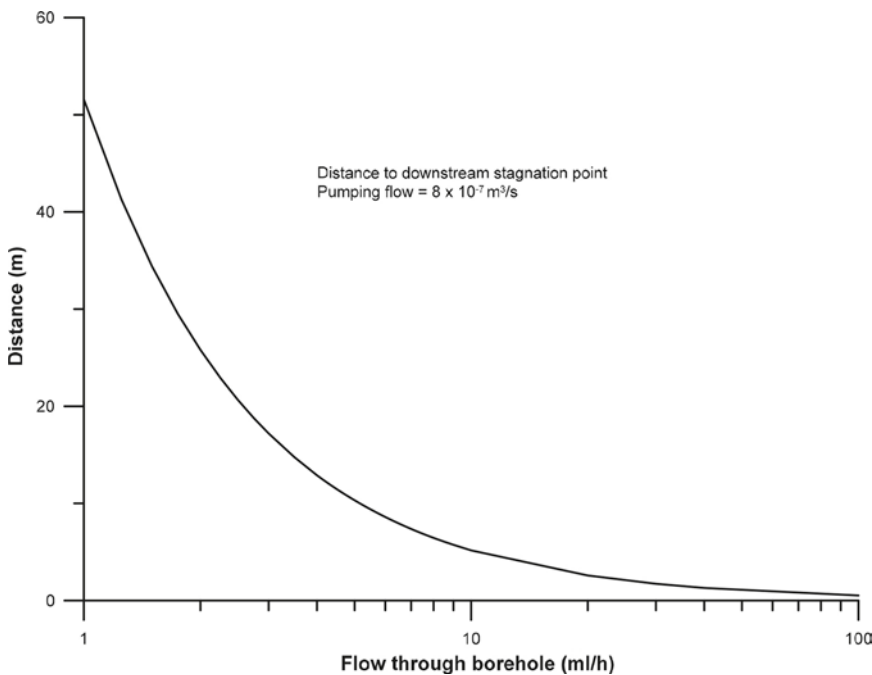

Figure 6-23. Stagnation point as a function of flow through a borehole (diameter = 56 mm).

Figure 6-24 illustrates the theoretical downstream travel distance at the end of the injection phase during SWIW4 in relation to the distance to the stagnation point during pumping. The travel distance is plotted as function of the specific discharge of the background uniform flow field, for a range roughly corresponding to Q_{bh} = 1–10 mL/h. Figure 6-24 may be used to get an indication under what conditions less than full recovery may be expected. A plausible upper limit for the background flow may be about 3 ml/h, corresponding to a specific discharge of about $7.5 \cdot 10^{-9}$ m/s (Equation 6-2), which would indicate that more or less complete recovery should be expected unless the actual aperture is very low.

During the waiting phase there is additional drift due to the background flow, which is given by:

$$d_{drift} = \frac{q_0}{n} t \tag{6-5}$$

The drift for a waiting time of 93 hours (SWIW test 5) is compared to the radial travel distance for an injected volume of 28.75 L as a function of aperture (per m thickness) in Figure 6-25.

Figure 6-25 gives an indication that the background flow may have to be carefully taken into account when interpreting the tracer results from SWIW 4 and SWIW 5. This is illustrated more explicitly in Figure 6-26, which shows simulations of SWIW tests with and without waiting phase and for two different background flow rates (1 and 3 ml/h, respectively) of the same magnitude as was estimated from dilution tests. Figure 6-26 indicates that for SWIW test 4, without waiting phase, the background flow has very little impact on the recovery breakthrough curve, even at the higher of the two flow rates. The simulations do not include diffusion or other time-dependent process. Therefore, the breakthrough curve for the case with a waiting phase should in the absence of background flow be identical to the case without waiting phase. The simulations with a waiting phase indicate that the background flow indeed has an effect on tracer breakthrough. For the higher of the two background flow rates, the effect is considerable. For the lower of the flow rates, the effect is much smaller but still significant. Although the simulated results are dependent on the choice of aperture value (which can be understood from Figure 6-25 above), Figure 6-26 indicates that a significant part of the experimental differences between SWIW test 4 and SWIW test 5 for individual tracers may be explained by drift during the waiting phase.

Figure 6-26 indicates that effects of background flow are small during SWIW test 4 but

that it may be significant during SWIW test 5. It is nevertheless of interest to examine whether inclusion of a background gradient would explain any of the late-time tailing observed for the added tracers in SWIW test 4. Figure 6-27 shows best-fit simulations of Li breakthrough in SWIW test 4 for several assumed values of the background gradient. It seems clear that the presence of background flow has very little influence of the late-time behaviour of the tracer breakthrough curve. The late-time behaviour is studied in more detail in a subsequent section (6.5).

Figure 6-27 shows that the late-time behaviour at low experimental values of C/C_0, may not be explained by the background groundwater flow. This is not un-expected in a homogenous transport domain, as a drift due to background flow during the waiting phase should not significantly affect the late-time behaviour (Haggerty et al. 2001). Having established that the late-time breakthrough of added tracers during SWIW test 4 indicates diffusive mass transfer irrespective of background flow, the next question is whether background flow may affect the early behaviour of tracers in SWIW test 5.

Best-fit simulations for Li and Cl data from SWIW test 5 is shown in Figure 6-28 and Figure 6-29, respectively. In both cases, the dispersion parameter φ is fixed using the values from SWIW test 4 simulations presented in Section 6.2.1. As a single estimation parameter, the background flow rate is estimated. This background flow is presented as flow through the borehole section, which is obtained using the "standard" assumption of a flow convergence factor of two. None of the fits are perfect, but sufficiently close to infer that the background flow may explain a significant part of what happens to the tracer during the waiting phase. It is interesting to note that the estimated values for the background flow is very similar for the added and removed tracer, and the value is well within the plausible range for the estimated values from the dilution measurements.
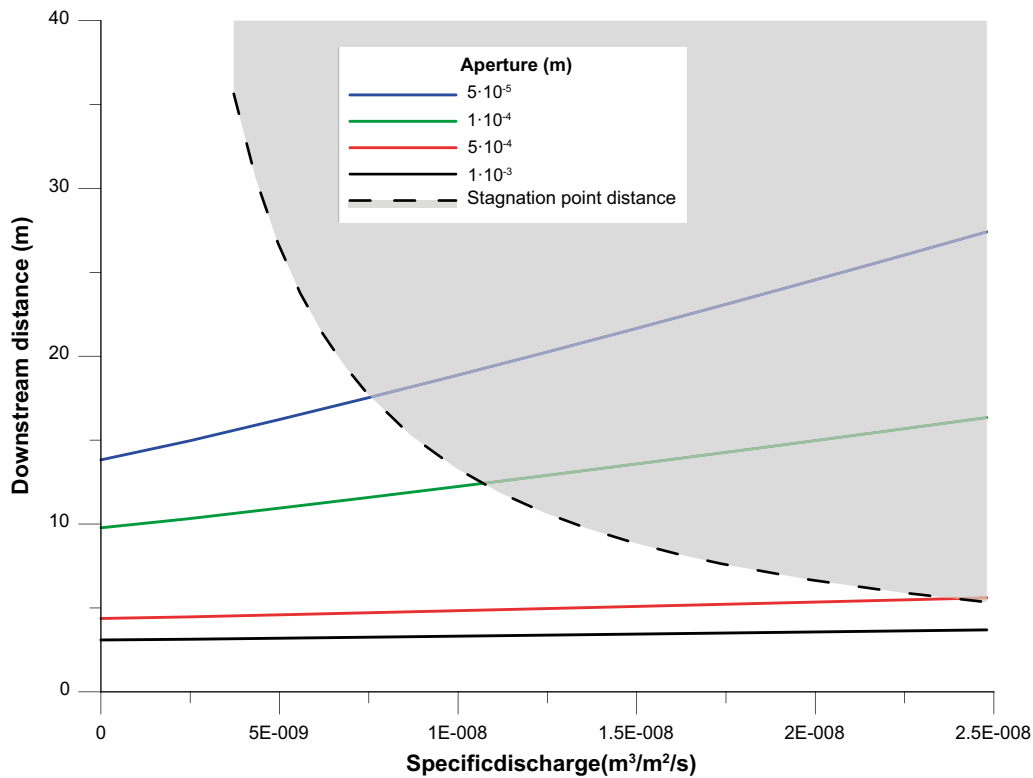
Figure 6-24. *Theoretical downstream travel distance, as a function of specific discharge for the background uniform flow field, for the advective front at the end of the injection phase for SWIW4 (10 h after start of injection with an injection pumping rate of 50 mL/min). Solid lines represent different values of aperture and the dashed line shows the distance to the stagnation point during recovery pumping. The shaded region indicates conditions where full tracer recovery is not possible.*
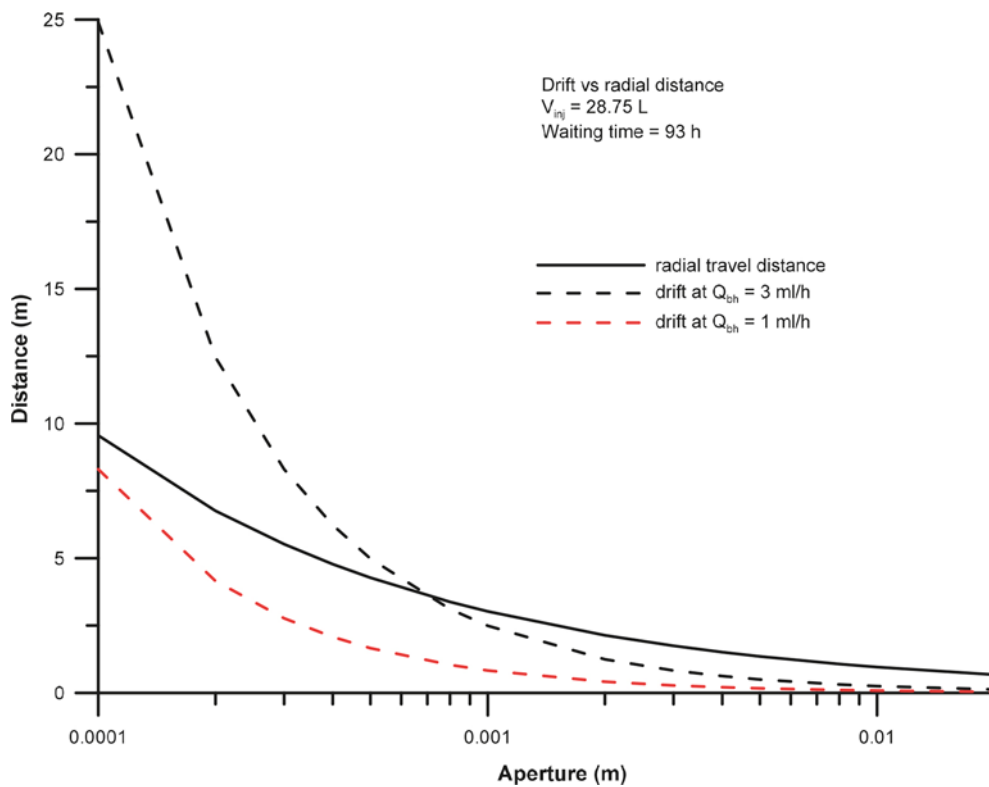

Figure 6-25. *Comparison of drift during the waiting phase and radial travel distance during the injection phase. Note that this example is simplified because the effect of drift during the injection period is neglected.*

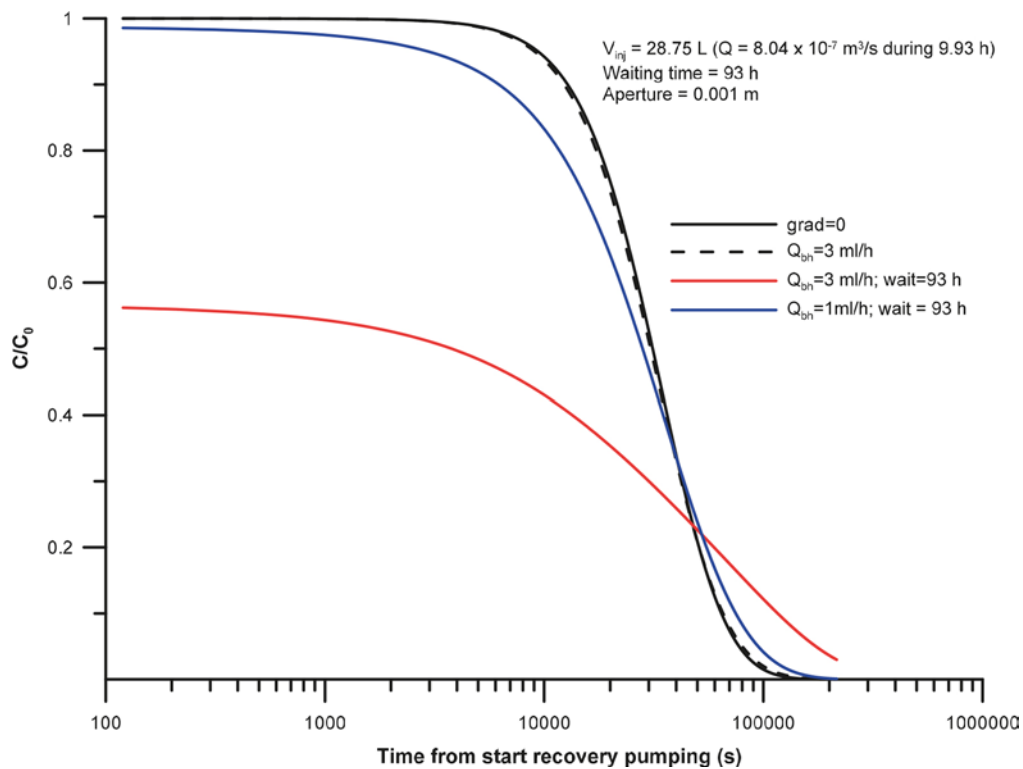***Figure 6-26.*** *Simulated breakthrough curves for two different background flow rates with and without waiting times, respectively.*
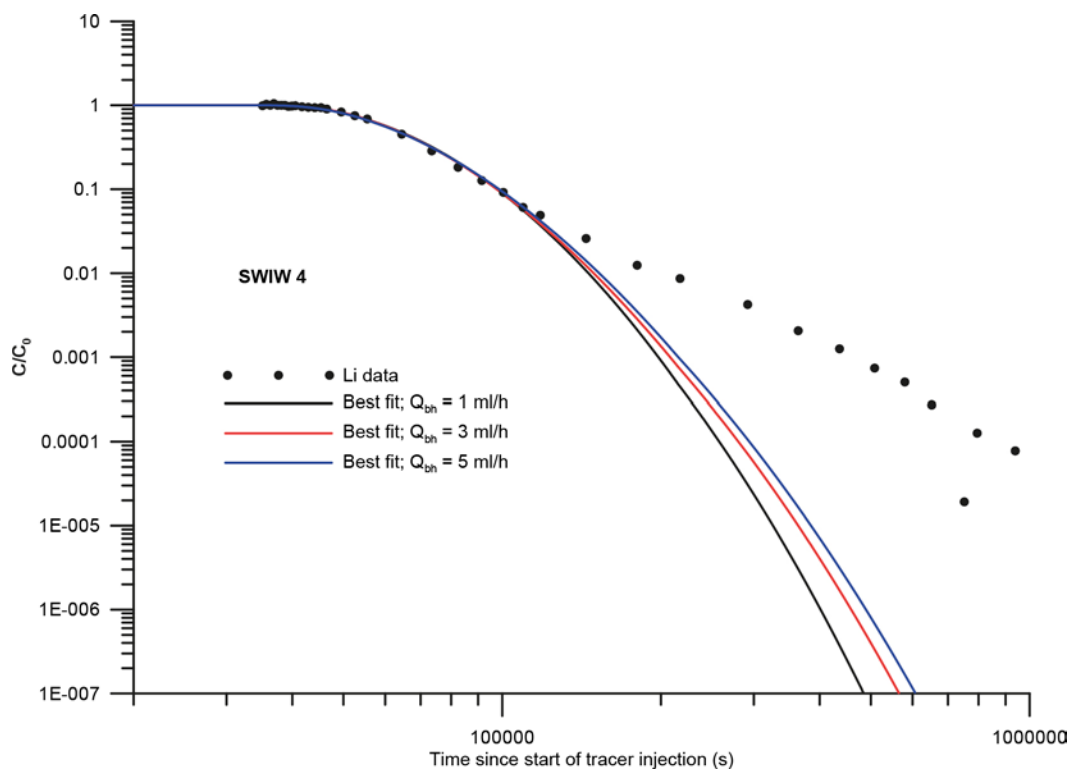
Figure 6-27. *Best-fit simulations of Li breakthrough in SWIW test 4 for a range of assumed background flow rates.*

Figure 6-28. *Best-fit simulation of Li data from SWIW test 5 assuming a uniform background flow. A single estimation parameter, Q_{bh}, is used; the dispersion parameter, φ, is assigned a fixed value obtained from analysis of Li data from SWIW test 4.*

Figure 6-29. *Best-fit simulation of Cl data from SWIW test 5 assuming a uniform background flow. A single estimation parameter, Q_{bh}, is used; the dispersion parameter, φ, is assigned a fixed value obtained from analysis of Cl data from SWIW test 4.*

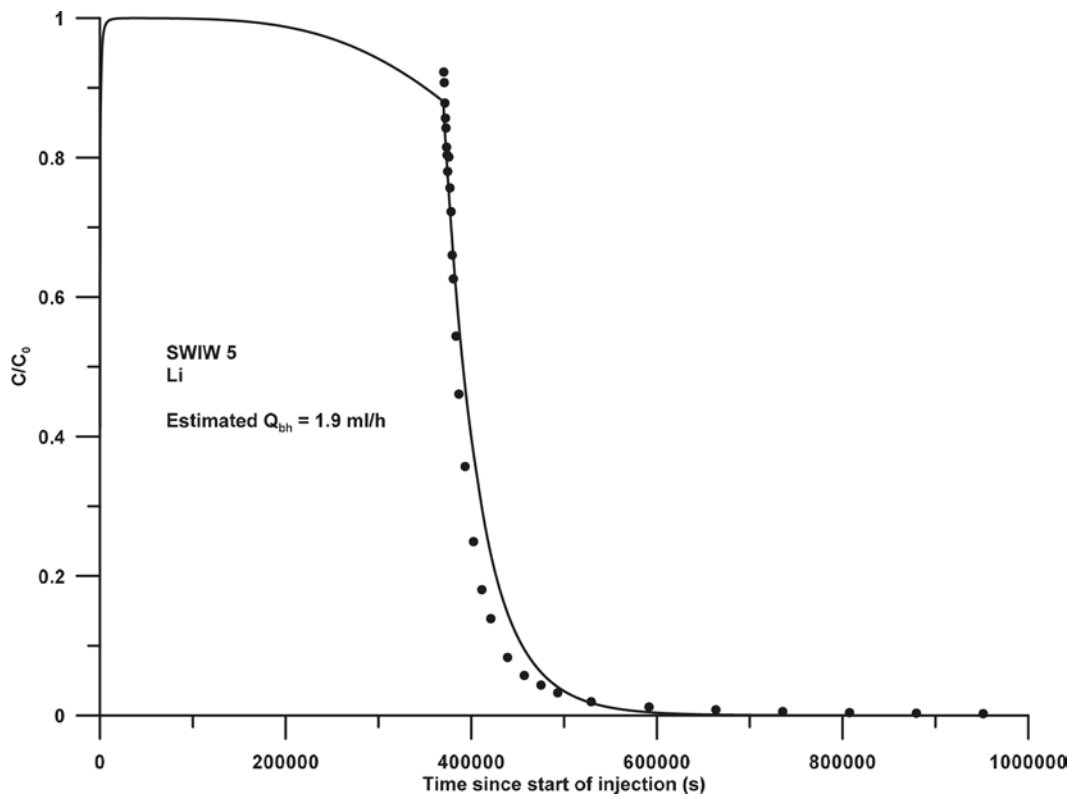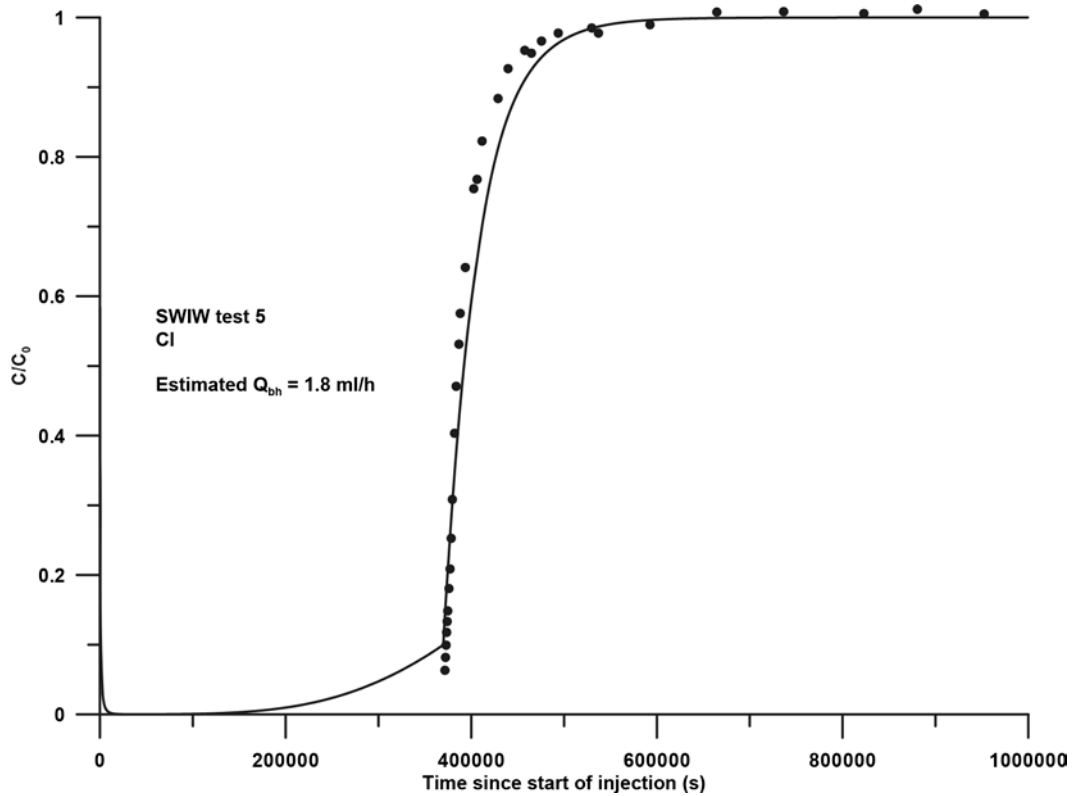In summary, the simulation examples above show that it is very possible, or even likely, that the (although small) background flow has an effect on tracer breakthrough for the tests with a waiting phase, such as SWIW test 5. However, it has also been shown that the gradient can not explain the late-time tailing in the breakthrough curves for added tracers, which is discussed in some more detail in the next section.

6.4 Analysis of late-time breakthrough of added tracers

Theoretical late-time behaviour in some simple systems

Analysis of the late-time appearance of tracer breakthrough curves, when plotted with logarithmic axes, has become a standard element of tracer test interpretation. In the synthetic SWIW experiments this applies to the added tracers, of course, as the removed tracers at late times reaches a plateau instead of having a tail. Plotting tracer breakthrough curves in log-log plots is commonly used as a tool to infer influence of diffusive mass transfer into hydraulically stagnant rock volumes.

The basic effect of diffusive mass transfer on the tracer breakthrough curve is the occurrence of a linear slope at late times. In a simple system with a transmissive fracture and a porous but hydraulically stagnant rock matrix, the slope approaches a value of -1.5 (e.g. Tsang 1995).

A few examples of simulated tracer behaviour in simple systems are shown below. The simulations are based on a simple radial model with an open plane-parallel fracture with a porous rock matrix. The simulations are made with the following experimental variables:

Injection and recovery pumping flow rates:	$8.3 \cdot 10^{-7}$ m³/s (50 mL/min)
Injection duration:	36,000 s (10 h)
Total injected volume:	0.030 m³
Extent of matrix from fracture centre:	0.2 m
Borehole diameter:	0.056 m

In these simulations, the effective matrix diffusion parameter A (see Section 4.4) is varied while the effective dispersion parameter (see Chapter 2), φ, is held at a constant value of $5.3 \cdot 10^{-4}$, which implies a relatively small dispersion effect in the fracture.

Figure 6-30 shows simulated tracer breakthrough curves, plotted with logarithmic axes, for a few cases with varying values of the effective diffusion parameter A. The differences between the values of A correspond to one magnitude difference in D_p. For example, assuming an aperture of 0.1 mm and a matrix porosity of $5 \cdot 10^{-3}$, the various values of A represent values of D_p varying from $2.5 \cdot 10^{-12}$ m²/s to $2.5 \cdot 10^{-9}$ m²/s.

Figure 6-30 shows how the diffusing tracers approach a slope of -1.5. The magnitude of the slope for the non-sorbing tracer increases indefinitely. The higher the diffusion effect (decreasing values of A), the sooner the straight-line part of the log-log slope begins and the transition between the advection-dominated and diffusion-dominated parts become more gradual. The two largest diffusion rates illustrate boundary effects when the rock volume available for diffusion limits the diffusive mass transfer away from the fracture. The latter can be seen as a slight "hump" followed by a rapid decline similar to the non-diffusing tracer. This effect may be referred to as "tail-end perturbation" (e.g. Jakob et al. 2003). Thus, a tracer diffusing into a finite matrix rock volume may exhibit log-log slopes of -1.5 that at some point in time transitions to a somewhat flatter slope.

Tracers that undergo linear equilibrium sorption (i.e. "K_d"-sorption) within the rock matrix also approach a log-log slope of -1.5, parallel to the log-log curves of tracers with no sorption ($R_m = 1$) or with other values of the sorption coefficient.

Figure 6-31 shows the breakthrough curves for a non-sorbing and a moderately strongly sorbing tracer (for a value of A=6,300 s$^{1/2}$, see preceding figure), together with the temporal development of the log-log slope for each tracer. One detail of interest is that the magnitude of the slope for the sorbing tracer is higher than for the non-sorbing tracer during the transition period from advection-dominated transport to the diffusion-dominated.

Figure 6-32 provides a further illustration of simulation results assuming a fairly large diffusion effect by showing simulation concentration profiles into the matrix at two different radial distances and at a few different pumping times.
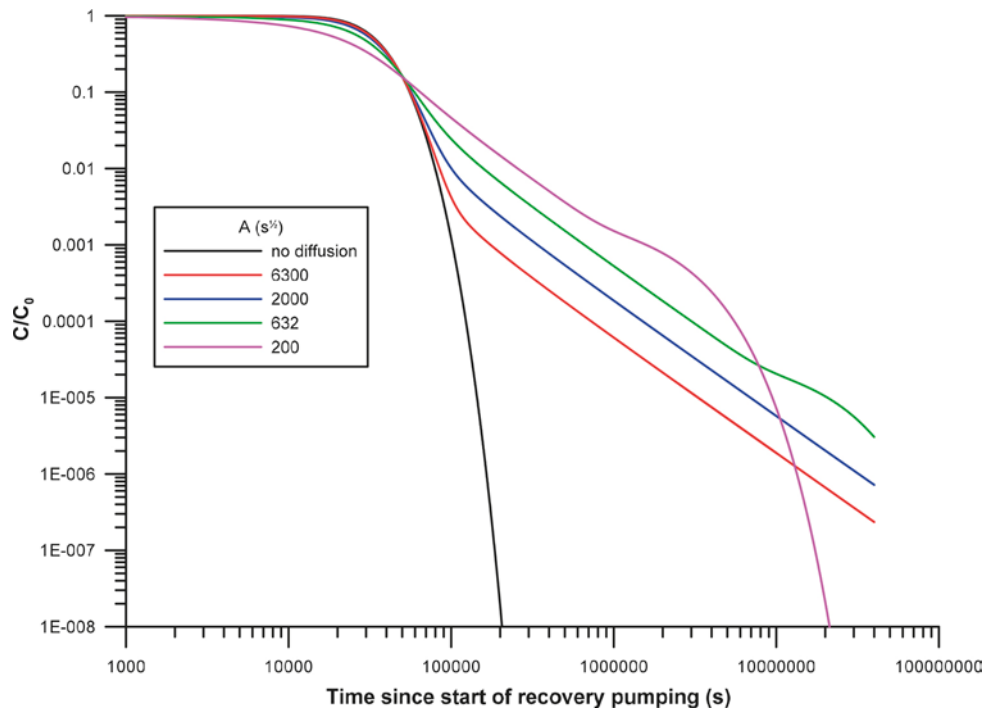
Figure 6-30. *Illustration of late-time behaviour in SWIW recovery breakthrough curves.*
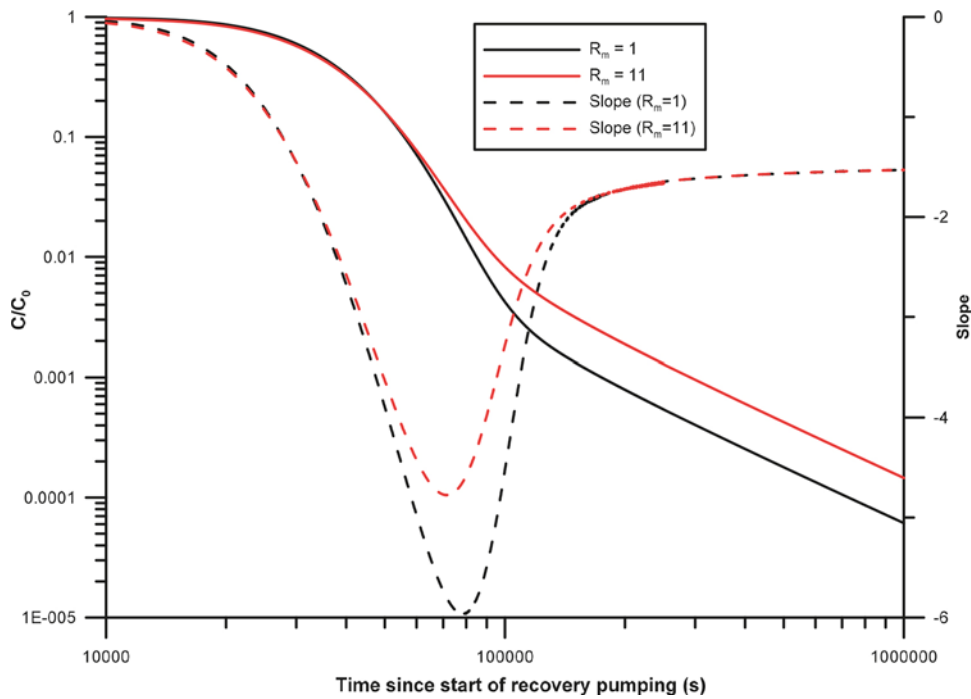

Figure 6-31. *Simulated SWIW recovery breakthrough for sorbing and non-sorbing diffusing tracers (for the case of A = 6,300 $s^{\frac{1}{2}}$, see above). The slope varies according to the dashed lines (right-hand axis).*
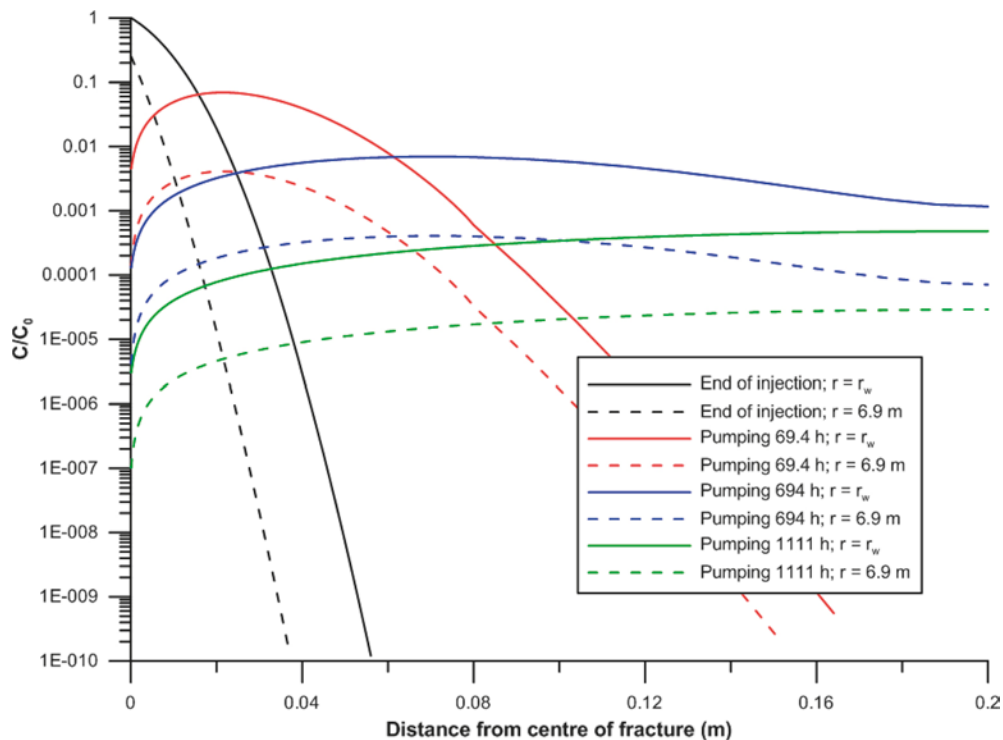
Figure 6-32. *Illustration of concentration profiles from the centre of the fracture into the matrix (finite matrix ending at 0.2 m from fracture centre) at a few different times. The assumed value of A is about 630 $s^{1/2}$, which implies a fairly large diffusion effect.*

The effect of employing a waiting phase on late-time behaviour is illustrated in Figure 6-33. The simulation is based on a waiting period of 90 hours, i.e. similar to the experimental time period applied in SWIW test 5. Figure 6-33 indicates that the waiting phase affects the log-log slope of the late-time breakthrough, resulting at a flatter slope than when a waiting phase is not used. For example, at around 10^6 s (about 280 hours) after start of recovery pumping, the log-log slope for the case without waiting phase is about –1.53 and the case with waiting phase is about –1.33. Both of the curves eventually approach a slope of –1.5 but this happens later for the case with waiting phase than for the case without. This general behaviour is interpreted to be an effect of employing a waiting phase and not that the matrix is finite. The waiting phase provides more time for the tracer to diffuse into the matrix before the recovery pumping starts, resulting in different "initial" conditions in the matrix before the recovery pumping starts.

These simulations only consider a few simple cases with matrix diffusion, with the purpose of qualitative comparisons with experimental data. More complex models explaining power-law behaviour in SWIW experiments in general may be found in, for example, Haggerty et al. (2000), Becker and Shapiro (2003) or Doughty and Tsang (2009).

Late-time slopes in log-log plots – experimental data

Experimental breakthrough curves for added tracers plotted in logarithmic diagrams are shown in Figure 6-34 and Figure 6-35 for SWIW 4 and SWIW 5, respectively. For all of tracers in both tests, a linear slope develops at late times, which typically is taken as an indication of diffusive mass transfer. For both of the tests, the slope varies among the various tracers. For SWIW 4, the slope varies from about –2.15 for NO_3 (although somewhat sparse data) to about –1.55 for Rb and Cs. For SWIW 5, the slope ranges from about –1.9 (NO_3) to –1.3 to –1.35 (Rb and Cs). If one disregards NO_3 (sparse data) and Uranine (anomalous behavior in general), there might be tendency that there is less spread in the slopes for SWIW test 5 than SWIW test 4.
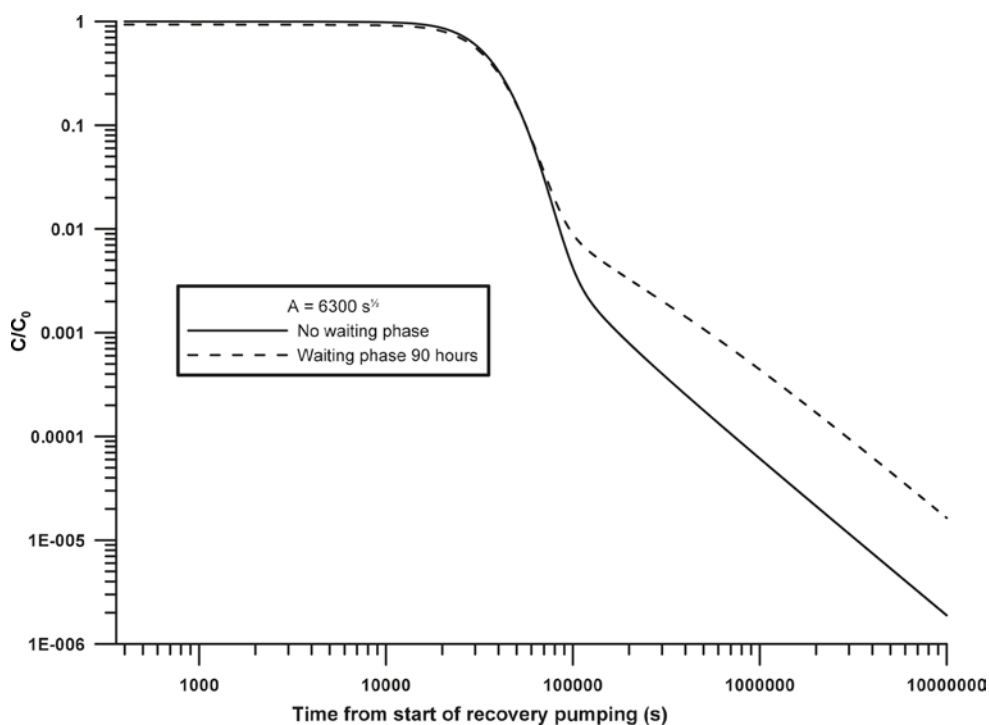
Figure 6-33. *Effect of employing a waiting phase (90 hours) on late-time breakthrough assuming a finite matrix.*

One characteristic of the log-log plots is that the various breakthrough curves show a very gradual transition from the initial breakthrough (presumably advection-dominated) to the straight-line parts at later times (presumably diffusion-dominated). At lower diffusion effects (see Figure 6-30), a moderate to low diffusion effect results in a fairly abrupt change in slope when diffusion begins to dominate the breakthrough curve; such effects are not seen in the experimental curves. The observation that the experimental curves have a very gradual transition to straight-line conditions may be an indication of a relatively large diffusion effect or at least that there is variability in diffusion rates and/or fracture aperture.

For SWIW 4 (Figure 6-34), the slopes for the relatively strongly sorbing tracers Cs and Rb are close to −1.5 while all other tracers have steeper slopes. In a homogenous system,, all tracers would approach a slope of −1.5 (see Figure 6-31 above). However, as was shown above, sorbing tracers theoretically attain flatter slopes somewhat earlier than non-sorbing tracers. One possible explanation for the differences in slope during SWIW 4 may therefore be that the system is in transition stage between advection-dominated transport and diffusion-dominated transport (as in the middle part of the graph in Figure 6-31 above).

The log-log slopes for both tests are summarised in Table 6-2. Common to the late-time log-log slopes from SWIW 5 is that all the slopes are flatter (i.e. less negative slopes) than in SWIW 4. The only exception to this is Uranine but, as discussed earlier, the behaviour of Uranine during the synthetic SWIW experiments is highly un-characteristic and Uranine results are therefore not considered representative. The general difference between SWIW 4 and SWIW 5 appears to make sense as the waiting time during SWIW 5 provides more time for diffusion (compare with Figure 6-33 above). The possible indication that there is less spread among the slopes for SWIW 5 (disregarding NO_3 because of sparse data and Uranine for previously mentioned reasons) may also be an indication of more influence of diffusion in SWIW 5 than SWIW 4, although this appears speculative. An additional remark regarding the results from SWIW test 5 is that the curves for Rb and Cs are less steep than a log-log slope of −1.5.
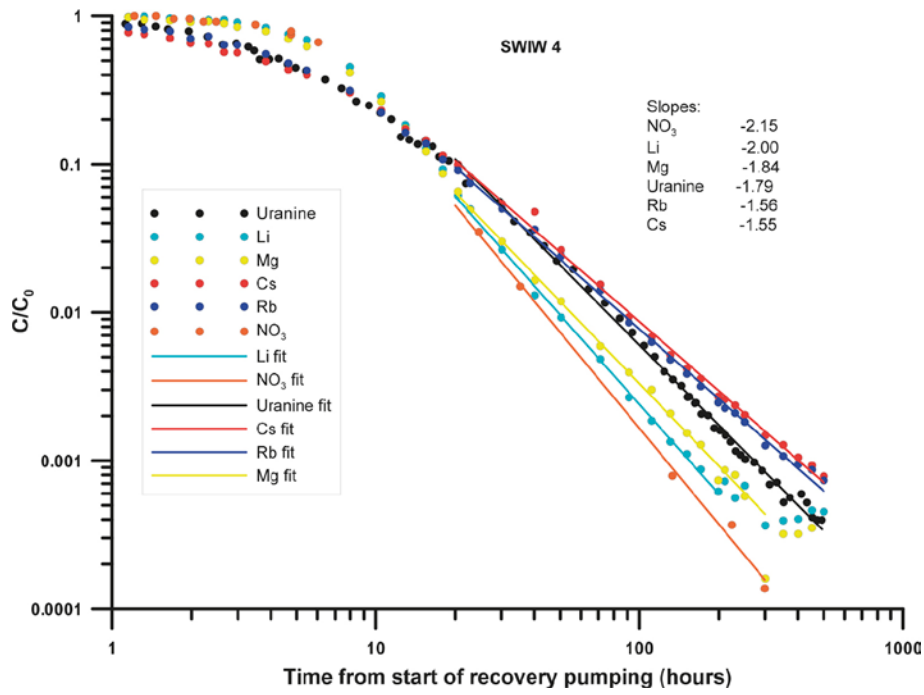
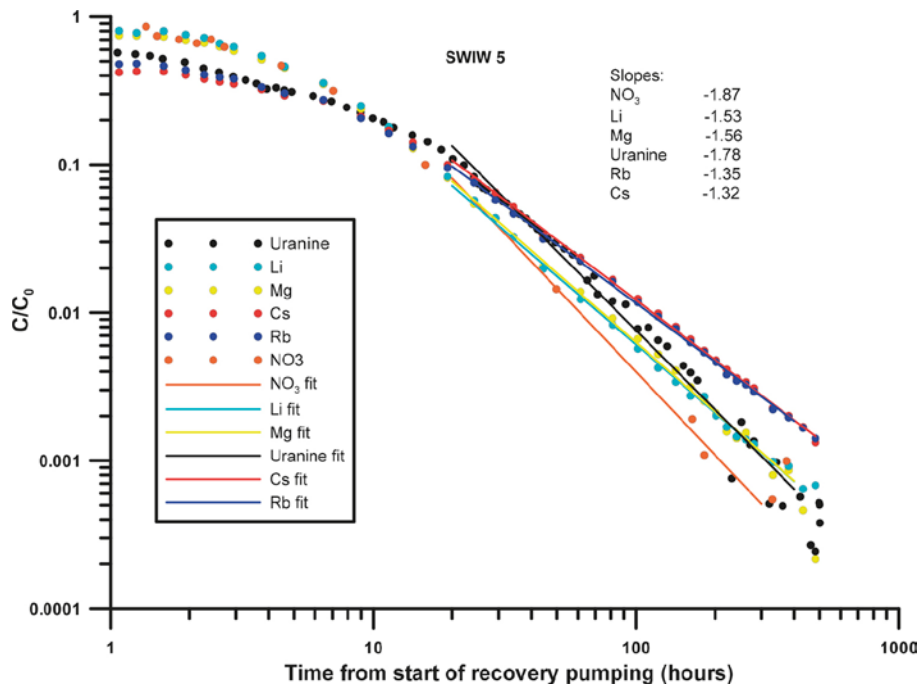*Figure 6-34. Late-time log-log slopes for added tracers in SWIW 4.*

Figure 6-35. Late- time log-log slopes for added tracers in SWIW 5.

Table 6-2. Summary of late-time log-log slopes.

Tracer	SWIW test 4	SWIW test 5
NO$_3$	–2.15	–1.87
Li	–2.0	–1.53
Mg	–1.84	–1.56
Uranine	–1.79	–1.78
Cs	–1.55	–1.32
Rb	–1.56	–1.35

The analysis of late-time behaviour of tracer breakthrough curves, plotted in logarithmic diagrams, may be summarized as follows:

- Consistent straight-line late-time slopes in log-log plots indicate that diffusive mass transfer is an active process during the synthetic SWIW experiments.

- There is a consistent difference in slope between SWIW test 4 and SWIW test 5, which may partly be explained by (as shown by generic simulation) diffusion during the waiting phase.

- There is also a difference in slope between sorbing and non-sorbing tracers, which might be an indication of spatial variation (the sorbing and the non-sorbing tracers, respectively, do not "experience" the same rock volume).

- Effects of a limited matrix, i.e. late-time perturbation, are not indicated.

6.5 Basic model analysis with matrix diffusion

The model simulations in this section are carried out with the matrix diffusion model described in Section 4.4. The results shown here should be seen as example simulations of selected experimental data, using only conservative tracers. Simulations are presented for Li (added tracer) in SWIW test 4 and SWIW test 5 as well as for Cl (removed) in SWIW test 5. Because of the ambiguity caused by uncertainty in the background flow (as discussed above), detailed modelling with sorbing tracers and matrix diffusion was not performed at this stage. Instead, the simulations presented here are intended as a semi-qualitative check whether homogenous matrix diffusion can provide an alternative explanation to background flow effects for the observed differences between SWIW tests with and without a waiting phase.

The first example is a simulation of Li data from SWIW test 4, shown in Figure 6-36. This figure also includes a case with an alternative background concentration for Li data, in order to illustrate the sensitivity to background concentration when plotting late-time log-log slopes. The simulation is made with values of $A = 630$ s$^{\frac{1}{2}}$ and $a_L^2\delta = 2\cdot10^{-5}$. This simulation suggests that a simple matrix diffusion model actually may be sufficient to explain the late-time behaviour of Li data in SWIW test 4. The simulated curve has at the end of the simulation a log-log slope of about -1.53. However, the data set with the alternative background values results in a steeper slope that is not possible to re-produce with the homogenous matrix diffusion model.

The early parts of the curve does not fit as well as with the simpler model with advection-dispersion only (Figure 6-14), although this is somewhat obscured by the logarithmic scale on the vertical axis in Figure 6-36. This was found to be the case irrespective of combination of parameter values, i.e. that the beginning of the curve can not be fitted well at the same as the late part of tail is fitted.

Next, an example of applying the matrix diffusion model to Li data from SWIW test 5 is shown in Figure 6-37. This figure shows two alternative model fits, one with more emphasis on fitting the tail ($A = 1,600$ s$^{\frac{1}{2}}$) and the other on fitting the early part of the breakthrough curve ($A = 6,300$ s$^{\frac{1}{2}}$). Although the former alternative fits the late parts (and almost the whole descending part) of the curve very well (which is not surprising because the log-log of Li data is about -1.5 for SWIW test 5), it fits poorly to the beginning of the curve (note that the vertical axis is in log scale). On the other hand, fitting the early parts better results in a poor fit of the late parts of the tail. This suggests that the homogenous matrix diffusion model is not able to simultaneously explain the early and late parts. Simple explanations to this could be either that the early parts are affected by the background flow or that different diffusion properties affect different parts of the curve; the early part of the curve being more representative for the rock volume close to the borehole section.

In addition to the above, the fits in Figure 6-37 require that the dispersion parameter φ is an order of magnitude higher than in the simulation shown above for SWIW test 4. Simulations (not shown) with a fixed value of φ (from fitting Li in SWIW test 4 with the advection-dispersion model), and emphasising the late-time tail in the fitting, resulted in very poor fits for the early part of the breakthrough curve.
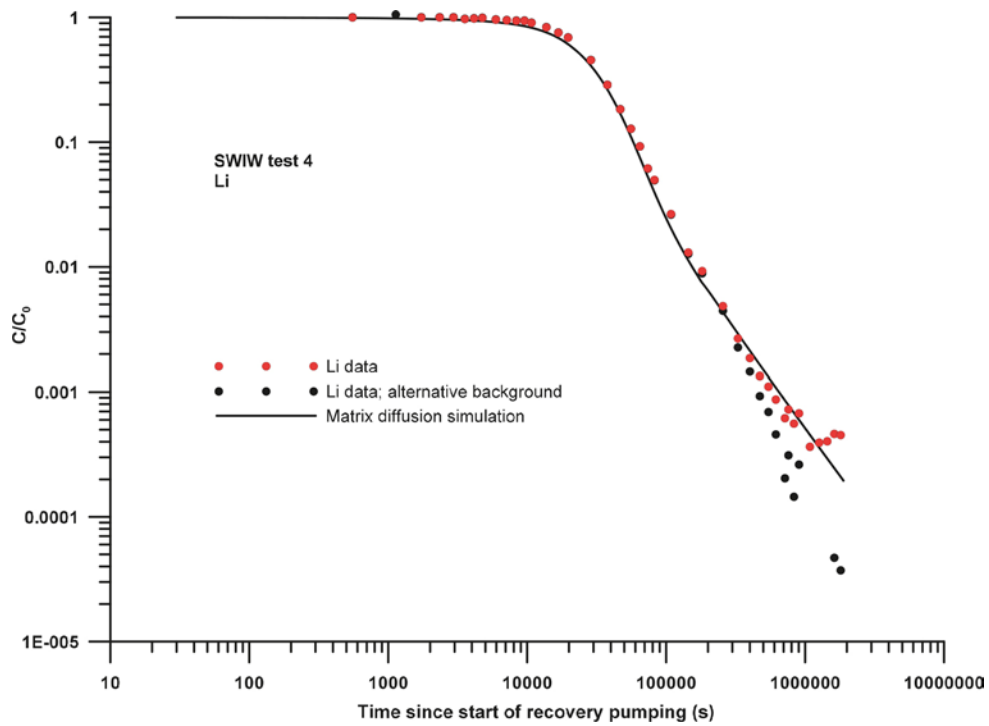
Figure 6-36. *Simulation of Li breakthrough data from SWIW test 4 with a matrix diffusion model.*
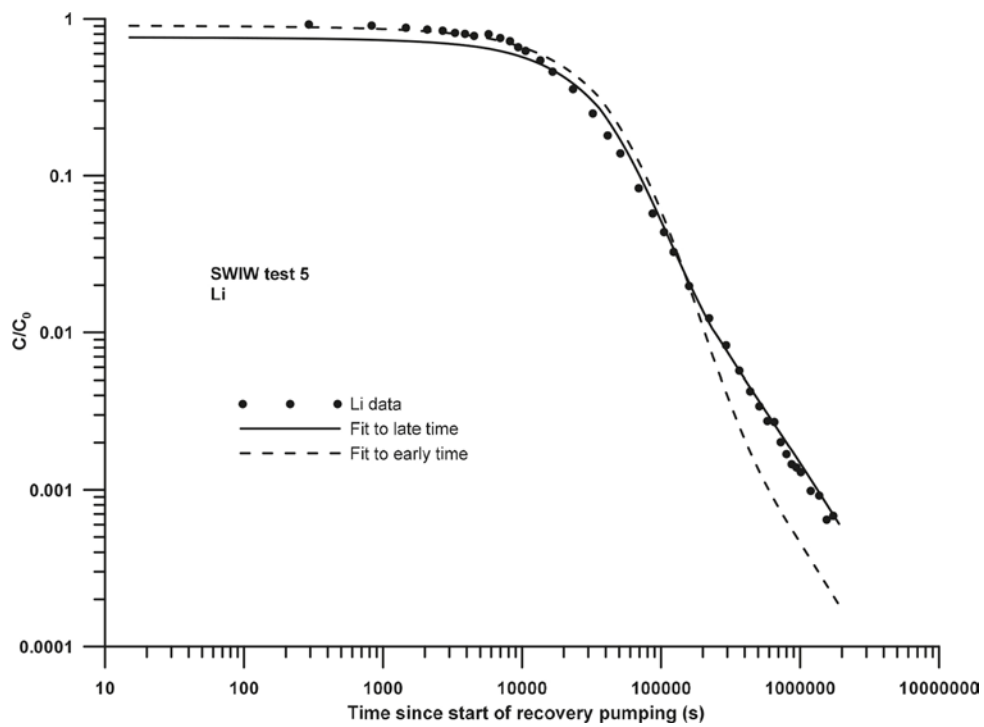

Figure 6-37. *Simulation of Li breakthrough data from SWIW test 5 with a matrix diffusion model.*

For the removed tracers there is no late-time tail to analyse. Instead, effects of diffusion may be visible in the early parts of the recovery breakthrough curves and then primarily when a waiting phase is applied. Therefore only SWIW test 5 is considered in this case, especially as Cl data from SWIW test 4 are fitted well using an advection-dispersion model without matrix diffusion. Figure 6-38 shows an example simulation of Cl breakthrough using the matrix diffusion model. The simulation is made with values of A = 7,000 $s^{\frac{1}{2}}$ and $a_L^2\delta = 5.5 \cdot 10^{-5}$, the latter was in this case fixed from the SWIW 4 analysis with the advection-dispersion model. The overall fit in Figure 6-38 is far from perfect but it is clearly demonstrated that the effect of matrix diffusion makes it possible to attain a starting level for concentration of Cl in SWIW 5 approximately corresponding to experimental data. As in the simulation of Li data from SWIW test 5, a relatively high value of A (i.e. lower matrix diffusion effect) is required to fit the early part of tracer breakthrough.

To summarise the matrix diffusion simulations, the presented examples suggest that homogenous matrix diffusion alone may only partly explain some of the effects during the waiting phase. Because influence of the background flow on tracer behaviour appears to be plausible and that diffusive mass transfer is indicated from the straight-line log-log slopes at late times, it appears reasonable to suggest that the early-time behaviour of SWIW test 5 data are affected both by the background flow and diffusive processes.
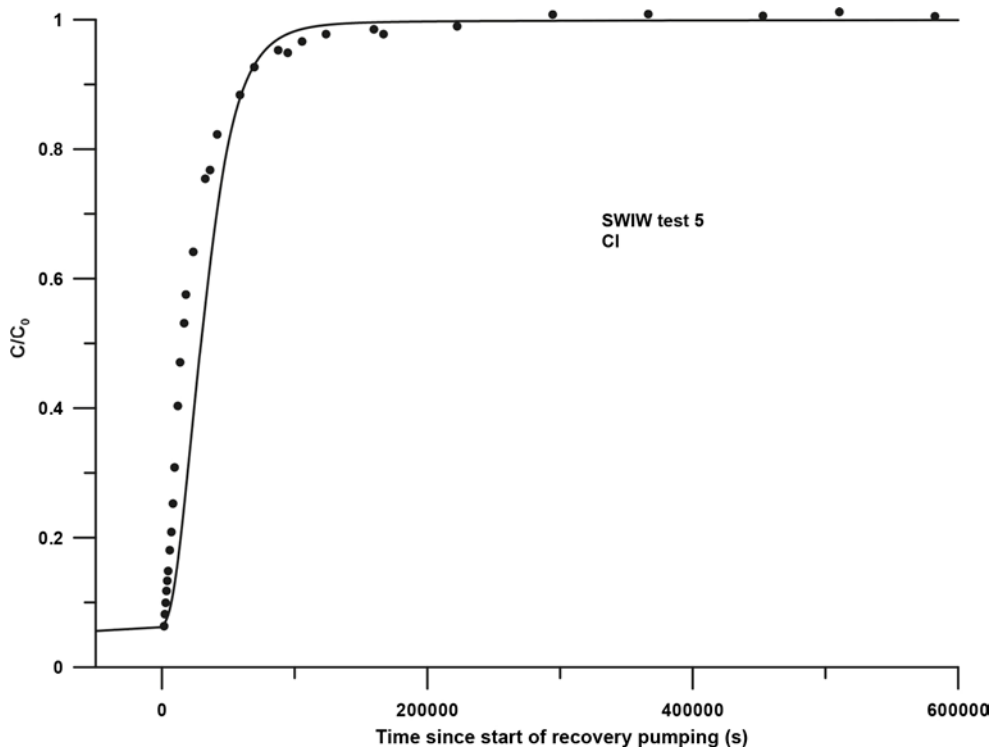

Figure 6-38. *Simulation of Cl breakthrough data from SWIW test 5 with a matrix diffusion model.*

7   Discussion and conclusions

This report presents a series of SWIW experiments involving a variety of tracers with different sorption and diffusion properties. Three preparatory tests were carried out prior to the two main SWIW tests. These tests were used to test experimental variables and performance. In the main tests, a synthetic groundwater was used for injection; the chemical composition of the injection water was prepared beforehand. The injection water was prepared so that some species naturally occurring in the groundwater would not be present in the injection water, while other tracers would be added. This is in contrast to a regular SWIW experiment, such as the ones performed within the site investigation program, where one or more tracers are added to native groundwater, extracted prior to the SWIW experiment.

The added tracers comprised Uranine, NO_3, Li, Mg, Cs and Rb, of which the latter two were expected to be relatively strongly sorbing. Removed tracers comprised Cl, Na, Ca, K and radon (Rn).

The SWIW tests were carried out without any chaser fluid but with or without a waiting phase. Thus, following injection of the tracer solution (i.e. synthetic groundwater), the back-pumping (recovery) started immediately for the cases without waiting case and otherwise immediately after the waiting phase. SWIW test 4 was carried out employing a total injection volume with synthetic groundwater of about 28.75 L. SWIW tests 5 included a waiting phase of about 93 hours, but experimental conditions otherwise as in SWIW test 4.

The primary results from the tests are the tracer breakthrough curves from the main tests, SWIW test 4 and SWIW test 5. All of the tracers resulted in fairly smooth breakthrough curves approximately consistent with prior expectations of advection and retardation properties. A simple homogenous advection-dispersion model with radial flow was found to be sufficient for explaining most of the tracer breakthrough of non-sorbing tracers (added as well as removed) during SWIW test 4 (without waiting phase), using a single composite dispersion parameter.

For sorbing tracers in SWIW test 4, tracer breakthrough was found to be explained fairly well by a homogenous radial flow and transport model with linear retardation. Based on this concept, i.e. without consideration other processes such as diffusive mass transfer, evaluated retardation factors ranged from about 1–2 to about 10–15. The latter range included the more strongly sorbed tracers Cs and Rb (added tracers) and K (removed tracer).

A surprising result is the anomalous behaviour of the tracer Uranine. This tracer has been extensively used as a very reliable conservative tracer in many previous SKB tracer experiments as well as in a large number of other tracer investigations and has proven to be at least as conservative as, for example Li (Lindquist et al. 2008). However, an examination of the results from SWIW test 4 and SWIW test 5 clearly shows that Uranine is not behaving as a conservative tracer in this case. Further study of Uranine results showed that the same behaviour occurred in the preparatory test that were carried using Uranine (SWIW test 1 and 3). Some checking of Uranine results were carried out but the cause of the anomalous behaviour is so far unknown. In retrospect, Uranine behaviour resulted in partly misleading information from the preparatory tests, which affected the planning of the main tests. Experimental data for Uranine is presented in overall plots but not considered for further analysis and interpretation. This is a drawback for the analysis of the experiment, as one of the added conservative tracers cannot be used as intended. It should be emphasized that Uranine sorption in the formation outside the borehole does not affect the evaluation of the dilution measurements. As tracer recovery for Uranine is very high, the anomalous behaviour cannot be explained by degradation. Instead, Uranine behaves a tracer undergoing strong (comparable to Cs and Rb) and reversible sorption. There are no obvious causes for strong Uranine sorption in this case. A study by Magal et al. (2008) showed significant sorption of Uranine in very saline waters, but the salinity during the synthetic SWIW experiment was very low compared with the mentioned study.

Tracer recovery results are very satisfactory for the main SWIW tests as well as the preparatory SWIW tests. Approximately full recovery is indicated for all added tracers (recovery does not apply for removed tracers). SWIW test 5 consistently show lower recovery than SWIW test 4 at the end of recovery pumping, which is due to the prolonged tailing observed when a waiting phase is applied.

Point dilution tests were carried out at several occasions in order to characterise the background flow rates through the experimental section. Estimated flow rates are in the approximate range of 1 to 3 mL/h. These are relatively low flow rates, approximately corresponding to the lower end of estimated flow rates for the SWIW experiments during the site investigation program (Nordqvist 2008). However, it is concluded here that a background flow rate in the range of 1–3 ml/h may have affected the results for SWIW test 5 (with a waiting phase of 93 hours). The main implication of this is that the beginning of the breakthrough curves for both added and removed tracers, in SWIW test 5, is difficult to interpret. The early parts of the SWIW 5 breakthrough curves are qualitatively consistent with diffusive mass transfer during the waiting phase. However, this effect may possibly also be caused by background flow. Because diffusive mass transfer is indicated from the later parts of the breakthrough curves (see further discussion of this below), it seems likely that it would be a combination of the two processes. It is also concluded here that the background flow did not have any significant effect on SWIW test 4 results.

The early parts of the breakthrough curves in SWIW test 5, for both added as well as for removed tracers, begin at different C/C_0-levels for different tracers. The differences are qualitatively consistent with the retardation factors evaluated for SWIW test 4 (see Section 6.2.1), which were fracture retardation factors without considering diffusion. However, if matrix diffusion with sorption in the matrix affects the concentration during the waiting phase (during which nothing would happen in the absence of diffusion or drift due to background flow), tracers with different matrix retardation factors would begin at different C/C_0 at the start of the recovery pumping.

Evidence for diffusion in the beginning of the recovery breakthrough curves in SWIW test 5 would be if two or more non-sorbing tracers with different diffusivity could be compared. Any differences between these would be due to diffusion only because they should be affected in the same way by the background flow. Among added tracers, Uranine would have been important for comparison with other non-sorbing tracers (NO_3 and possibly Li), but this is not possible because of the anomalous behaviour of Uranine during the synthetic SWIW experiment. A comparison of Li and NO_3 (which showed approximately identical behaviour in SWIW test 4) in SWIW test 5 shows that it is difficult to see any difference and that these two tracer start at about the same C/C_0-value. For the removed tracers, only chloride can be considered non-sorbing. Thus, one cannot use the results for non-sorbing tracers alone to conclude that diffusion is responsible for the observed differences between the early parts of SWIW 4 and SWIW 5 breakthrough curves.

As mentioned in the preceding paragraph, the effect of the waiting phase on Li and NO_3 appears to be about the same (see Section 6.1). On the other hand, a weakly sorbing tracer such as Mg is significantly more affected by the waiting phase and even more so for the more strongly sorbing Cs and Rb. It is unlikely that the differences caused by the waiting phase are due to the background groundwater flow only, as this would affect sorbing and non-sorbing tracer in a much more similar way. Thus, this would be relatively firm support that diffusion effects are significant also in early parts of SWIW test 5 breakthrough data.

In contrast to the potential ambiguities when interpreting the early pats of SWIW test 5 breakthrough data, the late-time behaviour of added tracers appear to more conclusively indicate that diffusive mass transfer occurs. Log-log plots of the breakthrough curves for added tracers result in straight-line slopes, often approaching the theoretical slope of -1.5 for matrix diffusion. The slopes vary among the different tracers; there appears to be a tendency for a more flat slope for sorbing tracers. In a homogenous system with matrix diffusion, the late-time log-log slopes should be the same (assuming linear equilibrium sorption in the matrix). Although generic simulations show that sorbing tracers can attain a flatter slope earlier than a non-sorbing, this would only be during a relatively short transition phase while experimental data indicate that the difference in slopes is more permanent. Because sorbing tracers do not "see" the same rock volume as non-sorbing tracers, it is possible that diffusion rates also differ.

There also appears to be systematically flatter late-time slopes in SWIW test 5 than in SWIW test 4. Generic simulations show that this might be a result of employing a waiting phase, but it is not clear whether this is the main reason for the differences between SWIW test 4 and SWIW test 5.

Modelling with a basic homogenous matrix diffusion model was carried out both for generic simulations as well as for exploratory evaluation of experimental data. Models including heterogenous formation properties may be more realistic, but is beyond the scope of this study and left for future work. The modelling with the homogenous model indicated that one may qualitatively explain the differences in initial C/C_0 values between SWIW test 4 and SWIW test 5. However, simulations of added tracers also indicated that it is difficult to explain the late-time tailing without altering the diffusion parameters. This could either be an indication that diffusion properties vary with distance from the borehole section, or that it is a result of a combination of diffusion into stagnant parts of the fracture and matrix diffusion. However, such specualtions are complicated by the indication that tracer drift, due to the background groundwater flow, might affect the early parts of the SWIW 5 curves.

The main findings herein from the series of SWIW experiment can be summarized in the following points:

- Anomalous behaviour of the assumedly non-sorbing tracer Uranine have in retrospect been found to have had significant effect on experimental planning and design.

- A unique and extensive data set is available for further analysis, including added and removed tracer from tests with and without waiting phase.

- Tracer recovery is very high in preparatory tests and as well in the main tests; available data does not indicate less than 100 percent recovery (with sufficiently long recovery pumping) in any of the tests.

- The background groundwater flow is low but might still have affected the tracer distribution in the formation during the waiting phase. The background flow was measured at several occasions but the uncertainty is relatively high due to high sampling rates relative to groundwater flow rates.

- SWIW test 4 results may be fairly well explained with a homogenous advection-dispersion model (without matrix diffusion) and a simple fracture retardation factor for sorbing tracers. Consistent results are obtained for both added and removed tracers.

- Differences between results from SWIW test 4 and SWIW test 5 are qualitatively consistent with diffusive mass transfer during the waiting phase. However, influence of the background flow can not be excluded.

- Late-time log-log slopes in breakthrough curves for added tracers indicate diffusive mass transfer during both SWIW test 4 and SWIW test 5.

The objectives as stated in Section 1.1 have been only partly fulfilled, based on the analysis presented herein. One ambition was to see whether it would be possible to distinguish between fast diffusion processes into stagnant water and slower diffusion into the rock matrix. Although it may be speculated that different diffusion rates (and thereby possibly indicating a a combination of diffusion into stagnant water and into the matrix) might be required to explain the beginning and the end, respectively, of the breakthrough curves, this likely requires further analysis that better accounts for the background groundwater flow. However, that diffusive mass transfers have occurred is strongly indicated by the late-time data for added tracers.

The synthetic SWIW tests were carried out in a slightly different way than the SWIW tests during the site investigation program. The main differences are that no chaser fluid was employed in the synthetic SWIW tests and that a relatively long waiting phase was employed. The overall behaviour of non-sorbing and sorbing tracers in the synthetic SWIW tests is consistent with the results from the site investigation SWIW tests. The possible influence of the groundwater background flow identified herein for SWIW test 5 is not relevant for the site investigation SWIW tests. In the latter, no waiting phase was employed and total injection volumes were considerably larger. The various simulations with background gradient effects presented in this report support previous conclusions (Nordqvist 2008) that the background flow was not an important factor in the site investigation SWIW tests,

This report comprises a summary and description of all experimental results. In addition, some basic modelling assuming homogeneous conditions and other analysis have been carried out in order to explore possible interpretations of experimental data. However, there is an abundance of data that may be further analysed. Some suggestions for possible further analyses include:

- Further analysis of data with consideration to effects of background gradient in the presence of matrix diffusion. This would include simultaneous consideration of gradient and diffusion. As part of this, it would be valuable to derive a more accurate correction for the sampling flow rate in evaluation of dilution tests.

- Further analysis of the behaviour of sorbing tracers compared with non-sorbing tracers, especially in SWIW test 5.

- Further model analysis of radon data could provide a valuable contribution in the overall analysis of the synthetic SWIW results, as the radon production represents an additional matrix process.

- Further analyses considering heterogeneous conditions.

References

SKB's (Svensk Kärnbränslehantering AB) publications can be found at www.skb.se/publications. References to SKB's unpublished documents are listed separately at the end of the reference list. Unpublished documents will be submitted upon request to document@skb.se.

Altman S J, Meigs L C, Jones T L, McKenna S A, 2002. Controls of mass recovery rates in single-well injection-withdrawal tracer tests with a single-porosity, heterogeneous conceptualization. Water Resources Research 38. doi:10.1029/2000WR000182

Bear J, 1988. Dynamics of fluids in porous media. Mineola, NY: Dover.

Becker M W, Shapiro A M, 2003. Interpreting tracer breakthrough tailing from different forced-gradient tracer experiment configurations in fractured bedrock. Water Resources Research 39. doi:10.1029/2001WR001190

Bodin J, Delay F, de Marsily G, 2003. Solute transport in a single fracture with negligible matrix permeability: 2. mathematical formalism. Hydrogeology Journal 11, 434–454.

Cvetkovic V, Cheng H, 2011. Evaluation of single-well injection-withdrawal tests in Swedish crystalline rock using the Lagrangian travel time approach. Water Resources Research 47. doi:10.1029/2010WR009627

Doughty C, Tsang C-F, 2009. Analysis of three sets of SWIW tracer test data using a two-population complex fracture model for matrix diffusion and sorption. Research Report 2009:09, Strålsäkerhetsmyndigheten (Swedish Radiation Safety Authority).

Drever J I, McKee C R, 1980. The push-pull test. A method of evaluating formation adsorption parameters for predicting the environmental effects on in-situ coal gasification and uranium recovery. In Situ 4, 181–206.

Gelhar L W, Collins M A, 1971. General analysis of longitudinal dispersion in nonuniform flow. Water Resources Research 7, 1511–1521.

Gelhar L W, Welty C, Rehfeldt K R, 1992. A critical review of data on field-scale dispersion in aquifers. Water Resources Research 28, 1955–1974.

Gouze P, Le Borgne T, Leprovost R, Lods G, Poidras T, Pezard P, 2008. Non-Fickian dispersion in porous media: 1 Multiscale measurements using single-well injection withdrawal tracer tests. Water Resources Research 44. doi:10.1029/2007WR006278

Gustafsson E, Morosini M, 2002. In-situ groundwater flow measurements as a tool for hardrock site characterisation within the SKB programme. NGU Bulletin 439, 33–44.

Güven O, Falta R W, Molz F J, Melville J G, 1985. Analysis and interpretation of single-well tracer tests in stratified aquifers. Water Resources Research 21, 676–684.

Haggerty R, McKenna S A, Meigs L C, 2000. On the late time behavior of tracer test breakthrough curves. Water Resources Research 36, 3467–3479.

Haggerty R, Fleming S W, Meigs L C, McKenna S A, 2001. Tracer tests in a fractured dolomite 2. Analysis of mass transfer in single-well injection-withdrawal tests. Water Resources Research 37, 1129–1142.

Jakob A, Mazurek M, Heer W, 2003. Solute transport in crystalline rocks at Äspö – II. Blind predictions, inverse modelling and lessons learnt from test STT1. Journal of Contaminant Hydrology 61, 175–190.

Lee T-C, 1999. Applied mathematics in hydrogeology. Boca Raton, FL: Lewis Publishers.

Lessoff S C, Konikow L F, 1997. Ambiguity in measuring matrix diffusion with single-well injection/recovery tracer tests. Groundwater 35, 166–176.

Lindquist A, Hjerne C, Nordqvist R, Byegård J, Walger E, Ludvigson J-E, Wass E, 2008. Forsmark site investigation. Confirmatory hydraulic interference test and tracer test at drill site 2. SKB P-08-13, Svensk Kärnbränslehantering AB.

Magal E, Weisbrod N, Yakirevich A, Yechieli Y, 2008. The use of fluorescent dyes as tracers in highly saline groundwater. Journal of Hydrology 358, 123–133.

Marquardt D W, 1963. An algorithm for least squares estimation of non-linear parameters. Journal of the Society for Industrial and Applied Mathematics 11, 431–441.

Moench A F, 1985. Transient flow to a large-diameter well in an aquifer with storative semiconfining layers. Water Resources Research 21, 1121–1131.

Molz F J, Melville J G, Güven O, Crocker R D, Matteson K T, 1985. Design and performance of single-well tracer tests at the Mobile Site. Water Resources Research 21, 1497–1502.

Moreno L, Neretniks I, Klockars C-E, 1983. Evaluation of some tracer tests in the granitic rock at Finnsjön. SKB TR 83-38, Svensk Kärnbränslehantering AB.

Neretnieks I, 2007. Single well injection withdrawal tests (SWIW) in fractured rock. Some aspects on interpretation. SKB R-07-54, Svensk Kärnbränslehantering AB.

Nordqvist R, 2008. Evaluation and modelling of SWIW tests performed within the SKB site characterisation programme. SKB R-08-104, Svensk Kärnbränslehantering AB.

Nordqvist R, Gustafsson E, 2002. Single-well injection-withdrawal tests (SWIW). Literature review and scoping calculations for homogenous crystalline bedrock conditions. SKB R-02-34, Svensk Kärnbränslehantering AB.

Nordqvist R, Byegård J, Hjerne C, 2008. Feasibility study of a Single Well Injection Withdrawal (SWIW) experiment with synthetic groundwater. SKB R-08-125, Svensk Kärnbränslehantering AB.

Nordqvist R, Byegård J, Hjerne C, 2012a. Complementary tracer tests – SWIW, CEC and multi-hole reciprocal cross flow tests at the TRUE-1 site. TRUE-1 Continuation project. TRUE-1 Completion. SKB P-11-27, Svensk Kärnbränslehantering AB.

Nordqvist R, Hjerne C, Andersson P, 2012b. Single-well and large-scale cross-hole tracer experiments in fractured rocks at two sites in Sweden. Hydrogeology Journal 20, 519–531.

Pickens J F, Grisak G E, 1981. Scale-dependent dispersion in a stratified granular aquifer. Water Resources Research 17, 1191–1211.

Schroth M H, Istok J D, Haggerty R, 2001. In situ evaluation of solute retardation using single-well push-pull tests. Advances in Water Resources 24, 105–117.

Tomich J F, Dalton R L, Deans H A, Shallenberger L K, 1973. Single-well tracer method to measure residual oil saturation. Journal of Petroleum Technology 25, 211–218.

Tsang Y W, 1995. Study of alternative tracer tests in characterizing transport in fractured rocks. Geophysical Research Letters 22, 1421–1424.

Voss C I, 1984. A finite-element simulation model for saturated-unsaturated fluid-density-dependent ground-water flow with energy transport or chemically-reactive single-species solute transport. Water-Resources Investigations Report 84-4369,U.S. Geological Survey, Denver, Colorado.

West J M, Aoki K, Baker S J, Bateman K, Coombs P, Gillespie M R, Henney P J, Reeder S, Milodowski A E, Yoshida H, 1997. Äspö Hard Rock Laboratory. Redox experiment in detailed scale (REX) – complementary laboratory work to examine microbial effects on redox. SKB HRL-98-14, Svensk Kärnbränslehantering AB.

Winberg A, Andersson P, Hermansson J, Stenberg L, 1996. Results of the SELECT project. Investigation programme for selection of experimental sites for the operational phase. SKB HRL-96-01, Svensk Kärnbränslehantering AB.

Unpublished documents

Nordqvist R, 2009. Usage of radon in SWIW with synthetic groundwater. SKBdoc 1217678 ver 1.0, Svensk Kärnbränslehantering AB.
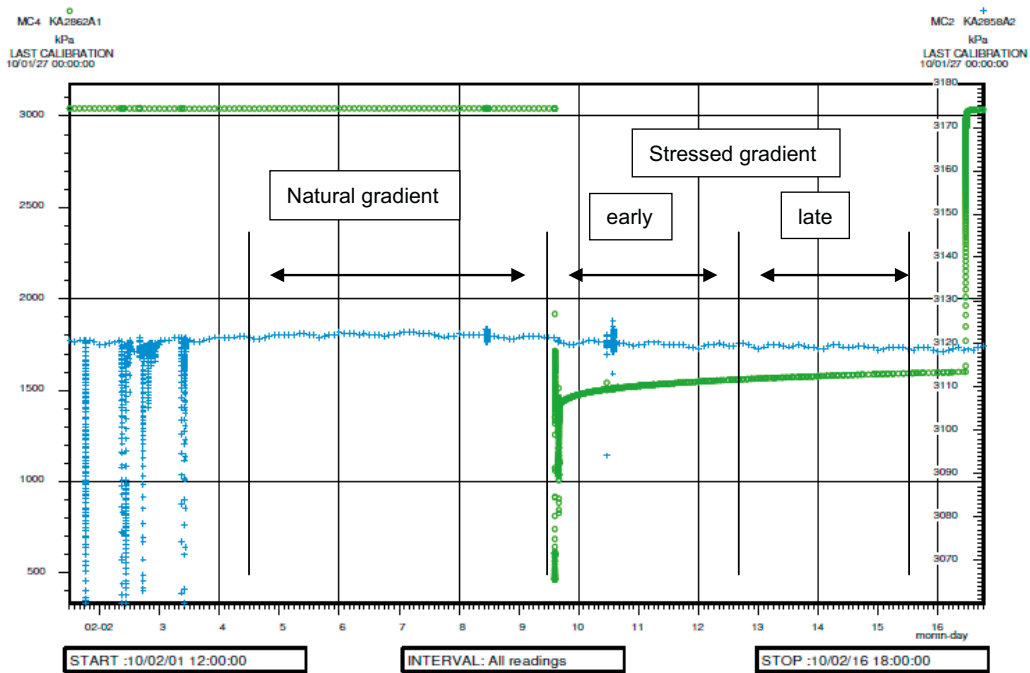
Groundwater flow measurements in KA2858A

Figure A1-1. *Pressure in KA2858A:2 (blue +) and in KA2862A (green o) during groundwater flow measurement 1 in KA2858A:2. The periods where evaluation is performed is marked in the figure.*

Figure A1-2. *The tracer dilution graph (logarithm of concentration versus time) for dilution measurement 1 in KA2858A:2 including straight line fits during both natural and stressed conditions.*

Figure A1-3. *Pressure in KA2858A:2 during groundwater flow measurement 2 in KA2858A:2. The periods where evaluation is performed is marked in the figure.*
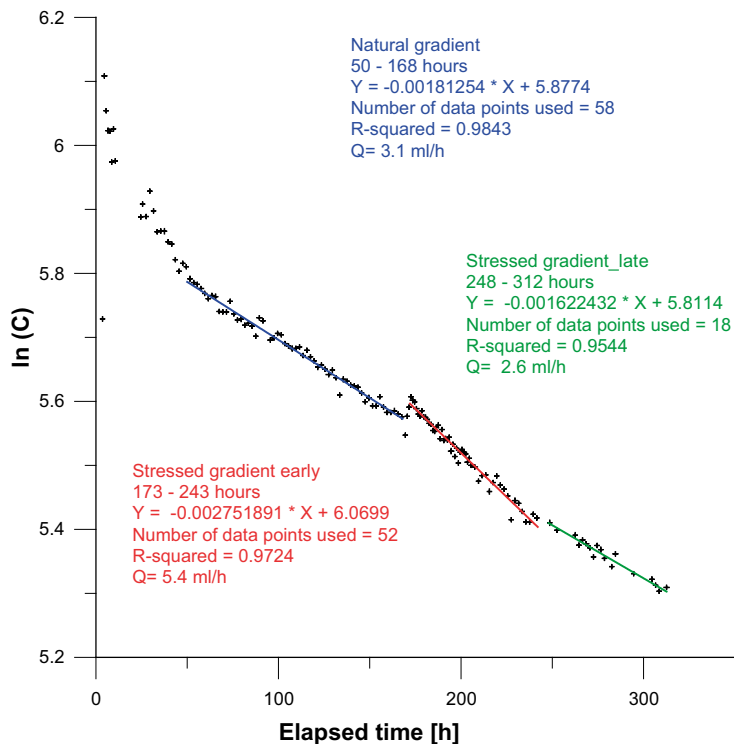

Figure A1-4. *The tracer dilution graph (logarithm of concentration versus time) for dilution measurement 2 in KA2858A:2 including straight line fit during natural conditions.*
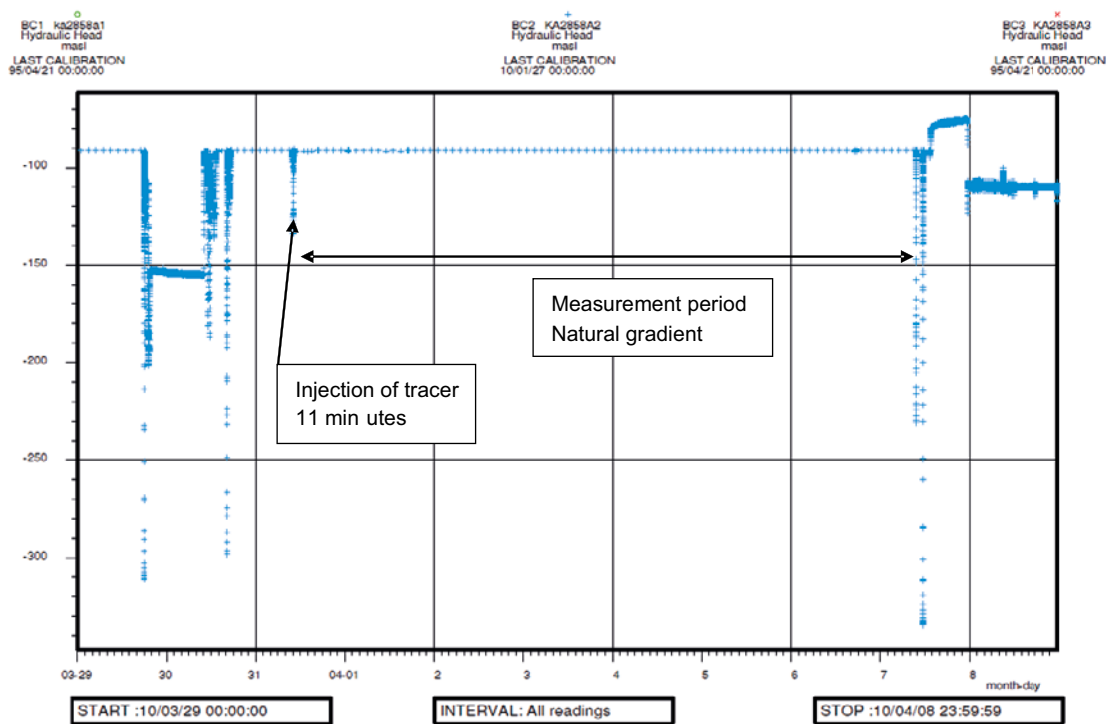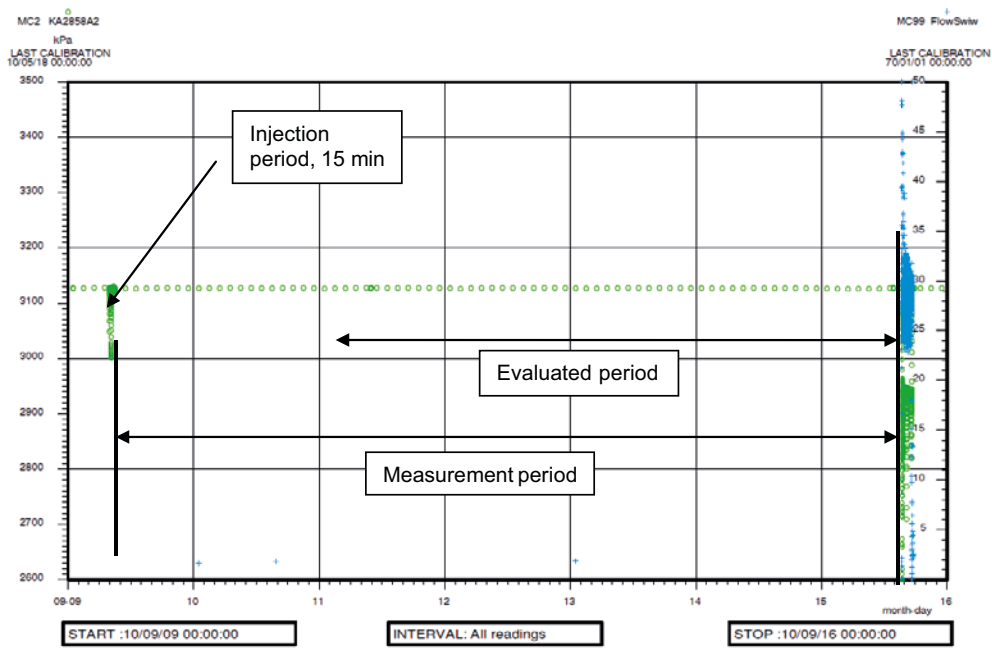
Figure A1-5. *Pressure in KA2858A:2 during groundwater flow measurement 3 in KA2858A:2. The periods where evaluation is performed is marked in the figure.*

Figure A1-6. *The tracer dilution graph (logarithm of concentration versus time) for dilution measurement 3 inKA2858A:2 including straight line fit during natural conditions.*

Figure A1-7. *Pressure in KA2858A:2 during groundwater flow measurement 3 in KA2858A:2. The periods where evaluation is performed is equal to the measurement period and is marked in the figure.*

Äspö HRLGroundwater flow measurement 4KA2858A
(39.77–40.77 m)

Natural gradient
11 - 187 hours
Y = -0.002680821 * X + 7.206849
Number of data points used = 47
R-squared = 0.7446
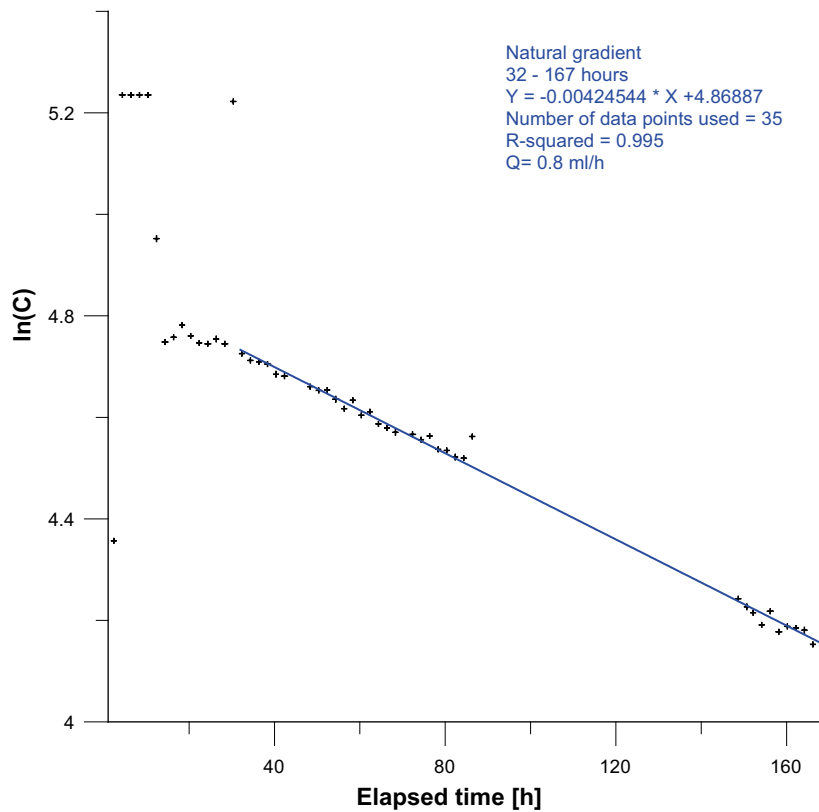Q_{bh}= 1.0 ml/h

Figure A1-8. *The tracer dilution graph (logarithm of concentration versus time) for dilution measurement 4 inKA2858A:2 including straight line fit during natural condition.*
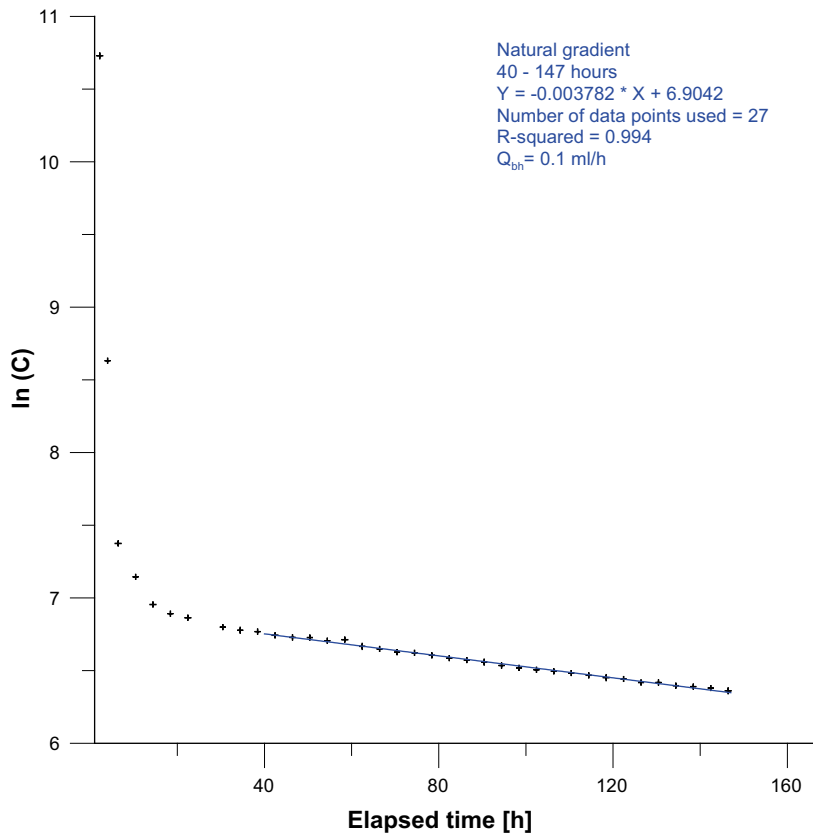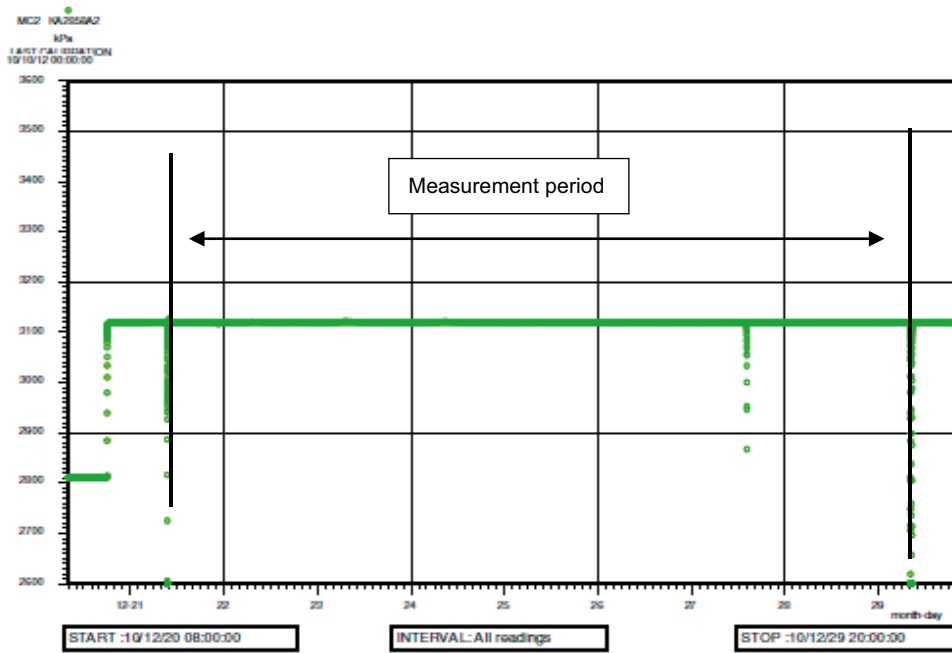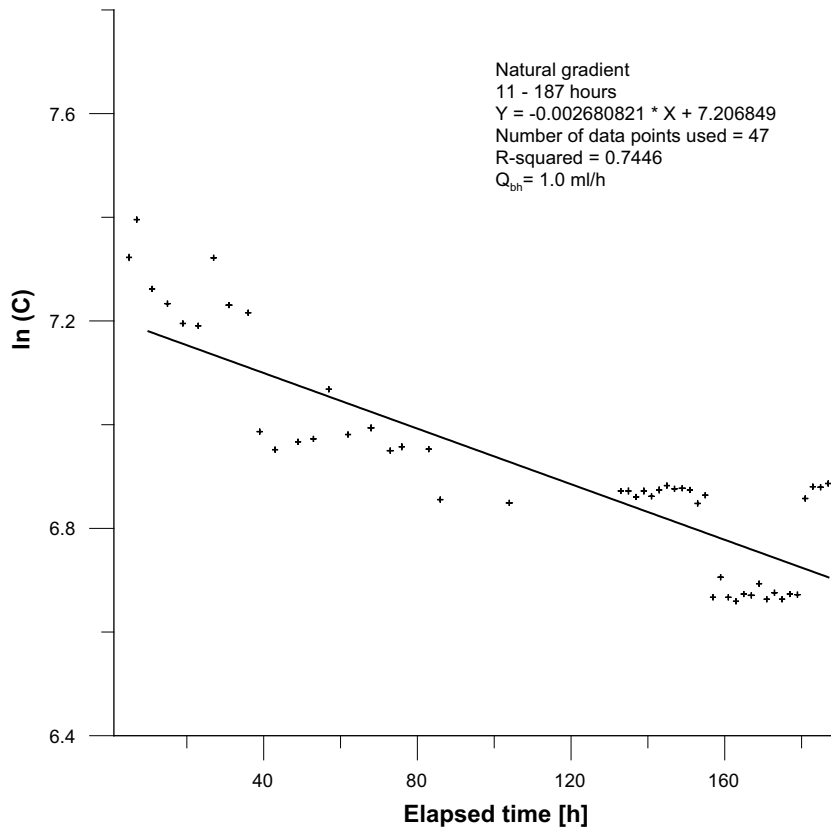
Water Composition, groundwater

Table A2-1. Water composition

Id code	Secup m	Seclow m	Sample no.	Sampling date	RCB %	Na mg/L	K mg/L	Ca mg/L	Mg mg/L	HCO_3^- mg/L	Cl^- mg/L	SO_4^{2-} mg/L	SO_4-S mg/L	Br^- mg/L	F^- mg/L	Si mg/L	Fe mg/L	Mn mg/L	Li mg/L
KA2858A	39.77	40.77	2298	1995-03-10	-2.76	2630	9.7	3360	49.7	9.0	10300	577		70.1		5.5	0.088	0.39	2.17
KA2858A	39.77	40.77	20106	2010-03-15	-0.4	3430	14	4770	47	4.7	13500	611		107	1.1	3.39	0.39	0.538	3.86(
KA2858A	39.77	40.77	20107	2010-03-16	-3.4	3490	14	4910	43	7.3	14700	623		111	1.6	6.09	<0,10	0.382	3.96(
KA2858A	39.77	40.77	20108	2010-03-29	0.96	3500	14.3	4810	42.2	7	13300	613	234	110	1.6	5.95	<0,10	0.382	4.33
KA2858A	39.77	40.77	20109	2010-04-26	0.01	3460	13.4	4990	34.1	7	13800	614	231	109	1.4	6.09	<0,10	0.321	3.77
KA2858A	39.77	40.77	20069	2010-01-27	-1.96	3420	12.8	4510	51.4	5.1	13500	624	223	107	1.3	5.17	<0.1	0.481	3.67
KA2858A	39.77	40.77	20070	2010-01-28	-2.78	3450	13.5	4580	46.3	6.8	13900	614	222	107	1.4	5.83	<0.1	0.397	3.92
KA2858A	39.77	40.77	20071	2010-01-29	-2.47	3450	13.9	4520	43.5	6.8	13700	613	218	107	1.6	5.81	<0.1	0.376	3.84
KA2858A	39.77	40.77	20447	2010-10-26	-1.2	3370	12.4	5150	35.5	6.8	14318	606	224	113	1.7	5.7	0.0219	0.328	3.78
KA2858A	39.77	40.77	20448	2010-11-03	76.6	558	7.56	914	2480	41	1390	543	205	13.3	1.3	2.12	<0.002	1.28	867
KA2858A	39.77	40.77	20449	2010-11-24	-1.1	3400	14.2	5170	33.3	6.9	14365	604	223	112	1.8	5.79	<0,2	0.294	3.73
KA2858A	39.77	40.77	20450	2010-11-29	47.1	1760	8.95	2620	1510	32	4675	549	214	103	2.1	3.48	<0,2	2.26	526
KA2858A	39.77	40.77	20451	2010-12-20	2.8	3430	14.1	5150	34.2	7.2	13277	543	223	98.9	1.7	5.74	0.019	0.279	4.04

- = Not analysed

< "value" = value below reporting limit

RCB % = Rel. charge balance error %

Table A2-1. Water Composition, continued

Id code	Secup m	Seclow m	Sample no.	Sampling date	Sr mg/L	pH_L	DOC mg/L	HS⁻ mg/L	Uranine µg/L	EC_L mS/m	NH₄-N mg/L	NO₂-N mg/L	NO₃-N mg/L	NO₂-N+NO₃-N mg/L	PO₄-P mg/L	PO₄-P_hlysis mg/L	Cs µg/L	Rb µg/L	Microorganisms cfu/ml
KA2858A	39.77	40.77	2298	1995-03-10	47.5	7.8	1.3			2650									
KA2858A	39.77	40.77	20106	2010-03-15	92.0	6.25		0.270	102	3500	0.0113	<0,0002	0.0214	0.0215	0.0008	0.0018	48	26.90	
KA2858A	39.77	40.77	20107	2010-03-16	94.2	7.82		<0,006	0.35	3550	0.0290	0.0002	0.0015	0.0017	0.0005	<0,0005	49	5.12	
KA2858A	39.77	40.77	20108	2010-03-29	96.7	7.79		0.006	0.7	3540	0.0293	<0,0002	0.0016	0.0017	0.0005	0.0015	50.7	5.12	
KA2858A	39.77	40.77	20109	2010-04-26	93.4	7.85		<0,006	0.9	3620	0.0342	<0,0002	0.0228	0.023	<0.0005	0.0015	54.5	5.33	
KA2858A	39.77	40.77	20069	2010-01-27	91.3	6.56			0.2	3450			0.008				43.4	4.26	
KA2858A	39.77	40.77	20070	2010-01-28	93.3	7.25			0.5	3490			0.0096				45.5	4.45	
KA2858A	39.77	40.77	20071	2010-01-29	94.7	7.57			0.1	3520			0.0006				45.9	4.49	
KA2858A	39.77	40.77	20447	2010-10-26	94.2	7.81	1.00	<0,019	3.7	3680			0.0026				5.21	51.2	18.0
KA2858A	39.77	40.77	20448	2010-11-03	86.5	9.06	3.50	<0,019	4027	3200			12				2430	15400	27.00
KA2858A	39.77	40.77	20449	2010-11-24	94.3	7.92	11.9	<0,019	1.7	3710			0.337				8.19	68.4	<10
KA2858A	39.77	40.77	20450	2010-11-29	91	8.88	2.8	0.048	502	3280			14				1520	9270	9.00
KA2858A	39.77	40.77	20451	2010-12-20	94.8	7.47	1.3	0.019	4.4	3713			1.71				10.6	85.2	18

- = Not analysed
< "value" = value below reporting limit
RCB % = Rel. charge balance error %